Environmental Tracking for Public Health Surveillance – Morain & Budge (eds)
© 2013 Taylor & Francis Group, London, ISBN 978-0-415-58471-5

Chapter 4

Air quality and human health

D.W. Griffin[1] & E.N. Naumova[2] (Auth./eds.) with; J.C. McEntee[3], D. Castronovo[4], J.L. Durant[5], M.B. Lyles[6], F.S. Faruque[7] & D.J. Lary[8]
[1]*US Geological Survey, Tallahassee, FL, US*
[2]*Tufts University School of Medicine, Boston, MA, US*
[3]*Cardiff University, Cardiff, UK*
[4]*Mapping Sustainability LLC, Walpole, MA, US*
[5]*Tufts University, Medford, MA, US*
[6]*US Naval War College, Newport, RI, US*
[7]*University of Mississippi Medical Center, Jackson, MS.; US*
[8]*W.B. Hanson Center for Space Science, University of Texas, Richardson, TX, US*

ABSTRACT: This chapter addresses how atmospheric constituents and events impact human health, and how environmental monitoring has aided our understanding of them. The principal focus is on planetary processes (volcanoes and desert dust storms); a secondary theme addresses surface emissions originating from anthropogenic sources.

1 INTRODUCTION

Earth's atmosphere is composed of chemically and physically distinct layers known as the troposphere, stratosphere, mesosphere, thermosphere, and exosphere (Figure 1). Between these layers are zones of transition known as the thermopause (where temperature no longer decreases with altitude), stratopause, mesopause, with each of these zones marking a change in temperature trend with increasing altitude above the Earth's surface. Environmental monitoring satellites orbit the Earth above the thermosphere and beyond from about 600 km to about 40,000 km. The lower atmospheric layer, the troposphere, ranges from an upper-level altitude of about eight kilometres over the Arctic and Antarctic to about seventeen kilometres over the equator. Approximately seventy-five per cent of Earth's atmospheric mass exists in the troposphere in addition to about ninety-nine per cent of its aerosols (particles and gas). The majority of all weather phenomena occur within this layer. Within the troposphere, humans exist in the planetary boundary, or atmospheric boundary layer, defined as the lowest part of the troposphere where winds are under the influence of surface topography. The planetary boundary layer typically reaches altitudes into the troposphere of about fifty metres over the Arctic and Antarctic to about two kilometres around the equator.

Humans and other animals have evolved to extract oxygen from the atmosphere through respiration. Consequently, air quality chemistry is an up-front and personal health risk for every person. Broad-scale weather events also impact health in context of disasters and hazards that if not managed properly lead to disease outbreaks or exacerbate well being issues within a population. A few sample data for weather-related mortality are presented in Table 1. Although lightning is a most intimidating hazard, the US Centers for Disease Morbidity and Mortality Weekly Report documented only 1318 deaths in the US between 1980 and 1995 (MMWR 2003a). The data also illustrate that weather-related mortality in the United States is linked to large storms and extreme temperature events. Globally, mortalities due to extreme-weather events have dropped about ninety-five per cent since the early 19th Century due to higher awareness and preparedness (Goklany 2007). Between

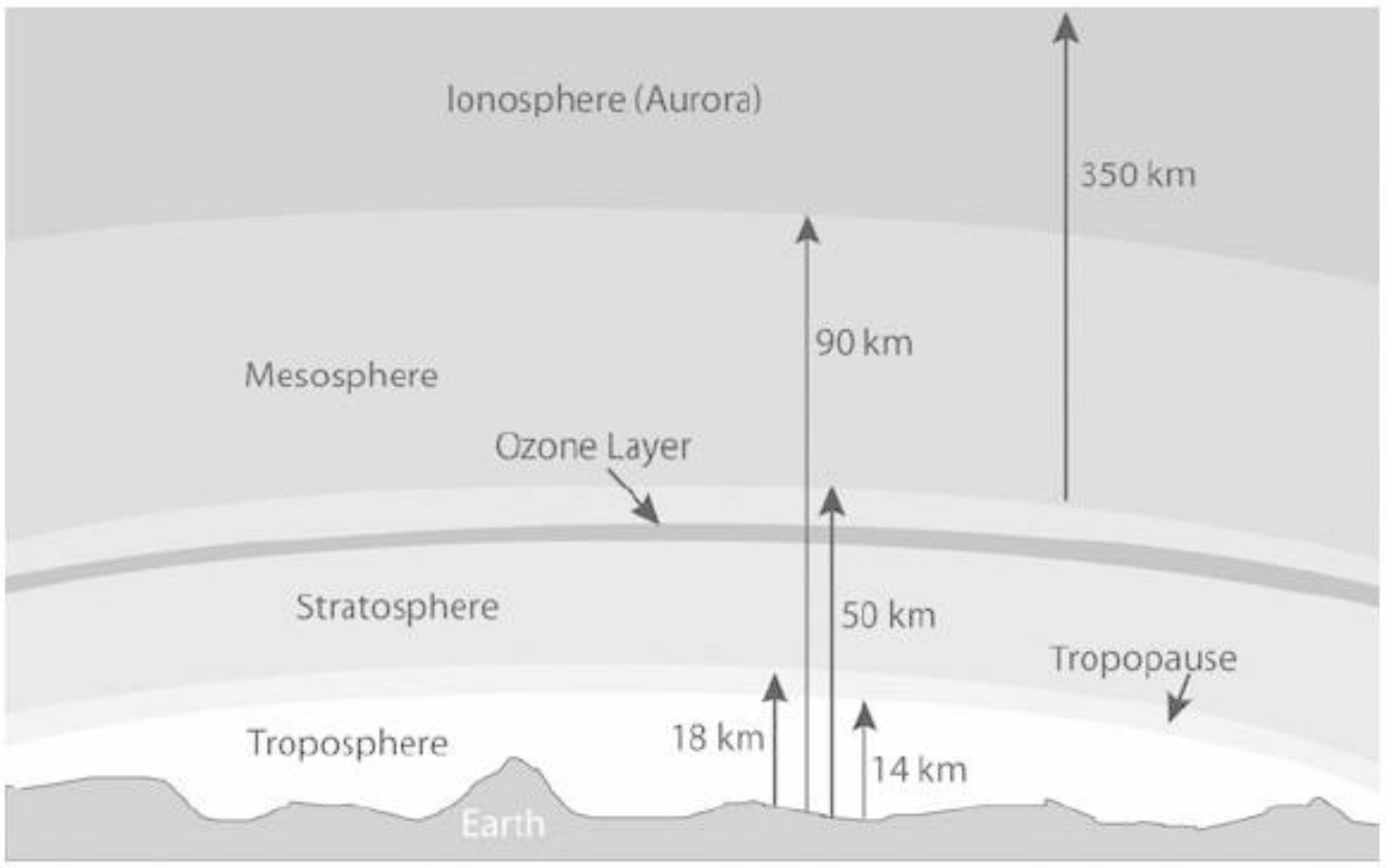

Figure 1. Earth's atmospheric layers, from the troposphere to the ionosphere.

Table 1. Weather-related deaths in the US, 2000–2008. Data courtesy NOAA, National Weather Service.

Year	Lightning	Tornadoes	Storms*	Extreme temp	Flood	Other**
2008	27	126	76	115	82	3
2007	45	81	28	152	43	2
2006	48	67	38	255	72	49
2005	38	38	1072	182	43	31
2004	32	35	108	33	82	35
2003	43	54	75	56	86	74
2002	51	55	96	178	49	53
2001	44	40	112	170	48	35
2000	51	41	95	184	38	49
Average	42	60	189	147	65	37

*Thunderstorm winds, tropical cyclones, winter
**Rain, dust storms, dust devils, mudslides, volcanic ash, high wind, misc

2000 and 2006, annual weather related deaths accounted for only about 0.03 per cent of total global deaths. These data pale in comparison to mortality caused by non-communicable illnesses (about fifty-nine per cent) and communicable diseases (about thirty-two per cent) These, include flu viruses that move from host to host through the atmosphere) (Goklany 2007). Economic health risk can be just as devastating. It has been estimated that ninety-six severe weather-events that occurred between 1980 and 2009 caused in excess of $700 billion USD in damages (NCDC 2010).

Although inclement weather poses obvious risks to human health, there are many respiratory health threats that are invisible to the unaided eye. The most indefensible challenge to the respiratory tract is caused by natural releases of toxic gases, such as carbon dioxide. In August 1986 approximately 1700 people were asphyxiated by carbon dioxide released from the depths of Lake Nyos in Cameroon, West Africa (Kling *et al.*, 1987; Giggenbach 1990). A similar event occurred several years earlier alongside another regional lake that asphyxiated thirty-seven people (Giggenbach *et al.*, 1991). Several degassing studies have been conducted in Italy to examine event fatalities of small numbers of humans and other life forms, and to develop strategies to limit future risks (Tassi *et al.*, 2005; Nadkarni *et al.*, 2008). Degassing events are not uncommon in tectonically active

areas and highly concentrated clouds of carbon dioxide may be emitted from water and soil that cause fatalities in exposed populations (Rogie *et al.*, 2001; Carapezza *et al.*, 2003). It is clear that changes in atmospheric gas composition can be fatal and are perennial risks to respiratory systems.

Respiratory tracts have evolved to protect life from inhaling particulates. The basic aetiology of lung inflammation begins with deposition of particles into the lung. Breathing patterns, the branched morphology of the airways, and particle size and shape can influence the location of particle deposition (Cullen *et al.*, 2002). The first line of defence in the human system lies with nasal hairs and mucus glands that provide moisture to the hairs to facilitate particle capture. For particles larger than five to ten micrometres in size, nasal filtering efficiency or entrapment is near 100 per cent compared to only about twenty-five per cent for particles in the 0.25 μm range (Brown *et al.*, 1950). The greatest deposition rate beyond the nasal chamber, from the trachea to the alveoli, occurs with particles between one to two micrometres in size, and continues to decrease as particle size approaches 0.25 μm. It then increases with further decrease in size. Among ultrafine particles (median diameter of twenty-six nanometres) deposition in the respiratory tract increases with a decrease in particle size (smallest particles, median diameter of 8.7nm) and deposition rate increases over 4.5-fold with exercise (Daigle *et al.*, 2003). Particles that penetrate and are deposited beyond the nasal cavity are cleared via secretion, mucociliary transport, and cough or ingestion. Optimal mucociliary transport occurs at 100 per cent humidity; and, decreases as lower humidity levels influence transport/clearance efficiency negatively humidity influence transport/clearance efficiency negatively (Corbett *et al.*, 1999). Research has demonstrated that carbonaceous ultrafine (100 nm) isotope-labelled particles remain in the lung system up to 3 days or more, but no evidence of movement across the interstitial barrier of the alveoli into the bloodstream was been noted (Wiebert *et al.*, 2006). Other investigations also reported that they were not able to detect movement through the interstitial barrier (Brown & Hovmoeller 2002; Mills *et al.*, 2006). In contrast, several studies have reported movement of ultrafine particles from the lung environment into the circulation system of humans and rats (Nemmar *et al.*, 2002; Takenaka *et al.*, 2006). Particles that become lodged in the main airways are cleared by the mucociliary escalator (Lehnert 1993). If a particle penetrates into the non-ciliated alveolar level, it may be cleared by phagocytic alveolar macrophages. However, if the particles impair macrophage-mediated removal they are not cleared. Some particles may directly penetrate the alveolar epithelium and reach the lung's deep lymph-node environment. Studies have demonstrated different immune responses based on particle size (Donaldson *et al.*, 2000; Samuelsen *et al.*, 2009). The latter has demonstrated that ultrafine particles in the range of 64nm elicited *pronounced inflammatory response* versus challenge with fine scale particles larger than 200 nm.

Studies addressing the accumulation of silica (most common mineral in Earth's crust) in the lung have demonstrated allergic response, asthmatic stress, and silicosis/pulmonary fibrosis risk (Norboo *et al.*, 1991; Saiyed *et al.*, 1991; Kwon *et al.*, 2002; Park *et al.*, 2005; Chang *et al.*, 2006). Macrophages have been shown to become inundated with inert particles, which subsequently halt the clearance of all particles at the alveolar level (Morrow 1992). Macrophages release toxins that destroy particles; however, the released IL-1, IL-6, tumour-necrosis factor (TNF), fibroblast-growth factor, and the affluence of polymorphonuclear neutrophils can damage lung tissue (Cullen *et al.*, 2002). The short-term effect of the above processes is lung inflammation, which manifests itself as difficulty in breathing and increased susceptibility to respiratory infections. Long-term prognoses include the possibility of fibrosis and carcinogenesis (Driscoll 1996).

Desert-dust storms are the primary naturally occurring means of both short- and long-term exposure to silica. Volcanic events are another primary source of exposure to atmospherically suspended soils. With both dust storms and volcanic events, significant quantities of mineral material can be entrained into the atmosphere with larger events capable of global dispersion (Simkin & Siebert 1994; Griffin 2007). Exposure to significant concentrations of soil particles is common over extended periods of time from dust storms and soil particles, or ash from volcanic eruptions. Earthquakes and landslides also can generate dust clouds that adversely impact human health (Schneider *et al.*, 1997; Cook *et al.*, 2005). Another source of heavy loads of airborne particulates consists of clouds of smoke from forest fires that can transport ash, soil, microorganisms

and other organic constituents thousands of kilometres from their point of origin (Morawska & Zhang 2002; Zhang & Morawska 2002; Mims & Mims 2004). A review of literature reveals that scientists have sought to characterize these heavy-particle-load events, to elucidate loading mechanisms, transport range, particulate composition, and their impact on ecosystems and human health. Earth observing satellites have contributed greatly to our understanding of transcontinental and transoceanic dispersal by providing data and imagery of atmospheric events as they develop. Assimilation of these data and/or fusion of data with imagery into numerical models are beginning to reveal associated risks from these processes.

Traditionally used to observe land-cover information and biogeophysical process phenomena on the Earth's surface, remote sensing has been used increasingly by scientists, engineers, public health communities, and epidemiologists to measure environmental variables that impact human health. A growing global network of atmospheric sensors is utilized for monitoring clouds, precipitation, chemistry, aerosols, oceanic winds, and changing environmental events (SMD 2012). Information on individual satellites can be found at (NASA 2012a). Satellites that provide full-colour, bird's eye views of Earth have produced incredible imagery of dust storms, volcanic eruptions, fire plumes, and other aerosols that have fostered a more comprehensive view of the nature of these events on a global scale, as well as the potential implications to human and ecosystem health in downwind environments. Many of these images can be accessed from websites hosted by national space agencies such as NASA's Earth Observatory (EO 2012). There are numerous other national and international databases from which to view images or to download spectral data for use in models.

Material in Section 2, volcanic ash, is provided by Doctors Naumova, McEntee, Castronova and Durant. Section 3, desert dust, is contributed by Doctor Griffin; Section 4, anthropogenic contaminants, is provided by Doctor Lyles; and Section 5, emerging Earth observing sensors and data, is contributed by Doctors Lary and Faruque.

2 VOLCANIC EMMISSIONS AND HEALTH

2.1 *Volcanic emissions, air quality and human health*

A 1985 earthquake in Mexico killed some 30,000 people, leading the United Nations General Assembly to designate the 1990s as the International Decade for Natural Disaster Reduction (IDNDR). One of the greatest risks is the danger of living near active volcanoes, as exemplified by the eruption of Nevado del Ruiz in the Columbian Andes, which resulted in 23,000 deaths (Villegas 2004). Prior to the IDNDR, most sensor data relating to volcanoes were limited to aerial photographs before and after the event (Villegas 2004). Today, Earth observing technology is used for a variety of increasingly complex volcano-related tasks, including pre-disaster loss estimations, integrated measurements, animations, and pre-event 3D modelled simulations. Remote-sensing data facilitate accurate and timely data collection to estimate human exposure to volcanic ashes in both highly accessible and hard-to-reach locations.

In the US, the Cascade Range of the Pacific Northwest has thirteen potentially active volcanoes extending across 1600 kilometres in highly populated areas of Washington, Oregon, and northern California. This range is the most volcanically hazardous area in the US with over 100 eruptions in the past 4000 years. On average, it has two volcanic eruptions per century including: Mount St. Helens from 1980–1986 and Lassen Peak, California from 1914–1917. The Mount St. Helens eruption 1980 caused fifty-seven deaths and over one billion US dollars in damages. There are more than one million residents at risk of a volcanic eruption from Mount Rainier, one of the Nation's most dangerous volcanoes, in the Seattle-Tacoma, Washington area (Smith *et al.*, 2005). Alaskan volcanoes also pose significant risk not only to local populations, but also to communities hundreds and even thousands of miles away. For instance, the ash cloud from the Augustine volcano drifted as far as Colorado, Arizona, and even Virginia (Kienle & Shaw 1979; Waythomas & Miller 1998). During the 1989–90 eruption of the Redoubt volcano, ash clouds were recorded as far as West Texas (Casadevall 1994; Waythomas & Miller 1998). While local communities typically experience the

most immediate effects of volcanic eruptions, distant areas can also be adversely affected. The long-distance transport of ash is not only possible, but probable if recent activity of the Alaskan and Cascadian volcanoes is any indication (USGS 2006; AVO 2010).

The hazards caused by volcanic eruptions are detrimental to human health. Recent developments in Earth observations make it possible to monitor these events from afar. Availability of these data combined with public health exposure information presents an opportunity to determine whether remotely acquired data can serve as a relative proxy for ground-based measurements. This Section explores the possibility by describing what is needed to establish an observational link to ground-based information. This is followed by a discussion of the health impacts of volcanic ash, and results from an actual application.

2.1.1 *Satellite monitoring of volcanoes*

Volcanoes emit gases and ash into the atmosphere that impact the human respiratory system (Delmelle *et al.*, 2001), natural environments (Robock 2000; Tank *et al.*, 2008), structures, and both ground-based and air-borne equipment, especially commercial aviation (Guffanti *et al.*, 2005). Traditionally, sensor data from volcanoes consisted of ground-based measurements collected at the source of degassing. Volcanologists are primarily interested in chemical species, such as H_2O, CO_2, SO_2, HCl, HF, and H_2S (McGonigle 2005), because fluctuations in chemical composition can indicate whether a future eruption is imminent. The direct impact of certain chemicals on human and natural environments is the primary concern here.

The standard procedure for ground-based measurements involves sample collection with subsequent laboratory analysis (Symonds *et al.*, 1994). However, this approach has a number of limitations including: (a) samples collected only where temperatures and safety permit, because such low-temp vents may not be representative of the whole volcano; (b) the potential for the chemical composition of the sample to be altered during storage; and (c) delays in analysis, making real-time applicability difficult (McGonigle 2005). Sensing technologies have improved continuously upon these limitations with advanced in situ and Earth observing equipment that permits relatively safe, accurate, and frequent measurement.

Advances in satellite-based observation systems have introduced an entirely new toolbox to researchers. Spectroscopic information of debris flows obtained from the SRTM (Stevens *et al.*, 2003) or the Air-borne Visible/Infrared Imaging Spectrometer (AVIRIS) (Crowley *et al.*, 2003) combined with digital elevation models (Glaze & Baloga 2003) are increasingly successful in predicting lava flow and lahar paths for risk zonation (Crowley *et al.*, 2003; Tralli *et al.*, 2005). Establishing the link between high ozone signals and ultraviolet (UV) radiation absorption made it possible to use satellite sensors for volcanic-plume monitoring (McGonigle 2005; Bluth *et al.*, 1993).

Both spectrally opaque and translucent clouds can be analysed using satellite acquired data (Webley & Mastin 2009; Webley *et al.*, 2009). To study opaque clouds, thermal infrared data ($\lambda = 10$–$12\,\mu$m) are used (Dean *et al.*, 2004), whereas translucent clouds are studied using the split-window-brightness temperature method (also known as the reverse absorption method) (Prata 1989; Pergola *et al.*, 2004). Once ash-clouds are detected, particle size, mass loadings, ash cloud volume, and even plume height estimations can be obtained (Webley & Mastin 2009; Holasek *et al.*, 1996). A number of satellite sensors are available for volcanic ash observation, including MODIS (Watson *et al.*, 2004) and ASTER (Pieri & Abrams 2004). In addition, techniques continue to be developed to improve the accuracy and sensitivity of sensors (Gangale *et al.*, 2009).

2.1.2 *Impacts of volcanic ash*

2.1.2.1 Societal impacts

Impacts of volcanic eruptions stretch far beyond geophysical damage. Evacuations, whether voluntary or mandatory, can have social, political, economic, emotional, and physical impacts on evacuees and surrounding residents. The response to eruption warnings is closely related to the perception of risk (Inhorn & Brown 2000). Middle and higher socioeconomic classes are able to call on family and friends to assist with moving belongings, while lower economic classes are at a distinct disadvantage. Day labourers often do not have access to telephones and may not learn about

an evacuation until the work day is over. Evacuation may be further complicated by cessation of public transportation and roads clogged with personal vehicles. Forced military evacuations often target the poor unfairly causing fear and resentment among this group. Wealthier families relocate with greater ease than their poorer counterparts, who lack automobile access and are forced to evacuate with less notice. Shelters are typically over-crowded with unsanitary communal facilities and few health-related resources. These conditions lead to nutritional deficiencies and weakened resistance to illness, resulting in the spread of infectious diseases such as chickenpox and measles (Inhorn & Brown 2000). Emotional conditions worsen when families are separated during the evacuation process. Increased stress and psychological disorders are common among resettled people. Evacuees, especially children, suffer increased health problems due to unfamiliar climates and disruption of normal nutrition (Whiteford & Tobin 2004). Strife between evacuees and locals is amplified when resettled people are seen as getting *unfair* amounts of aid. The resettled people may have sold their homes and land or have lost their jobs or agricultural assets. Most likely they have no source of income while they are displaced. In their newly settled areas, resettled people are excluded from politics and feel no sense of community, history, or future. Consequently, despite the health risks, many displaced people return to their own towns (Whiteford & Tobin 2004). All of these well being issues exacerbate direct respiratory health effects in individuals.

2.1.2.2 Human health impacts

Volcanic eruptions are associated typically with toxic emissions; pyroclastic flows (the mixture of rock fragments and superheated gases that can achieve speeds over 100 km/hour and temperatures over 300°C); the release of ash; volcanic gases containing a host of harmful compounds such as carbon dioxide, water vapour, sulphur dioxide, hydrogen chloride, hydrogen sulphide, hydrogen fluoride, among others; and polycyclic aromatic hydrocarbons produced whenever any complex organic material is burned by hot pyroclastic flows (Cullen *et al.*, 2002; Hansell *et al.*, 2006). Despite the fact that almost ten per cent of the global population of seven billion people live within the potential exposure range of an active volcano, information on the acute and chronic respiratory health effects of volcanic emissions is relatively sparse. A few studies have begun to document these impacts (Baxter *et al.*, 1981; Small & Naumann 2001; Horwell & Baxter 2006; Horwell 2007). The acute effects of volcanic ash falls and gases on respiratory conditions vary from undetected to well-defined (Hansell *et al.*, 2006; Horwell & Baxter 2006). During and shortly after eruptions with heavy ash fall, the transient, acute irritant effects of volcanic ash and gases on mucus membranes in the upper-respiratory tract and the exacerbation of chronic lung diseases have been documented (Nania & Bruya 1982; Baxter *et al.*, 1983). These effects have been found following eruptions in Cerro Negro, Nicaragua, in 1992 (Malilay *et al.*, 1997); Mt. Sakura-jima in Japan (Wakisaka *et al.*, 1988); and Mt. Tungurahua in Ecuador (Tobin & Whiteford 2001; Tobin & Whiteford 2002a,b).

Volcanic ash is capable of inducing acute respiratory problems in susceptible people, especially children and those with a history of respiratory illness such as asthma or bronchitis (Johnson *et al.*, 1982; Baxter *et al.*, 1983; Horwell & Baxter 2006). The precise mechanism causing these problems has not been well defined; however, its complexity has been outlined (Baxter *et al.*, 1983; Horwell & Baxter 2006). The irritant effects of volcanic ash, on human airways depend on the physical and chemical properties of the ash including particle size (Baxter *et al.*, 1983; Martin *et al.*, 1986), the concentration of respirable ash particles, mineralogical composition, and duration of exposure (Horwell & Baxter 2006). They also depend on how well one's respiratory tract is functioning, such as ventilation rate, nasal filtration efficiency, and the mucociliary clearance rate (Martin *et al.*, 1986). Several in-vitro and in-vivo experiments on different lung cells and animals suggest that inhaled volcanic ash is less toxic to the lung than other compounds like fine and coarse ambient particulate matter, quartz, or free crystalline silica.

Some observations support the notion that volcanic ash is not a potent stimulus to lung inflammation since it does not stimulate the release of IL-8, a quimiotactic factor for neutrophils, nor does it depress γ-interferon and TNF-α secretion from either human alveolar macrophages or normal human bronchial epithelial cells (Martin *et al.*, 1984; Becker *et al.*, 2005). However, it has been shown that physical immunologic barriers such as ciliary beating frequency and mucus lining can be

altered after a short exposure to volcanic ash (Schiff *et al.*, 1981). It has been reported that humoral immunologic parameters can also be affected by volcanic ash; for instance, workers exposed to volcanic ash had significantly lower C3 and C4 levels as well as a marked decrease in serum immunoglobulin-G (IgG) levels when compared to unexposed controls (Olenchock *et al.*, 1983). Immunological assays have shown that IgA, IgG, and albumin, airway proteins, play a protective role in mediating the effect of inhaled dust in human lungs (Martin *et al.*, 1986). Therefore, young and malnourished children with pre-existing low levels of immunoglobulin are at a higher risk for respiratory problems than healthy children. Moreover, some rodent models indicate that exposure to different particulate air pollutants, including volcanic ash, stimulates immuno-competent cells (e.g. monocytes) more strongly than alveolar macrophages to produce oxidative response (Becker *et al.*, 2002). Exposure to volcanic ash was also found to be related to an impairment of stimulated superoxide production while resting superoxide anion production is normal, indicating that volcanic ash might pose a risk for infection by compromising phagocyte antibacterial functions (Castranova *et al.*, 1982). Such mechanisms may explain why individuals with underlying lung impairment, including chronic inflammation, are more susceptible to the harmful effect of air contaminants than healthy individuals.

At high altitudes where oxygen demand is high, even a small increase in CO, SO_2, CO_2, and similar compounds that might affect haematocrit level may trigger a substantial increase in emergency room (ER) visits for asthma exacerbation, especially during fumarole activity. Very little is known about the effects of fresh fractured silica particles on developing lung tissue in young children. One may speculate that rough edges of silica particles due to micro-abrasion may damage the epithelial lining and promote pathogen colonization. Due to a child's high susceptibility for viral infections, exposure to silica particles may explain an increase in acute lower-respiratory infections of bacterial origin in young children.

2.1.3 *Monitoring volcanoes using air-borne and satellite sensors*

Distance imaging and chemical monitoring provide quick, accurate, and timely methods for monitoring exposure to health hazard outcomes, and improving communication of health risks to the public. Such data and imagery also can provide advanced situational information for volcanoes that are under-monitored. The ability to forecast volcanic activity and to mitigate hazard exposure depends upon knowledge of previous activity at a site and at similar sites worldwide. Sensing technology has been used increasingly by geographers and public health professionals to predict, monitor, and quantify the impacts of natural disasters.

2.1.3.1 Estimating hazardous human health exposure from ash & sulphur dioxide

In a four-year longitudinal study of children aged six to thirty-six months in Quito, Ecuador, 4450 cases of acute upper-respiratory infection and 518 physician-diagnosed cases of pneumonia were observed. Among these six (1.2 per cent) required hospitalization (F. Sempertegui, personal communication). Among all the acute upper-respiratory infection episodes, 102 (2.3 per cent) progressed into acute lower-respiratory infection. Therefore, it is anticipated that for every case of hospitalization due to pneumonia, there are approximately eighty-six cases of mild pneumonia. If true, this observation testifies to the severity of respiratory conditions. In fact, the observed effect was very similar with a reported increase in acute upper-respiratory infection (2.6 times), acute lower-respiratory infection (2.5 times), and asthma (2.1 times), after eruptions of Tungurahua in 1999 (ReliefWeb 2010).

Quito was affected by several episodes of ash emission between October and December, 1999; April, 2000; and July, 2000. Figure 2 is a composite of ash advisories available from the volcano ash advisory archive (VAAA) (NOAA 2012). It is possible that estimates of the ER rates before and after the eruptions in April may have been elevated by these prior eruptions, causing the effects to be underestimated. It is also plausible that the effects of volcanic activity were exacerbated due to little or no rain, which can clean the air between eruptions. Additional studies are needed to better quantify the effect of ash fallouts and related pollutants.

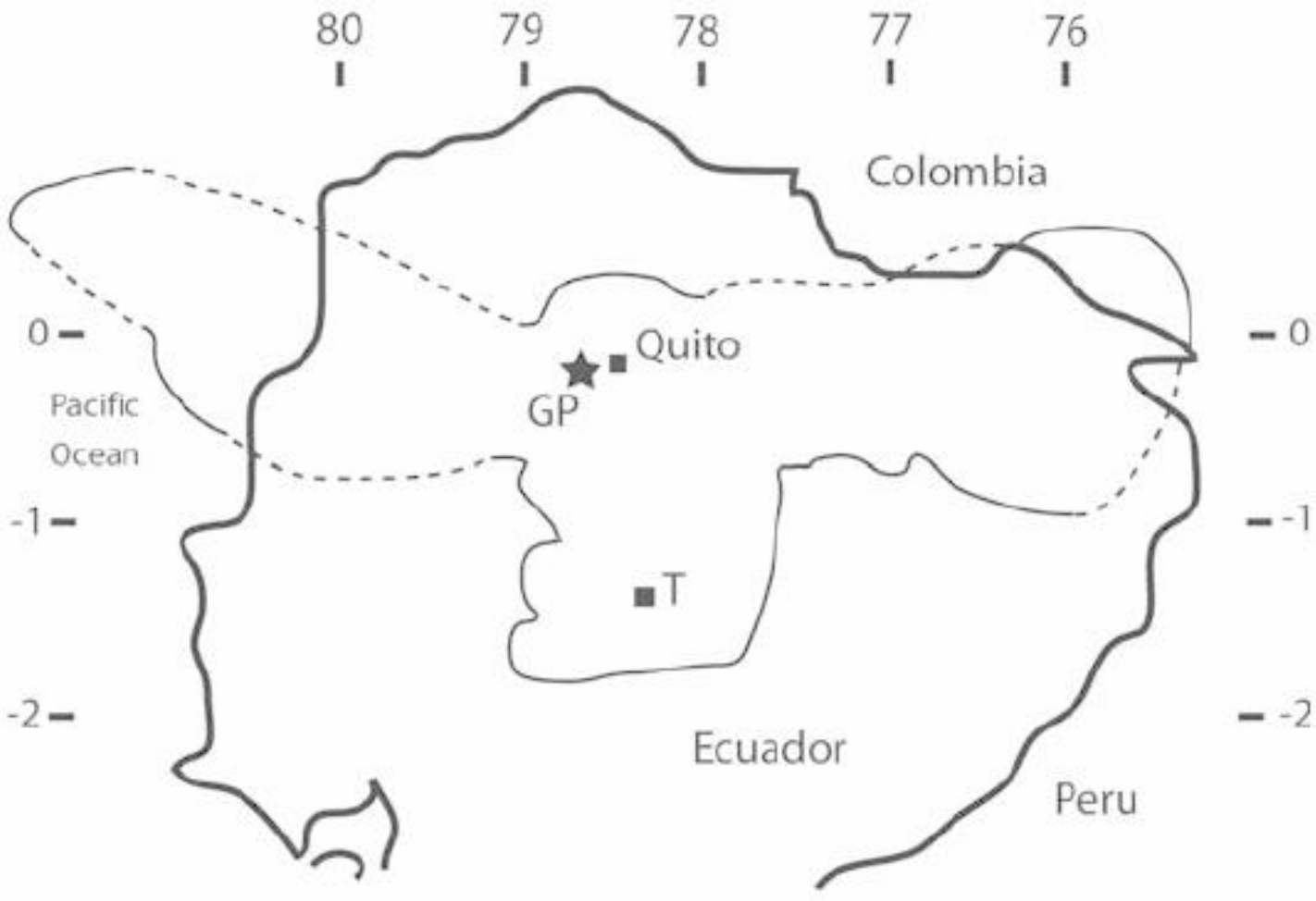

Figure 2. Extent of Guagua Pichincha ash deposition (thin line) compiled from NOAA ash advisories October 1999–July 2000 (Courtesy Geophysical Institute of Ecuador).

2.1.3.2 Significance

Recent research has emphasized the spectrum of health problems associated with direct and indirect effects of volcanic ash and gasses, including displacement, disruptions in infrastructure (Tobin *et al.*, 2002; Whiteford *et al.*, 2002), and soil, air, and water contamination (Delmelle *et al.*, 2001; Loehr *et al.*, 2005). Studies stress the need for implementing efficient surveillance systems to monitor the health effects associated with various environmental and socioeconomic factors, especially in the most vulnerable populations (Malilay *et al.*, 1997). In the absence of such surveillance systems, respiratory health outcomes that often reflect the most severe conditions requiring ER visits and hospitalization cannot be characterized. The results of these efforts provide important information for environmental public-health policy and a better understanding of the short-term health effects of environmental exposure to volcanic ashes. Observed effects in Quito's children most likely reflect an increase in severity of acute respiratory infections and exacerbation of pre-existing asthma-related conditions. Because no surveillance systems exist, health outcomes from urgent ER visits and hospitalizations were used, reflecting the most severe conditions. It is expected that young children with pneumonia and asthma-related conditions are more likely to be hospitalized than older children or those with acute upper-respiratory infection.

2.1.3.3 Limitations

Observed increases in respiratory infections in April, 2000 were most likely triggered by aerosols and ash falls produced by Pichincha eruptions. However, it is important to consider that the main limitation in this analysis; that is, the absence of direct measures of exposure, must be considered. It is also plausible that ash particles deposited during 1999 ash falls could have been re-suspended in the air without elevated volcanic activity. Unfortunately, systematic monitoring of air quality in Quito for critical air pollution was initiated after 2000, so only indirect proxies such as satellite imagery for ash emissions and daily records on seismic activity of Pichincha can be used to establish the timing of high exposure (NOAA 2012).

In this four-year longitudinal study, the correlation between ER visits and timing of high exposure was examined. However, limitations to this approach exist. First, health effects of volcanic aerosols and ambient traffic-related pollution are difficult to separate. Secondly, volcanic activity is a continuous process in which the delayed health effects of one event may overlap with others. Thirdly, a seasonal elevation in incidence of respiratory infections and pneumonia could coincide

with the eruption and therefore bias the results. Finally, temporal variations in ER visits could be prompted by a number of social factors (e.g. weekends, holidays, strikes) as well as by changes in perception associated with volcano alerts. Although potential confounding factors from air pollution, continuous volcanic activity, seasonal infection rates, and reporting bias could have affected this study, their role most likely is not substantial.

2.1.4 *Need for air-borne and satellite sensors: A case for Quito and Guagua Pichincha*

Volcanic ashes worsened the already poor air quality in Quito (Estrella *et al.*, 2005). Typically, the chemical compositions of these ashes have been distinguished from by-products of anthropogenic air pollutants in urban settings. However, one of the most predominant components of particulate matter (PM_{10}), are found in automobile emissions as well as volcanic ash. In fact, a few samples of PM_{10} concentrations collected in urban Quito in the late fall of 1999 demonstrated extremely high levels in both the northern and southern parts of the city. Data reveal that during the 1999 Pichincha eruption, PM_{10} increased progressively from 58 $\mu g/m^3$ on September 30, to 407 $\mu g/m^3$ on October 6–7, to 1487 $\mu g/m^3$ on November 26, 1999. All of these exceeded the allowed level by eight to twenty-eight times (OPS 2005). Unfortunately, specific information on ash composition, transport, and deposition is limited, especially for eruptions prior to 2000 (Diaz *et al.*, 2006). Reported ash composition had substantial respirable material and elevated cristobalite content (Baxter *et al.*, 1999; Baxter 2003; Garcia-Aristizabal *et al.*, 2007). For three consecutive eruptions in November 1999, July 2000, and February 2002 percentages of PM_{10} in the Guagua Pichincha ash ranged from 7.9 to 13.6; not dissimilar to the Mount St. Helens 1980 ash composition (Baxter *et al.*, 1983, 2003). Data from the 2001 eruptions of Tungurahua and El Reventador volcanoes in Ecuador indicated that the ash layer in the Quito area was mainly composed of medium-to-fine ash particles with about twenty per cent free crystals (Le Pennec *et al.*, 2006). That study indicated that the ash was re-suspended during the windy afternoons and caused ocular irritation, respiratory troubles, and other health problems.

Although higher levels of respiratory disease in Quito's children after volcanic activity have been documented, the studies acknowledge that the absence of direct measures of exposure was a considerable limitation. The authors suggest that ash composition and deposition can be monitored using air-borne and satellite sensors, thereby enabling detailed tracking and exposure assessments of events that may be detrimental to human health.

2.1.5 *A novel methodology to estimate hazardous human health exposure*

For epidemiology, use of imagery and data collected by remote systems is a relatively new and emerging field with most studies surfacing in the past two decades. Several techniques based on remote surveillance have been developed to assess the ability of detectors to monitor volcanic plume composition (Prata 1989; Yu, *et al.*, 2002; Pieri & Abrams 2004; Watson *et al.*, 2004). It is essential to investigate whether acquired data can serve as a proxy for ground-based air-quality assessment (Andronico *et al.*, 2009; Carter & Ramsey 2009; Tupper & Wunderman 2009; Lyons *et al.*, 2010). Reliable methods and algorithms are needed for linking remotely sensed data with outcomes observed through public health surveillance.

2.1.6 *Detecting and measuring ash dispersal using existing sensor methodologies*

Volcanoes emit a mixture of acid gases, water, and solid-phase ash particles. The fates of these species are typically complex, involving physical (i.e. aggregation, absorption, and fallout) and chemical processes (i.e. the oxidation of sulphur dioxide [SO_2] to H_2SO_4). They pose a hazard to air traffic safety as well as ground conditions in the local environment; and, in sufficient volume, the global climate system. In almost every case they pose hazardous environments for human health. A variety of techniques has arisen to monitor each of these species using satellite-based instruments (Prata 1989; Krueger *et al.*, 1995; Seftor *et al.*, 1997; Krotkov *et al.*, 1999; Schneider *et al.*, 1999; Wright *et al.*, 2002; Ellrod 2003; Ellrod *et al.*, 2003; Tupper *et al.*, 2004; Chrysoulakis *et al.*, 2007; Filizzola *et al.*, 2007). However, measurements are still commonly taken on the ground (Prata &

Table 2. Sensors and associated bandwidths.

Sensor	Bandwidths (μm)	Target species	Spatial resolution (km)	Repeat times (days)
OMI	0.3–0.34	SO_2, aerosols	~14	1–2
GOES	11–12	ash, ice	>14	~0.01
MODIS	7.3, 8.6, 11–12	SO_2, ash, ice	1	0.5
ASTER	8.6, 11–12	SO_2, ash, ice	0.09	16

Bernardo 2009), such as on the shield volcanoes of Hawaii (Dockery 2006; Sutton *et al.*, 2006) where accessibility is not a major obstacle.

Today, algorithms utilize a wide range of wavelengths to detect, track, and model volcanic plume components, including silicate ash and sulphur dioxide (SO_2) (Watson *et al.*, 2004). Each technique is dependent on a series of sensor-based observational issues relating to temporal, spatial, and spectral resolution (Pieri & Abrams 2004). Satellite data can quantify the horizontal spreading velocity of a volcanic cloud, allowing for prediction of future movement (Oppenheimer 1998; Tralli *et al.*, 2005). MODIS AVHRR, the Total Ozone Mapping Spectrometer (TOMS), and GOES sensors supply data for the majority of studies attempting to identify and quantify volcanic-ash- and gas-containing clouds (Prata 1989; Wen & Rose 1994; Krueger, Walter *et al.*, 1995; Seftor *et al.*, 1997; Krotkov *et al.*, 1999; Schneider *et al.*, 1999; Wright *et al.*, 2002; Ellrod 2003; Ellrod *et al.*, 2003; Tupper *et al.*, 2004; Watson *et al.*, 2004; Gu *et al.*, 2005; Chrysoulakis *et al.*, 2007; Filizzola *et al.*, 2007; Novak *et al.*, 2008). Sensors on both geostationary and polar-orbiting satellites are acquiring data. Geostationary satellites about 36,000 km above Earth orbit at the same velocity as Earth's rotation, maintaining a constant observation window over a particular region of the globe. Polar-orbiting satellites collect data at 700 km to collect nearly global coverage on a predictable revisit cycle. A trade-off exists between these two orbit types: geostationary satellites re-acquire images every few minutes but have a spatial resolution of several kilometres, whereas polar-orbiting satellites make no more than one or two measurements of the same location per day with resolutions at the meter scale. Each sensor has a different suite of attributes, making it useful for particular phenomena. Table 2 provides details on commonly used sensors and Figure 3 shows the footprints.

2.1.7 *Remote data acquisition*

Periods of heightened volcanic activity can be identified by examining imagery from the Smithsonian Institute global volcanism program archives and the MODVOC global-hotspot archive (MODVOC 2009; Smithsonian 2009). For each study period, instances when substantial ash was dispersed are identified and EO data for these instances are collected. Satellite imagery can be retrieved through file transfer protocol (FTP) servers for GOES-8 East (hereinafter GOES-8), MODIS, ASTER, and OMI archives. GOES-8 data are archived at the University of Wisconsin-Madison Space Science and Engineering Center (SSEC). Data are delivered in the man computer interactive data access system (McIDAS) format and converted into GeoTiff format using image processing software (SSEC 2005). MODIS sensor data are distributed through NASA's Level 1 atmosphere archive distribution system (LAADS) (NASA 2009). ASTER data are available from the NASA data gateway (NASA 2009). After data are acquired, they are analysed using digital image-processing software.

2.1.8 *Ash detection*

Ash presence can be estimated using GOES-8, MODIS and ASTER data. Prata developed the brightness temperature difference (BTD) technique using two spectral channels at 10.3–11.3 μm and 11.5–12.5 μm, which are atmospheric spectral windows where the effects of other atmospheric gases are minimized (Prata 1989). These channels are used to discriminate volcanic from meteorological clouds containing ice, water vapour, and water droplets. The BTD method involves

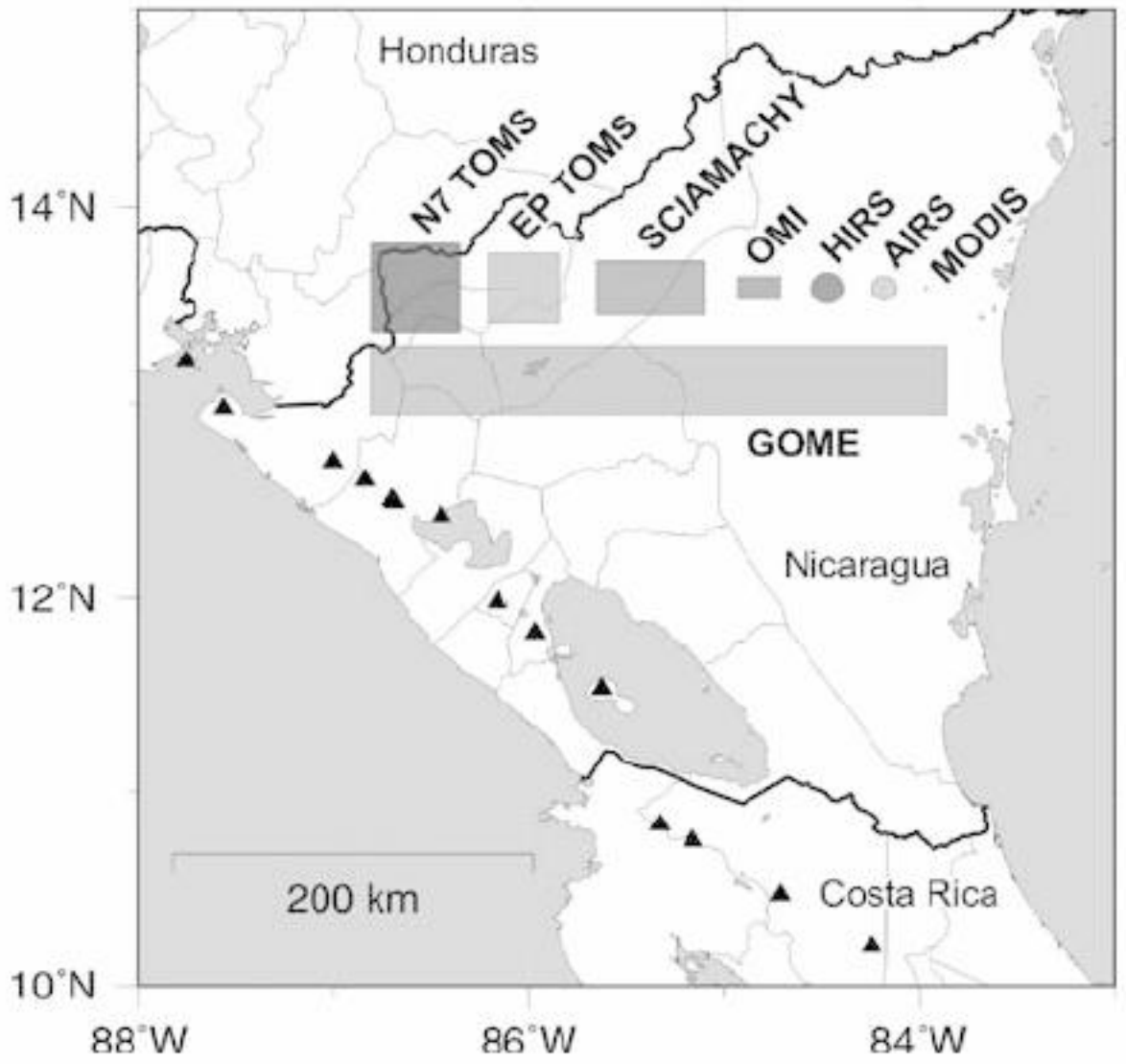

Figure 3. The nadir footprint of SO_2 sensors, excluding ASTER, whose footprint would not register at this scale. GOES has a slightly larger footprint than MODIS (Courtesy Carn, University of Maryland, Baltimore County). (see colour plate 20)

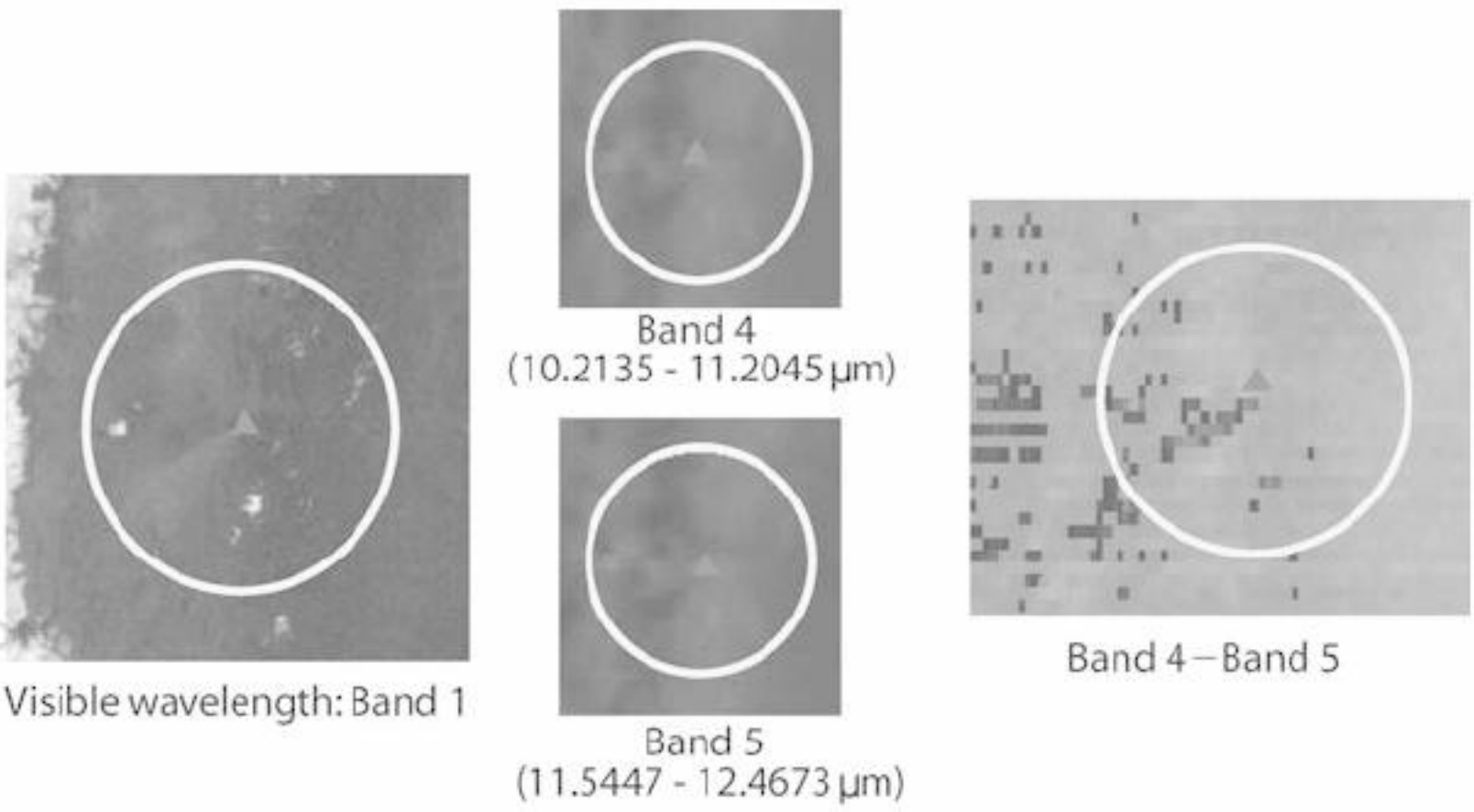

Figure 4. GOES-8 imagery, Tungurahua Volcano, Ecuador 14:45 UTC 16 September 2001. (see colour plate 21)

subtracting GOES channel-5 image data from channel-4 data (T4–T5). T4 greater than T5 indicates the presence of hydro meteoric clouds, whereas T4 less than T5 indicates the presence of silicate-rich ash with stronger negative numbers representing greater ash richness (Wen & Rose 1994; Watson *et al.*, 2004). The BTD method acquires data both day and night because the sensors operate in the thermal infrared region. The same strategy can be used for GOES-8 channels 4 (10.2135–11.2045 μm) and 5 (11.5447–12.4673 μm) (Figure 4) and the MODIS channels 31 (10.780–11.280 μm) and 32 (11.770–12.270 μm) (Figure 5).

Both GOES and MODIS data are used because they offer different temporal and spatial resolutions. The GOES platform is advantageous when monitoring smaller eruptions with a lifespan of no

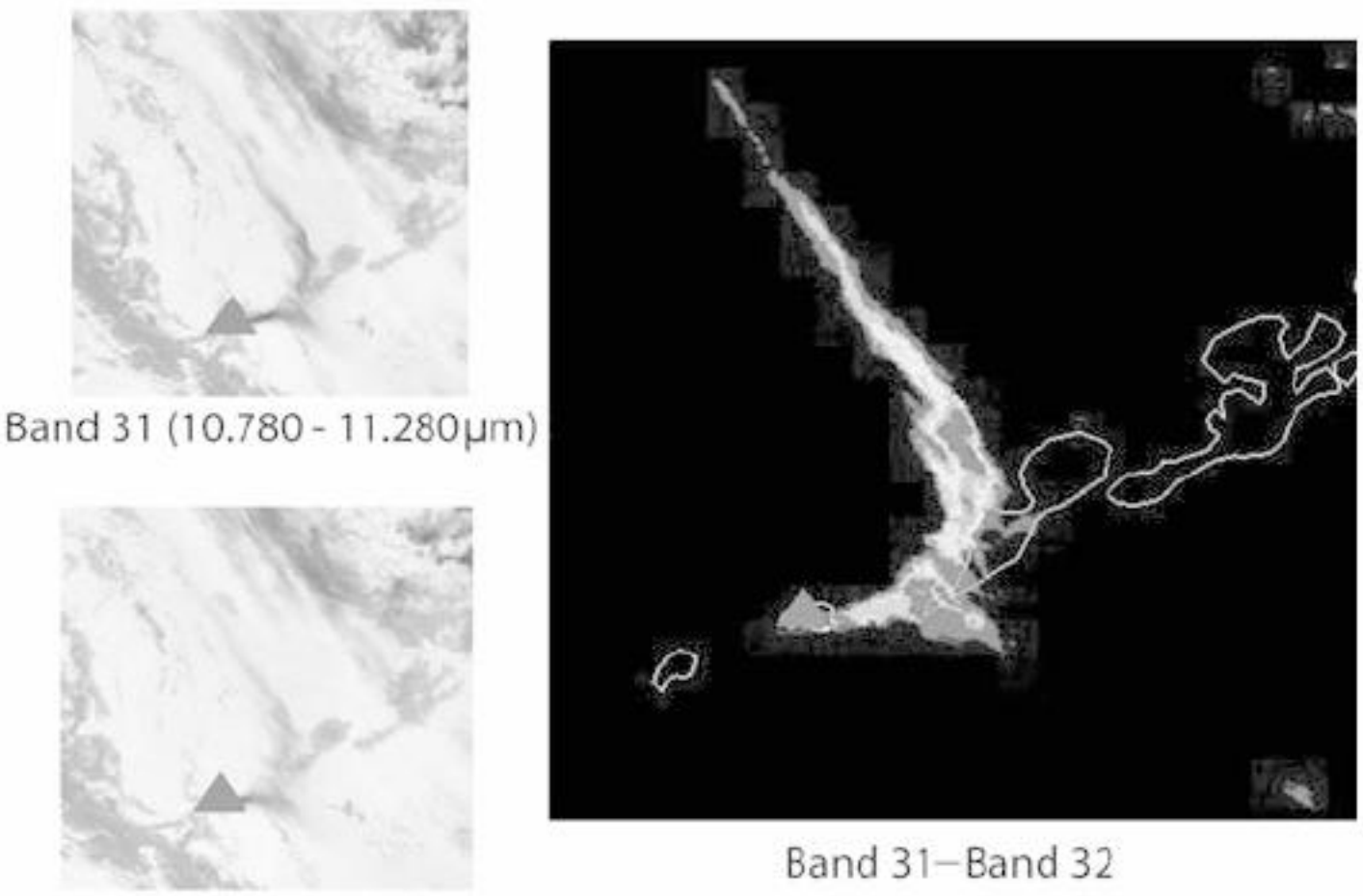

Figure 5. MODIS Imagery, Mount Cleveland Volcano, Alaska 23:10 UTC 19 February 2001. (see colour plate 22)

longer than a few hours, because the sensor updates every thirty minutes and has a four kilometre spatial resolution. Currently, MODIS imagery for many locations on the Earth is acquired once a day, but has a one kilometre spatial resolution. Whereas the temporal resolution for the MODIS instrument is less frequent, its spatial resolution is finer. By integrating both data types into the analysis, volcanic ash-plume trajectories are identified, tracked, and illustrated using a GIS. Volcanic ash plumes can be confirmed using advisories from NOAA's Volcanic Ash Advisory Centre. These advisories are disseminated as both text and graphic messages and are updated on a daily basis. Findings can be confirmed by using a dispersion model.

2.1.9 *Dispersion model*

Although remote sensing data are a powerful tool for observing and analysing volcanic-plume dispersal (including plume footprint, horizontal size and location), satellite data cannot forecast ash trajectories. Volcanic ash transport- and dispersion-models are used for predicting ash trajectories. Dispersion models can obtain data relating to ash trajectory; ash transport, concentration, size distribution, vertical dimensions, and age of cloud (Searcy *et al.*, 1998; Draxler & Hess Pudykiewicz 1989). Dispersion models and sensor data are used for reciprocal validation by comparing observed data with modelled data. Modelling the spatial extent of ash clouds, including details such as particle size and future trajectories, is particularly informative in complimenting and verifying sensor data, especially when imagery is obscured by meteorological conditions (e.g. clouds) (Peterson *et al.*, 2009).

Data can be used to create rolling thirty minute GOES and daily MODIS volcanic plume maps for air-borne ash particles within a GIS. Volcanic plumes can be compared with ground-based air-quality monitoring data from the same location and dispersion-model results from the same time period. By having frequent ground-data measurements and dispersion model results to compare with sensor data from the same time period, one can determine whether there is a correlation between what is observed in the air and what has fallen to the ground. This helps to establish whether sensor data can serve as a relative proxy for ground-based measurements. It is probable that higher amounts of ash particles in the air correspond with higher amounts on the ground, although the magnitude of the relation is unknown. Determining what proportion of ash does end up on the ground warrants further investigation. Some studies have explored this issue (Andronico

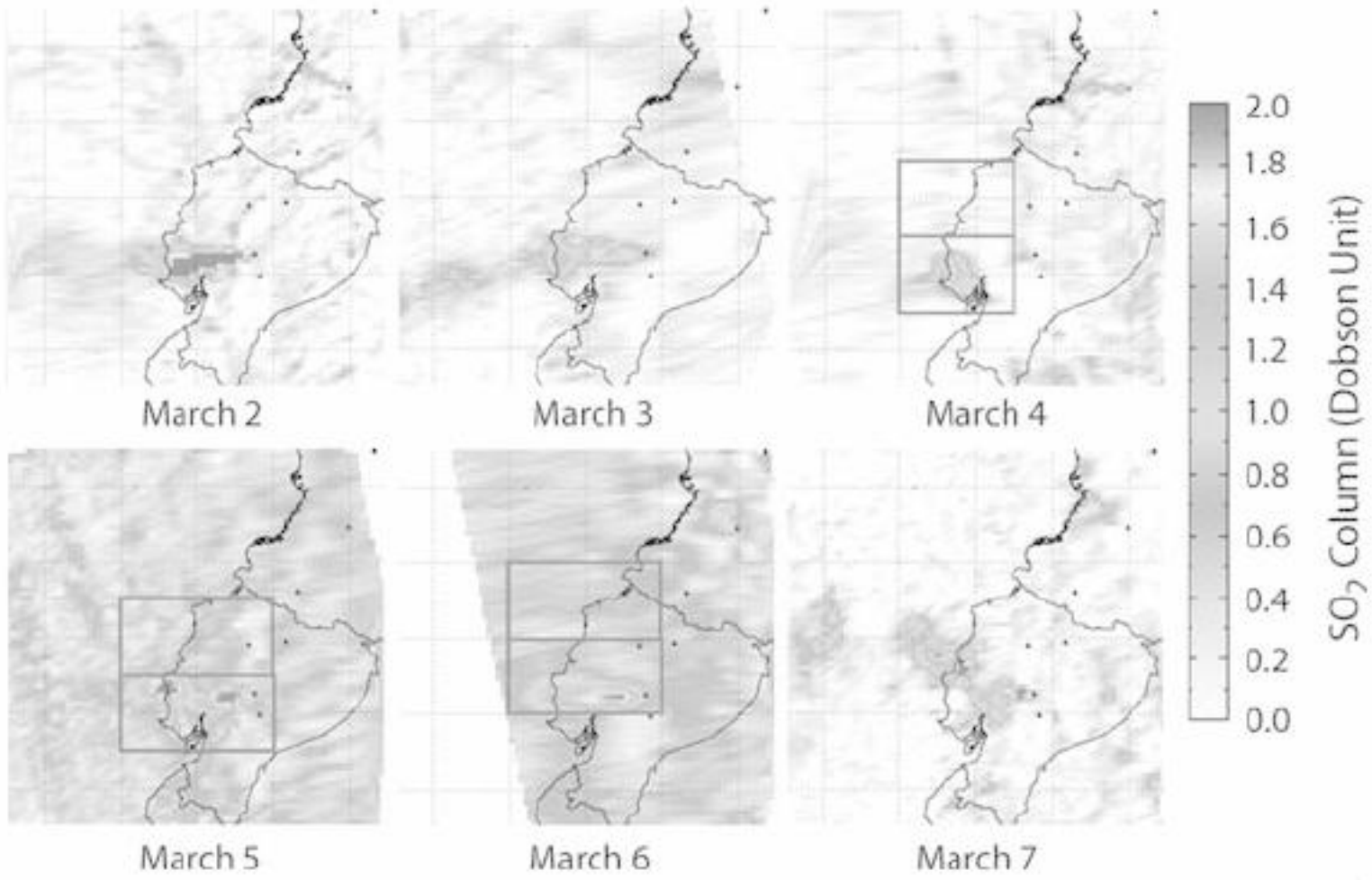

Figure 6. OMI SO_2 imagery for Tungurahua volcano, Ecuador, March 2007. (see colour plate 23)

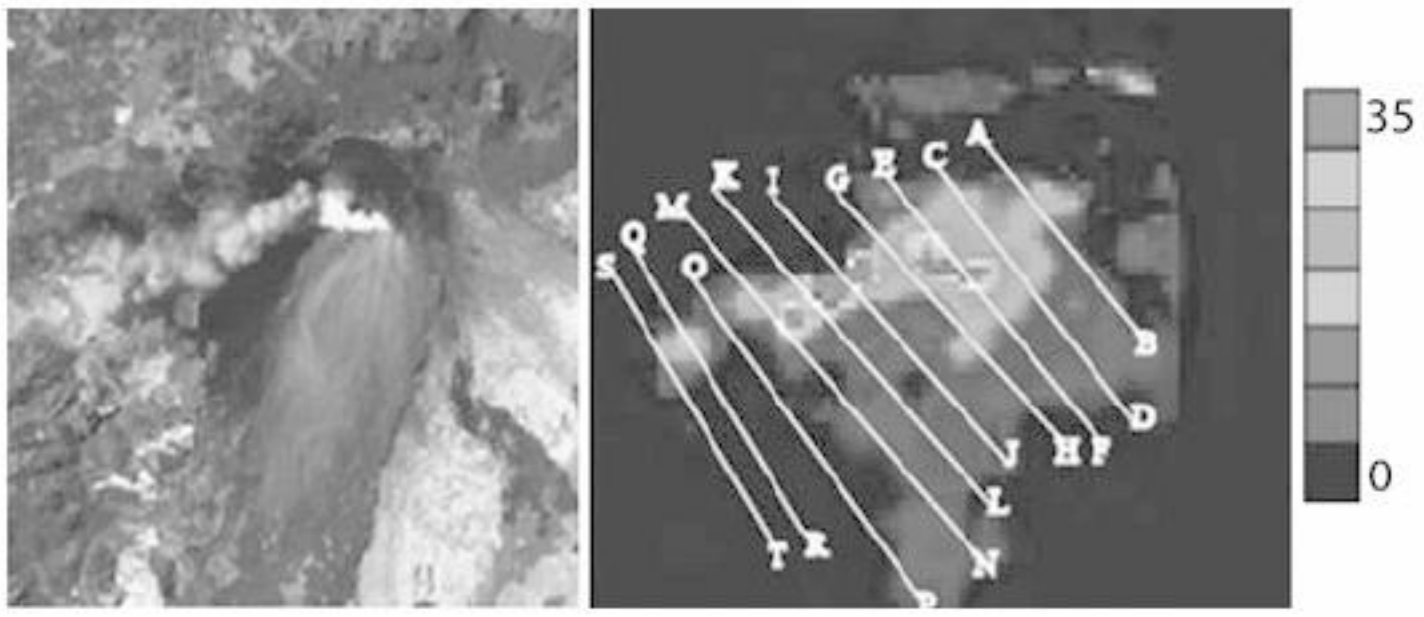

Figure 7. Emissions from Pacaya volcano, Guatemala are similar to emissions from Tungurahua (Courtesy Watson, University of Bristol). (see colour plate 24)

et al., 2009; Carter & Ramsey 2009; Tupper & Wunderman 2009; Lyons *et al.*, 2010) but none has undertaken these efforts with explicit focus on public health consequences.

2.1.10 *SO_2 detection*

Multiple sensors are used for SO_2 data acquisition to optimize the temporal and spatial resolution. For SO_2 detection, data are acquired by the Ozone Monitoring Instrument (OMI), MODIS, and ASTER. Having ninety metre pixels, ASTER can provide the finest detail. Advanced SO_2 detection uses a tool known as interface description language (IDL) developed at the Jet Propulsion Laboratory (JPL).

OMI imagery was used to estimate SO_2 dispersal from the Tungurahua volcano. Figure 6 shows SO_2 emissions from this volcano moving westward. Dynamic series of these maps can provide a visual-analytical method for viewing plume-dispersion, such as those shown in Figure 7 (Castronova *et al.*, 2009).

Sulphur dioxide data also are acquired by the OMI on board NASA's Earth Observing System (EOS) Aura Satellite. The OMI sulphur dioxide group (SDG) produces daily composited SO_2 images for select areas. Archived images are available from May 2006 and are available within two to three days after each acquisition. Archived data dating back to 2004 are also available from the SDG website (OMISDG 2007).

The MODIS sensor on board EOS Terra and Aqua platforms use channels 28 (7.2–7.5 μm) and 29 (8.400–8.700 μm) to measure SO_2. Each band uses a different measurement method (Realmuto *et al.*, 1994; Realmuto *et al.*, 1997; Realmuto 2000; Watson *et al.*, 2004). Channel-28 measures differences in radiance between SO_2-filled atmosphere and SO_2 free atmosphere. Channel-29 identifies SO_2 by measuring the difference in radiance between clear ground measurements and ground measurements with SO_2 cloud cover (Novak *et al.*, 2008).

Channels-10 to -12 of ASTER are sensitive to SO_2 and capable of detecting small-scale degassing (Watson *et al.*, 2004). Because of its high spatial resolution, ASTER is the only instrument in orbit that detects plumes less than 1.5 km wide (Pieri & Abrams 2004).

2.1.11 *Developing volcanic ash and SO_2-exposure maps*

Remotely collected SO_2 data can be fused or assimilated with geospatial data and relevant dispersion models to simulate exposure to SO_2. Simulations can be created every half hour from the GOES sensor and augmented with daily data from MODIS. They can also be overlaid with demographic data to assess how many people might have been affected. Dynamic maps of these time-stamped outputs can be created to provide an initial visual assessment for how well areas of elevated exposure correspond with health surveillance data obtained from ER records (Castronovo *et al.*, 2009).

2.1.12 *Linking sensor data with health outcome data*

Working with data from a variety of sources requires a sound research hypothesis, developing a conceptual framework, selecting potential candidates for measures of exposure, and outlining properties of health outcomes clearly (Jagai *et al.*, 2007). Also, there needs to be compatibility among health outcome measures and exposure measures derived from sensor data. This is achieved analytically by considering normalization schemes, inclusion of a proper indicator in the modelled procedure, stratification, and other techniques. Though it is rarely possible, there should be complete uninterrupted temporal and spatial overlap in health and exposure data. Temporal completeness expands the array of applicable analytical techniques because many statistical methods for time-series data have serious limitations if there are gaps in the series. Poor overlap may lead to a substantial reduction in statistical power to detect an effect, since the sample size available for the analysis will be smaller in a joint time series. Typically, time-referenced health outcomes are recorded as daily, weekly, monthly, quarterly, or annual counts of health-related events. The temporal period of availability of satellite-acquired data depends on their orbital designs and parameters (e.g. every thirty minutes or daily; sun-synchronous or geostationary). Therefore, to properly link sensor data with health outcome data, it is important to ensure convertibility of time units and perform a basic time unit alignment. Finally, the spatial alignment has to be carefully addressed. Health outcomes are typically derived from specific geographic areas and may differ by specificity, sensitivity, and population coverage. Moreover, these data must have geographic coordinates to ensure proper selection of the target or catchments area for abstracting sensor data.

Detection of a meaningful increase in number of health-related events by using statistical scanning in a given location should then be linked to an elevated exposure, if a causal relationship exists. The ability to detect such a link depends on characteristics of geographical area, spatial adjacency, and a spatial distribution of event occurrences. In practice, rarely do uniform or normal distributions correctly reflect population density. Similarly, a simple regular shape like a concentric circle (a primary choice in many spatial-clustering algorithms) rarely represents a geographic area of interest in a proper manner. For example, a geographical area representing communities effected directly by a chemical plume is likely to resemble a funnel with respect to factors contributing to contamination; that is, wind speed, wind direction, diffusion, and photochemical reactions (Naumova *et al.*, 1997). Similarly, a pattern of communities effected by a hurricane is likely to resemble a storm trajectory (Chui *et al.*, 2006). In some situations, assumptions related to cluster properties are reasonable as, for example, when a point-source exposure is well defined; when everyone is affected in a similar way; or, when the population within a study area is relatively stable. Examples include diseases that can be effectively scanned for clustering are exacerbations of chronic disorders (e.g. asthma) or injuries. But even in well-defined cases, spatial methods have to take into consideration

Figure 8. Aerial photograph of Quito, Ecuador. Pichincha volcano lies west of Quito in the central background. A narrow zone of haze stretches from left to right across the city (Geophysical Institute of Ecuador). (see colour plate 25)

complex non-Euclidean topologies of an outbreak signature. Such topologies are very likely to be observed in spatio-temporal patterns of diseases when transmission is amplified by re-suspended ash deposits, or distorted by multiple population relocations, when tracking of exposure location is unwarranted. Complex spatial patterns of georeferenced exposure-transmission-detection pathways have to be better understood. An example illustrates the potential for using remote sensing data to better understand health effects of volcanic eruptions.

2.2 *Potential applications: Guagua Pichincha*

2.2.1 *Guagua Pichincha in April 2000*

Quito, capital of Ecuador, is located 2800 m above sea level and is surrounded by four active volcanoes: Guagua Pichincha, Cotopaxi, Antisana and Tungurahua (de la Cadena 2006). The strato-volcano Guagua Pichincha is located thirteen kilometres west of Quito and became active in 1998 with emissions of vapour, ashes, and fumes after 340 years of dormancy. In spring, 2000, volcanic ash containing silica, sulphurs and particulate matter were again reported, and yellow alerts were issued for Quito. Nestled in a long, narrow valley between the base of the mountain range to the west and the precipitous canyon of the Machángara River to the east, Quito possesses an unmatched setting: a dangerous chamber created by nature and enhanced by humans (Figure 8).

Over the last two decades, rapid urbanization and sprawl have resulted in hazardously high levels of air pollutants (Jurado & Southgate 2001; Cifuentes *et al.*, 2005). The unique topographical location of Quito and the pattern of prevailing wind, traps stagnant, contaminated air. At that altitude, where the demand for oxygen is high, even a small increase in air pollution may trigger a substantial increase in ER visits for respiratory conditions.

Studies indicate strong effects of air pollution on respiratory health in Quito children (Estrella *et al.*, 2005). In this study, elevated rates of ER visits for acute and lower-respiratory infections and asthma-related conditions were documented in the younger children of Quito in association with the volcanic activity of Guagua Pichincha in April 2000. Before, during, and after ash falls in Quito, fluctuations in paediatric ER visits represented the negative impact volcanic activity has on human health. In all 5169 ER records were abstracted for patients treated between 1 and 10 December 2000, and were subsequently classified into three non-overlapping categories: acute upper-respiratory infection (2392); acute lower-respiratory infection (2319); and, asthma-related hospitalizations (431). Volcanic activity was documented from a variety of governmental and media sources and was compared with a time series of daily counts of respiratory infections in the studied population. Applying a Poisson regression model to examine the relations between the timing of the eruption and ER visits, it was found that increases in daily cases relative to the annual average were significant for all ER visits and for each disease group.

After geocoding 4786 records (93.4 per cent), categorizing them into the city of Quito, the city suburbs, or the area outside the city's metropolitan boundaries, the spatial distribution of cases and changes during eruption was examined. The daily means of ER visits in the youngest children were two times higher during the four periods of volcanic activity than pre- and post-eruption, after adjusting for baseline differences. In addition to the level of six to eight cases per day typically observed in girls and boys treated in the ER, respectively, a 2.25-fold increase in daily ER visits was observed in all parts of the city. Overall, during twenty-eight days of volcanic activity and ash releases, on average, 138 girls (CI-95 per cent = 104, 207) and 206 boys (CI-95 per cent = 137, 252) were treated in ER in contrast to the typically observed level of 6.17 and 8.18 cases per day in girls and boys, respectively. Not only did this study demonstrate an increase in ER visits to the Baca Ortiz Hospital after volcanic activity, it emphasized the usefulness of hospital-based surveillance for monitoring the health effects associated with volcanic activity.

Rapid deployments of disease surveillance systems that incorporate novel data collection technologies demonstrate the potential for increasing information exchange. The list of prospective candidates for disease monitoring is growing and includes not only traditional hospitalization records and laboratory-confirmed tests, but also the data streams driven by new information technologies. Personal digital assistant (PDA)-based records collected directly from outbreak investigations, hits and queries targeting specific websites, and searches for media and news are examples of these new data streams. These novel data sources are the primary candidates for linkages with sensor data.

2.2.2 *Eyjafjallajökull volcano, Iceland April 2010*

A volcanic eruption of Eyjafjallajökull in Iceland reminded everyone of the need to better understand risks associated with volcanic activity (Gudmundsson 2011). Eleven centuries of settlement in Iceland were marked by an explosive eruption of Eyjafjallajökull that started on 14 April 2010. Eyjafjallajökull is a glacier volcano that rises to 1666 m above sea level on the southern shore of Iceland about 150 km from Reykjavik. The explosive interaction of magma at over 1000°C with ice and water generated large volumes of finely comminuted ash. Erupting from beneath the ice cap, the plume of ash and vapor reached heights of almost ten kilometers on the first day. Alerts were issued to people with respiratory illnesses. The next three days of sustained tephra production resulted in ash dispersal in the southeast area populated by several hundred people. Fortunately, the Reykjavík metropolitan area of some 300,000 inhabitants was located just outside the margins of the active volcanic zone. Eruptions halted by the end of May 2010. Since then, on windy days, released ash is re-suspended into the air and, as a result, particulate matter concentration levels have been unusually high in southern and southwestern Iceland, including Reykjavik. Ash-fall deposits can remain in the environment, sometimes for decades and can be redistributed by wind and by human activities.

The up-to-date studies suggest that the acute and chronic health effects of volcanic ash depend on: a) particle size and its respirable fraction; b) mineralogical composition, especially the crystalline silica content; and, c) physico-chemical properties of the surfaces of ash particles. The effects vary between volcanoes and even between eruptions, making the comparison of specific effects difficult. The fresh ash from Eyjafjallajökull was very well characterized: it contained twenty-five per-cent respirable particles (i.e. less than 10 μm). The main constituents were sixty per cent SiO_2, sixteen per cent AlO_3 and ten per cent FeO with the negligible content of crystalline silica content. The plume was carefully monitored via remote sensing. Such large-scale events offer opportunities for detailed investigation of the long-term effects of ash deposition on human and animal health and the health of ecosystems.

3 DESERT DUST STORMS AND HEALTH

Deserts account for approximately thirty-three per cent of Earth's terrestrial environments. The two largest deserts are the cold deserts of the Arctic and Antarctica, with each covering approximately 13×10^6 km^2. Although they are the largest, they are in general covered by snow and ice for most

of the year and their surface soils contribute little to Earth's annual atmospheric desert-dust load. Current global estimates for the quantity of desert dust moving some distance in Earth's atmosphere ranges between one-half to five billion metric tons per year, and some believe that the upper limit is an underestimate (Goudie & Middleton 2001).

Dust particles are loaded into the atmosphere by storm fronts that generate high winds across the surface. These winds cause saltation, which is the movement and bounce of soil particles along the surface (Grini & Zender 2004). Saltation in conjunction with sandblasting of downwind surfaces by particles results in dust-cloud formation characterized by fine grain sizes, typically less than 10 μm (Cahill *et al.*, 1998; Gillette *et al.*, 2004; Grini & Zender 2004). These less than one micrometre, ultrafine particles are capable of long-range global dispersion, although grain sizes as large as 75 μm have been identified at distances up to 10,000 km from their source (Betzer 1988). Atmospheric particulate load for a 1995 African dust storm that impacted air quality in Tampa Bay, Florida more than 6500 km from the source, was over ten times that observed during normal atmospheric conditions; and, over ninety-nine per cent of the particles were less than one micrometre in diameter. This small size is capable of penetrating into the deep lung environment (Griffin 2007).

Primary sources of dust entrained into Earth's atmospheric boundary layer are the Saharan and Sahelian zone of North Africa. These regions are currently believed to contribute approximately fifty to seventy-five per cent of the total desert dust budget (Moulin *et al.*, 1997; Goudie & Middleton 2001; Prospero & Lamb 2003). The second greatest source is the desert region of Asia that includes the Gobi, Takla Makan and Badain Jaran deserts. Dust storms also are common from other world regions. The major ones include North America's Great Basin and Sonoran deserts, Mexico's Chihuahuan desert, South America's Patagonia and Atacama deserts, South Africa's Etosha and Mkgadikgadi deserts, Australia's Sandy and Great Victorian deserts, and the Syrian and Arabian desert regions of the Middle East. Due to periodic short-term fluxes in climate that influence regional rates of precipitation and anthropogenic influences (i.e. deforestation), these smaller desert regions can contribute significantly to atmospheric-particle loading. This is best demonstrated by the American Dust Bowl of the 1930s and in the recent large dust storms originating on the continent of Australia (Griffin *et al.*, 2002; De Deckker *et al.*, 2008).

3.1.1 *North African dust storms*

Large dust storms capable of transoceanic movement occur year round in the Saharan and Sahelian zones. Common transport routes from the northern fringe of the Sahara are into and over the northern Atlantic, Europe and Middle East during the spring months (Graham & Duce 1979). Less frequently, large dust storms moving out of North Africa have been tracked eastward over the Middle East, across Asia, over the Pacific, and into North America (McKendry *et al.*, 2007). Yearly dust storms generated on the mid- and southern Sahara and Sahel move west across the Atlantic Ocean and impact air quality in the Caribbean and Americas. Typically, between the Northern Hemisphere summer months of May through October, dust storms move across the Atlantic dust corridor between 15N–25N latitude and impact air quality in the Caribbean and south eastern US (Graham & Duce 1979). A cloud of dust arising off the west coast of North Africa typically takes three to five days to reach the Caribbean, and in cases of prolonged transmission can form atmospheric bridges of dust across the Atlantic (Figure 9).

The equatorial trade winds drive and carry dust and hurricanes across the Atlantic. Between the Northern Hemisphere's winter months (November–April), transatlantic transport is farther south due to equatorial shifts of Hadley cells and dust moves to the southern Caribbean and South America (Swap *et al.*, 1996; Giraudi 2005). The primary source regions of transatlantic dust are the Bodele Depression and Lake Chad regions of the Sahara (Goudie & Middleton 2001; Koren *et al.*, 2006). Fine textured sediments from lakebeds are more easily mobilized into the atmosphere than coarse textured terrestrial soils.

Interestingly, Lake Chad is only five per cent of its 1960's area due to a combination of climate change and anthropogenic diversion of its source waters for cultivation. Similarly, the dried lakebed of Owens Lake in southern California and the exposed sediments of the Aral Sea are prime sources

Figure 9. An atmospheric bridge of dust observed on 8 August 2001 extends along the arrow from its source in North Africa to the Caribbean (Courtesy NASA & ORBIMAGE). (see colour plate 26)

of entrained dust that is due primarily to engineering diversions of source waters for consumption and agricultural purposes (Griffin *et al.*, 2001). Another influence on dust transport is natural and anthropogenic desertification along border regions. Although desertification has been documented on annual scales, the overall size of the Sahara has not changed significantly in recent geologic time (Tucker & Nicholson 1999).

Naturally occurring climate cycles that are driven by large-scale planetary processes like the North Atlantic Oscillation (NAO) and El Niño influence long-range dust transport out of Africa significantly (Prospero & Nees 1986; Moulin *et al.*, 1997; Giannini *et al.*, 2003). The NAO is a duel pressure system that moves annually in a northerly and southerly flux over the equatorial and North Atlantic Ocean. When this system is in a more southerly position, there is more annual rainfall over North Africa and thus less dust transport off the continent. Likewise, when the NAO is in a more northerly location, there is less rainfall over North Africa and greater dust transport out of the region. Since the late 1960s the NAO has predominantly held a more northerly location. This started the current long-running North African drought that has resulted in a noted increase of North African dust transport across the Atlantic to the Caribbean and Americas (Prospero & Nees 1986; Moulin *et al.*, 1997). Looking at annual dust-transport records collected on Barbados, this increase in transport is apparent. A majority of peak-transport years between the early 1960s and the late 1990s occurred during El Niño years (Prospero & Nees 1986). Approximately forty million tons of Saharan and Sahelian dust are deposited in the Amazon Basin each year (Swap *et al.*, 1992; Koren *et al.*, 2006). Nutrients such as iron, phosphorus, and nitrogen carried in desert dust impact primary production in oceans on both long- and short-term temporal scales (Graham & Duce 1979; Ridgwell 2003). Aeolian iron influx in oceans has been estimated between about one to ten billion mol/year using dust-iron solubilities of one and ten per cent, respectively (Fung *et al.*, 2000). Ice-core analyses of dust deposition on geological time scales has demonstrated that during glacial periods of elevated dust transport, oceanic productivity increased and atmospheric carbon concentrations decreased (Broecker 2000; Ridgwell 2003; Lambert *et al.*, 2008). Although some organisms may benefit from this nutrient rich dust, the same dust may be harmful to others. Correlation has been made between African desert-dust deposition in Florida Bay and algal blooms of *Karinia brevis*, the red tide agent. Blooms of this algae routinely impacts marine ecosystem and human health negatively (Lenes *et al.*, 2001; Walsh & Steidinger 2001).

3.1.2 *Asian dust storms*

Clouds of dust moving out of Asia's deserts occur primarily in the spring between February and May. Like the NAO's influence on transatlantic transport of North African dust, the Pacific decadal oscillation (PDO) influences dust transport from Asia to the Americas, and during larger scale dust events, around the globe (Gong *et al.*, 2006; Hara *et al.*, 2006). The PDO spawns El Niño/La Niña-like events that are characterized by sea surface temperature anomalies above the latitude of 20°N. They typically occur on time scales of two to three decades but there is great variability in their frequency and duration. During positive-phase events there is typically less dust transport from Asia

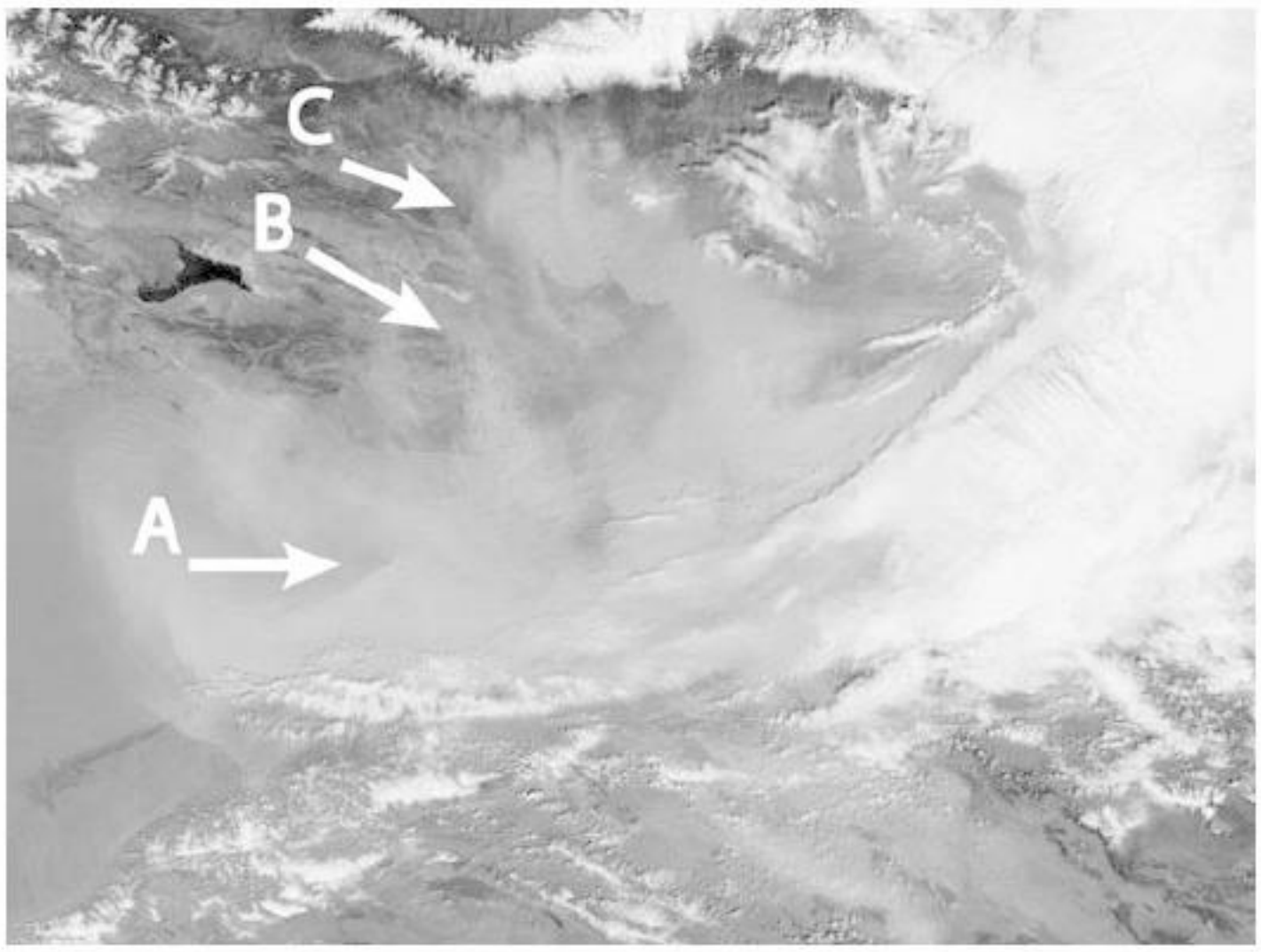

Figure 10. A large dust storm originating in western China on 24 April 2010. This storm resulted from dust converging from three locations. Arrows indicate direction of dust movement from each source region (Courtesy MODIS image, NASA). (see colour plate 27)

across the Pacific to North America than during negative-phase periods, when the eastern Pacific cools. Positive-phase PDO reduces the movement of northern fronts into and across the deserts of Asia restricting the transpacific transport window. The increase in large clouds of Asian dust moving eastward to North America has coincided with recent negative-phase years. El Niño and La Niña events influence dust transport out of Asia with transport across the Pacific occurring at roughly 45°N latitude during El Niño years (greater dust transport) and 40°N during La Niña years (less dust transport) (Gao *et al.*, 2003; Hara *et al.*, 2006). The desertification rate along Asia's desert borderland averaged approximately 2100 km^2 per year between 1975 and 1987 (Zhenda 1993). Anthropogenic activities contributing to this rate are deforestation, overgrazing and population growth. A report from the US Embassy in China in April 1998 cited range wars in the Ningxia Hiu Autonomous Region between herders grazing the border region grasslands and farmers harvesting them (Griffin *et al.*, 2001). A dust storm that impacted air quality in China's Gansu and Xinjiang Provinces in April 2010 (Figure 10) was reported to be one of the largest in since the early 1990s, with visibility in some areas approaching zero and reports of three deaths and one missing person (Tan 2010). Although early web-based reports of this storm indicated that it was restricted to the Asian continent, large dust events such as that one are capable of global dispersion. The chemical fingerprint of a 1990 Asian dust storm moving eastward off the Asian coast crossed the Pacific, North America, and the Atlantic and was detected via isotopic analysis in samples collected in the French Alps (Grousset *et al.*, 2003). Similarly, a large Asian dust storm that impacted North American air quality in 1998 reduced solar-radiation levels by as much as forty per cent and left a chemical fingerprint inland to the state of Minnesota (Husar *et al.*, 2001).

3.2 *Desert dust and human health*

3.2.1 *Exposure to desert dust*

Silicosis is a disease caused by chronic inhalation of silica. This disease is typically occupational in nature and is a health risk to those most frequently exposed to mineral dusts, such as miners and cement workers. It is caused by silica penetrating into the lungs where it causes nodular lesions. The disease causes impaired lung function and can be fatal. One understudied field regarding silica

and human health is the occurrence of this disease in populations that are frequently exposed to desert dust-storms. These include populations close to dust sources as well as those who reside within downwind dust-transport corridors.

Studies focused on the incidence of silicosis have demonstrated potential risk. For example researchers detected silicosis in fourteen of sixteen screened Himalayans in a group residing in a common region of dust, compared to ten of twenty-four in a region where dust exposure was less common (Norboo *et al.*, 1991). In a related study, where dust storm silica concentrations were as high as seventy per cent, the average prevalence of silicosis in 449 individuals from three different regional villages was 16.5 per cent, and in one village as high as 45.3 per cent (Saiyed *et al.*, 1991). This study further noted many cases of massive fibrosis; that is, nodules larger than one centimetre.

In a study conducted in China, where populations are commonly exposed to dust, the silica content in regional soils ranged from about fifteen to twenty-six per cent, the soil particle size range of two to five micrometres was twelve to twenty-five per cent and the prevalence rate of silicosis was seven per cent for 395 screened individuals, or about twenty-one per cent for those over forty years of age (Xu *et al.*, 1993). Those authors also reported the occurrence of silicosis in a village camel and that no human cases of silicosis were detected in a control group (Xu *et al.*, 1993).

Another concern of dust exposure is the development of asthma and the risk to those susceptible to respiratory stress. High asthma rates and the risk to children developing the disease in populations frequently exposed to desert dust have been documented (Bener *et al.*, 1996; Al Frayh *et al.*, 2001). Interestingly, the asthma rates on Barbados increased seventeen-fold between 1973 and 1996, the period corresponding to a Saharan drought and an increase in transatlantic dust transport (Howitt *et al.*, 1998 Prospero 1999). On Trinidad, researchers have demonstrated a link between African desert-dust and paediatric respiratory stress (Gyan *et al.*, 2005). The link between Asian desert dust exposure and human morbidity and mortality has been established by numerous research teams (Kwon *et al.*, 2000; Kwon *et al.*, 2002; Park *et al.*, 2005; Chang *et al.*, 2006; Yang 2006; Kan *et al.*, 2007; Meng & Lu 2007; Belser *et al.*, 2008; Chan *et al.*, 2008; Chiu *et al.*, 2008).

A widely reported but poorly understood illness associated with exposure to desert dust is a disease known by a number of names: desert-dust pneumonia; Al Eskan disease; Gulf War syndrome; and Persian Gulf War syndrome. Cases of desert-dust pneumonia were widely reported during the 1930's American Dust Bowl. Rates then were a hundred per cent higher than those reported during periods of lower dust storm frequency; but, the causative agent was not identified (Brown *et al.*, 1935). It was rumoured that the disease was caused by breathing through wet cloth, a method used for protection during dust events (Egan 2006).

A similar dust-related disease has been widely reported in military personnel deployed in the Middle East during the first and second Gulf Wars (Korenyi-Both *et al.*, 1992; Korenyi-Both 2000; MMWR 2003b; Shoor *et al.*, 2004; Aronson *et al.*, 2006). A survey of over 15,000 deployed personnel between 2003 and 2004 reported that over sixty-nine per cent experienced some form of respiratory illness (Sanders *et al.*, 2005). In addition to respiratory stress, deployed personnel have reported neurological illnesses, fever, and fatigue; and, although some epidemiological studies have shown a link between deployed personnel and disease relative to non-deployed control groups, others have shown no differences between deployed and control groups (Haley *et al.*, 1997; Rook & Zumla 1997; Fukuda *et al.*, 1998; Ismail *et al.*, 1999; Doebbeling *et al.*, 2000; Knoke *et al.*, 2000; Hyams *et al.*, 2001; Gray *et al.*, 2002; Kang *et al.*, 2002; Lee *et al.*, 2002; Hooper *et al.*, 2008; Smith *et al.*, 2009). In recognition of the health risk to personnel from dust-storm exposure, the US military currently provides dust-storm warnings in Korea via its web-based Yellow Sand Activity Warning System (YSAWS) (KMA 2008). This system provides a real-time, colour-coded flag system to provide health advisories to personnel. Ground-based monitoring and satellite sensors are being utilized by China, Korea, and Japan to monitor KOSA (yellow sand) activity to protect public and economic health, address mitigation strategies, and understand the influence of climate change (Yamamoto 2007).

The Dust Regional Atmospheric Model (DREAM) has been utilized to forecast dust entrainment, transport, and deposition in south western US and in China (Nickovic *et al.*, 2001; Papayannis *et al.*, 2007; Yin *et al.*, 2007; Sprigg *et al.*, 2009). In the south-western US, this model is nested within the

Figure 11. African dust-borne microorganisms transported across the Atlantic Ocean between 22 May and 30 June 2003: Ocean Drilling Program, Leg 209. The black bars are CFUs and the Y-axis on the left shows their values in $\mu g/litre^3$ of air; the dotted line shows modelled NAPPS dust concentrations on the right side Y-axis in $\mu g/litre^3$ of air. (see colour plate 28)

National Weather Service NCEP/eta weather forecast model to assimilate satellite digital surface terrain observations that enable forecasting of dust cloud evolution, movement, and deposition over periods of 24–72 hours (Morain *et al.*, 2007; Morain *et al.*, 2009; Morain & Budge 2010). Similarly, the Naval Aerosol Analysis and Prediction System (NAAPS) Global Aerosol Model uses digital satellite and surface measurement data to predict the distribution of dust aerosols at various altitudes on a global scale (Johnson *et al.*, 2003; Schollaert *et al.*, 2003; Honrath *et al.*, 2004; Reid *et al.*, 2004). This model accounts for mobilization, spatial mixing, advection, wet removal and dry deposition, and has been utilized successfully to measure desert-dust-associated microbial concentrations in the tropical mid-Atlantic (Figure 11) (Griffin *et al.*, 2006). Image A shows a series of satellite images of African dust crossing the Atlantic, and the location of a marked research site, May 26, 2003; image B is a contoured unit-less optical depth global aerosol model output for May 26, 2003 with the same marked research site in A. Image C shows total bacterial- and fungal-colony-forming unit (CFU) concentrations obtained from atmospheric samples normalized to per cubic meter for the study period 22 May to 30 June 2003. The blue line shows the trend of predicted

NAAPS dust concentrations per cubic meter at ten metres above sea level for those dates that were acquired several months after the cruise. The majority of CFU was detected during periods of elevated dust (Griffin *et al.*, 2006). Both the NAAPS and DREAM/eta models have great potential for public health dust advisories and monitoring.

3.2.2 *Dust-storm microorganisms & their transport*

The number of bacteria found in a gram of forested, arid, and other types of soils ranges from 10^7 to 10^9, respectively (Whitman *et al.*, 1998). Within these samples there are an estimated 10,000 bacterial types (Torsvik *et al.*, 1996; Torsvik *et al.*, 2002). The number of fungi found in soil has been reported at 10^6/gram (Tate 2000). Viral concentrations have been reported as high as 10^8/gram (Reynolds & Pepper 2000; Williamson *et al.*, 2003). Factors that influence microbial survival and diversity in soils include pH, temperature, elemental composition, nutrient content, and moisture concentration (Yates & Yates 1988; Gans *et al.*, 2005; Janssen 2006). Growth of microorganisms in laboratory cultures has been the historical approach for their identification in soil samples. However non-culture techniques, such as direct-count assays in which cell or nucleic stains allow accurate counts per weight or volume of soil and water, have demonstrated that less than one to up to nineteen per cent of bacteria are culturable in any given sample (Torsvik *et al.*, 1990; Amann *et al.*, 1995; Sait *et al.*, 2002). Clearly, the limitations of culture-based methods prevent the determination of viability for many microorganisms; but, modern molecular-based assays such as the polymerase chain reaction enable one to determine presence/absence in samples (Griffin 2007). Studies of desert microorganisms have reported concentrations of bacteria and fungi per cubic meter of air during normal atmospheric conditions to be 0–1000 CFU and 0–291 CFU, respectively. In these same environments during periods when dust storms were present, concentrations ranged from 0–15,700 CFU and 0–703 CFU, respectively (Griffin 2007). On an international scale, dust storm microbiology studies have demonstrated that very diverse communities of both bacteria and fungi are capable of surviving long-range atmospheric transport (Griffin 2007). Atmospheric sources of stress to dust-borne microorganisms include exposure to UV, desiccation, temperature, and both high- and low-humidity levels (Mohr 1997). Several factors influence the ability of many microorganisms to withstand the rigors of long range transport. These include: (a) attenuation of UV light by up to fifty per cent depending on particle load; (b) the interactions among particles like partial UV shielding and particle tumbling during transport; and (c), variable humidity levels as dust clouds move over aquatic environments (Gregory 1961; Mohr 1997; Herman *et al.*, 1999; Dowd & Maier 2000; Griffin 2007). Various species of both bacteria and fungi are more capable of surviving long-distance transport or suspension at extreme altitudes because their cell pigmentation provides some UV shielding, tolerance to extreme UV doses, or the ability to form spores that provide stress protection (Griffin 2004; Griffin 2007; Griffin 2008; Smith *et al.*, 2010).

With regard to bacteria, one of the most well-known pathogens associated with dust storms is *Neisseria meningitides*. Outbreaks of meningitis are reported frequently following dust events in the meningitis belt of North Africa. These outbreaks typically occur between February and May of each year and effect on the order of 200,000 individuals (Molesworth *et al.*, 2003; Sultan *et al.*, 2005). The current belief is that inhaled dust particles cause abrasions in the nasopharyngeal mucosa allowing virulent strains residing in the nose access to its host's bloodstream, and thus the ability to cause infection (Molesworth *et al.*, 2002). Recently, *N. meningitides* was cultured from settled dust samples collected in Kuwait, demonstrating that dust storms may serve as a vector for this pathogen (Lyles *et al.*, 2005). Other species of bacteria known to cause disease in humans and isolated in a number of different desert-dust storm studies include *Bacillus licheniformis* (peritonitis), *Ralstonia paucula* (speticemia, tenosynovitis), *Acinetobacter calcoaceticus* (respiratory infections), Kocuria rosea (bacteremia), *Brevibacterium casei* (sepsis), *Staphylococcus epidermidis* (endocarditis), and *Pseudomonas aeruginosa* (can cause fatal infections in burn victims) (Griffin 2007). Dust-storm exposure of personnel to ubiquitous pathogens such as *Acinetobacter baumannii* may present significantly unique human health risk in desert environments (Holt 2007).

The most well documented human pathogen known to be transported in dust clouds is the fungus *Coccidioides immitis* (Fiese 1958). This pathogen is only found in the Americas, and outbreaks

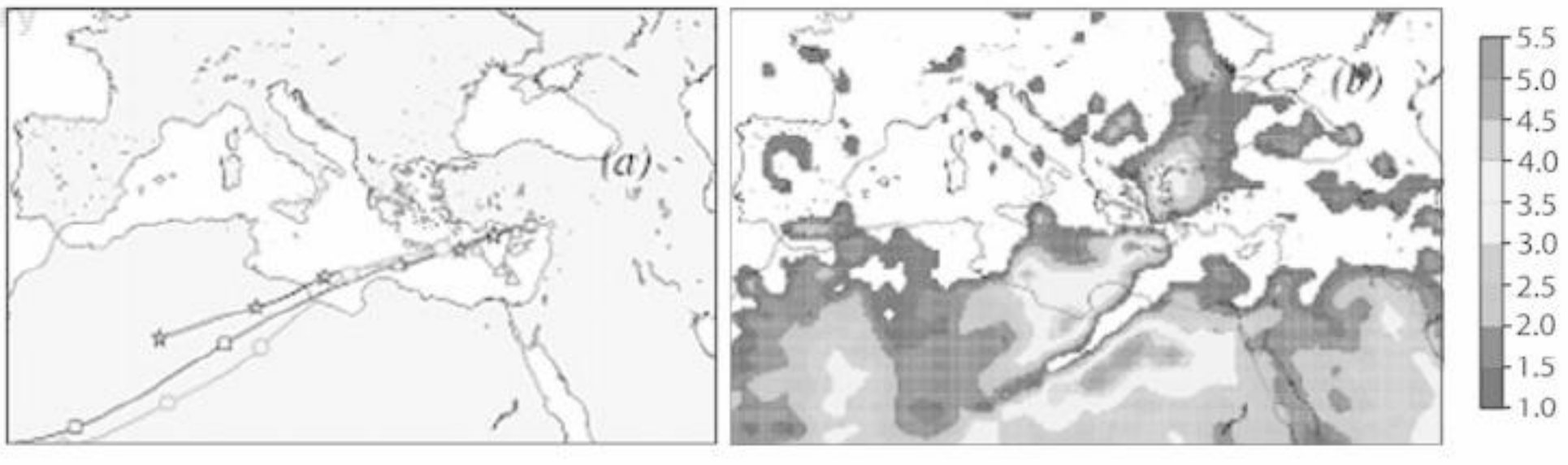

Figure 12. (Left): Air-mass back-trajectory from Erdemli, Turkey; (Right): Earth Probe TOMS satellite data (trajectory data courtesy ECMWFTOMS; TOMS image courtesy NASA). (see colour plate 29)

of the disease known as coccidioidomycosis are reported annually following exposure to clouds of desert dust (Jinadu 1995; Hector & Laniado-Laborin 2005). Groups at highest risk include, African-Americans, Asians, and people younger than twenty years old (Williams *et al.*, 1979; Durry *et al.*, 1997). Infections by this pathogen can be fatal (Schneider *et al.*, 1997). Other genera of fungi that have been identified in desert-dust studies, and whose spores are known to be human allergens include *Acremonium*, *Alternaira*, *Aspergillus*, *Cladosporium*, *Curvularia*, *Emericella*, *Fusarium*, *Nigrospora*, *Paecilomyces*, *Pithomyces*, *Phoma*, *Penicillium*, *Trichophyton* and *Ulocladium*) (Griffin 2007). In a desert-dust study conducted at a coastal Mediterranean research site in Erdemli, Turkey, fungal CFU were more commonly recovered from atmospheric samples during dust events than bacterial CFU. This differed from what was observed in the Caribbean where bacterial CFU were equal to Bacterial CFU, or in Mali, Africa where bacterial CFU were more frequently recovered (Griffin *et al.*, 2003; Kellogg *et al.*, 2004; Griffin *et al.*, 2007). These data demonstrate different microbial dust-storm fingerprints that were influenced by distance from source, distance of transport, and difference in storm source regions. In the Turkish dust samples, the dominant fungal CFU were species of *Alternaria*. Spores of this fungus are known to be potent human allergens. Childhood exposure to spores of *Alternaria* in semi-arid environments has been associated with the onset of asthma (Halonen *et al.*, 1997). Figure 12 illustrates the combined use of satellite data to visualize dust aerosol transport into Turkey from Africa and air mass back-trajectory data. Back-trajectory is used to determine the origin of an air mass to determine impact regions as related to observed microbial CFU. These data clearly illustrate an increase in microbial CFU as the dust cloud passed over the research site, and the air mass/dust-cloud source region as the deserts of North Africa (Griffin *et al.*, 2007). The top image shows a seventy-two hour air mass back trajectory identifying Africa as the source. The red line is 1000 hPa; the grey line is 850 hPa; the green line is 700 hPa; and the blue line is 500 hPa. One thousand hPa is about one per cent of atmospheric pressure, or one millibar. The TOMS image on the bottom shows African dust impacting the research site in Erdemli, Turkey.

Table 3 lists bacterial and fungal CFU aero microbiology data for April 14–16, 2002. CFU = colony-forming units. Blank # = negative controls. CFU data show few fungal CFU and no bacteria CFU at the research site on 14 April 2002, followed by an increase and peak (at 1733 hrs.) in CFU on the 15th of April as the dust storm impacted the site, followed by a decrease in CFU on the 16th as the storm passed and the atmosphere started to clear of particulates.

One of the most neglected fields of desert-dust microbiology is virology, which is reflected in the limited number of papers cited in scientific literature. An atmospheric study of African desert dust in the Caribbean reported viral concentrations of 1.8×10^4/cubic metre during normal atmospheric conditions and 2.13×10^5/cubic metre during a dust event (Griffin *et al.*, 2001). A report demonstrated an increase in concentrations of air-borne influenza viruses during dust versus non-dust events in Asia (Chen *et al.*, 2010). This report is particularly noteworthy, given that transpacific atmospheric transport of infectious influenza viruses from Asia to North America was previously hypothesized (Hammond *et al.*, 1989).

Table 3. Aero-microbiology for Erdemli, Turkey (courtesy Griffin *et al.*, 2005).

Sample	Date	Time	Bacterial CFU	Fungal CFU
24	4/14/02	09:00	0	4
25	4/14/02	14:54	0	2
Blank 5	4/14/02	15:16	0	0
26	4/15/02	08:27	5	38
27	4/15/02	13:42	3	35
28	4/15/02	17:33	6	121
29a	4/16/02	15:03	1	33
29b	4/16/02	15:03	0	34
Blank 6	4/16/02	15:47	0	0

With regard to dust-storm microbiology, it is still unclear how microbial ecology in various desert soils differs; and, more importantly, how the ecology of air-borne dust-associated communities change with distance travelled. Nor is it clear how susceptible community members succumb to stress or how new organisms are added as particles sand-blast downwind environments and new members are added when air masses from different sources mix. Smoke transport of fungi from the Yucatan to Texas across the Gulf of Mexico has been reported (Mims & Mims, 2004). This potential vector of long-range atmospheric transport warrants investigation. Obviously, more investigations are needed of dust-borne viral transport given the recent influenza report by Chen (*et al.* 2010). In addition to the direct transport of human viral pathogens in dust-storms, there is the possibility that bacteriophages, known to move virulence genes from pathogenic strains of bacteria to non-pathogenic strains, may be capable of surviving long-range dust transport and thus are shuttling these genes between distant populations. Many of the molecular tools that will advance these fields have only recently become available; but, it seems clear that these methods will be augmented by aerial and satellite technology.

4 ANTHROPOGENIC POLLUTANTS

Loads of chemicals and hazardous wastes have been introduced into the atmosphere that didn't even exist in 1948. The environmental condition of the planet is far worse than it was 42 years ago (Gaylord Nelson, Earth Day 1990).

4.1 *Air-borne dust and chemicals*

Another desert-dust related health risk is exposure to anthropogenic chemicals that are utilized in dust-cloud source regions and are present in surface soils or are scavenged by the dust clouds. Scavenging occurs when emitted chemicals adhere to particles and are entrained in the interstitial spaces of the clouds as the clouds pass over emission areas (agriculture and industrial). In the late 1960s an air-quality research project conducted on samples from Barbados found that atmospheric-dust samples were of European and/or African origin and contained pesticide residues. Based on pesticide concentrations in these samples, the study concluded that atmospheric delivery of these chemicals to oceans was greater than from river sources (Risebrough *et al.*, 1968).

Dusts entrained around the Aral Sea have been shown to carry agricultural pesticides. A pesticide known as phosalone has been detected in regional air-borne dust at a concentration of 126 mg/kg and hospitalizations due to phosalone exposure have been reported (O'Malley & McCurdy 1990; O'Hara *et al.*, 2000). Worse, the surface area of this Sea has decreased by half since 1960, primarily due to the diversion of source waters for agricultural irrigation (Micklin 1988; Nandalal & Hipel 2007). This has left a dry shoreline area over 27,000 km^2 of exposed sediments that, in addition to

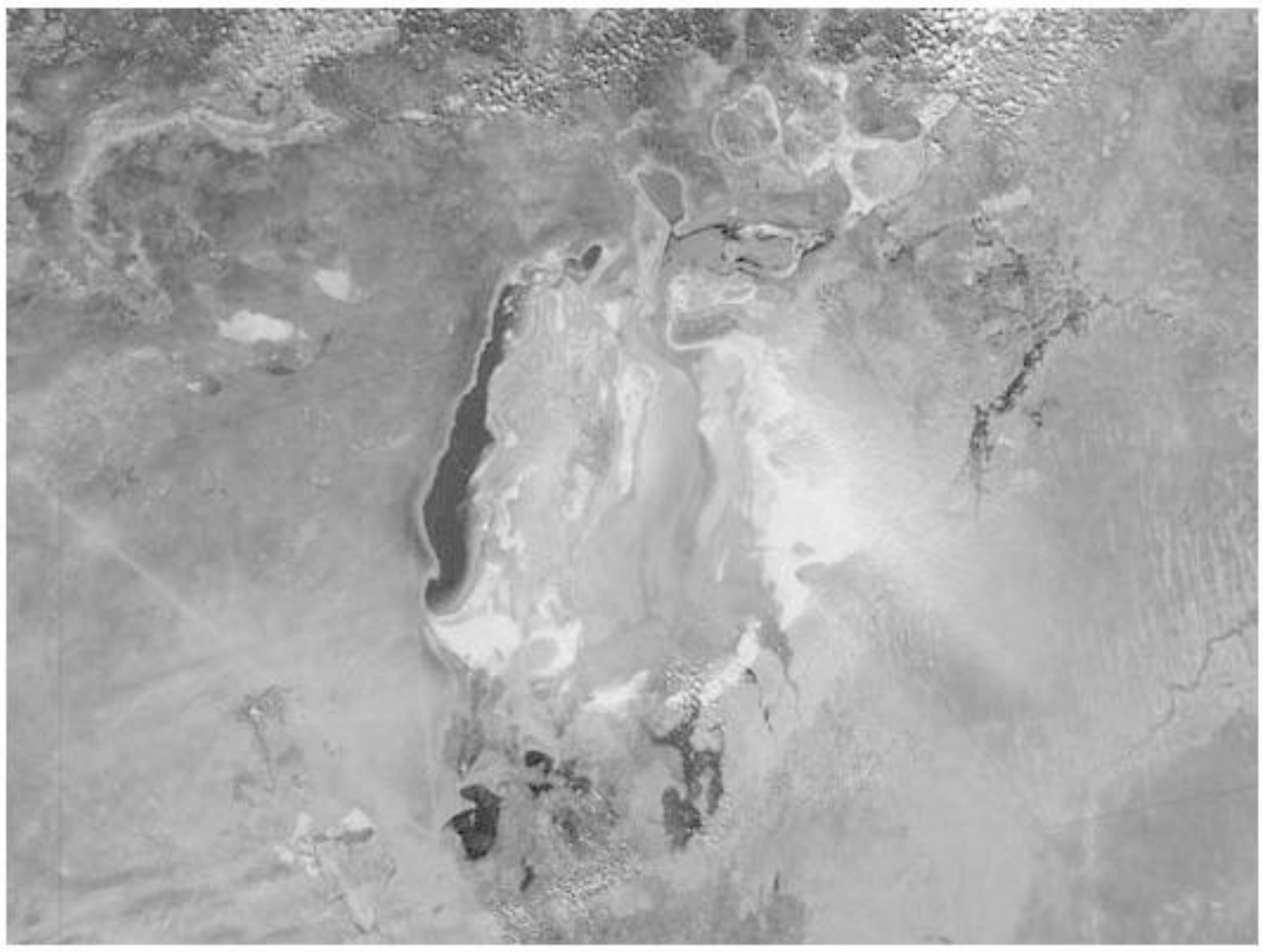

Figure 13. MODIS image for 26 March 2010 showing a dust event originating in the Aral Sea region and moving to the southeast, along the Kazakhstan/Uzbekistan border (Courtesy NASA Earth-observatory). (see colour plate 30)

regional agricultural lands, are a prime source for atmospheric dust (Micklin 2007). Research has detected pesticides such as DDT in the breast milk of women and in the blood of children at some of the highest concentrations ever reported (O'Malley & McCurdy 1990; Hooper *et al.*, 1998). The extent of this environmental disaster has yet to reach its pinnacle. The Aral Sea region is a prime example of how humans can contribute significantly to an increase in the quantity of dust moving in Earth's atmosphere.

The Aral Sea disaster has been widely monitored by Earth-observing satellites. The USGS has a website (http://earthshots.usgs.gov/Aral/Aral) that contains a time series of satellite images from 1964 that dramatically illustrate the demise of the sea. NASA's Earth-observing satellites routinely capture images of dust storms in the region and this can be seen in Figure 13.

Long-range transport of industrial pollutants from Asia to North America, with and without associated desert dust, was identified during six events that occurred between 1993 and 2001 (Jaffe *et al.*, 2003). Industrial pollutants, which included carbon monoxide, peroxyacetyl nitrate, and non-methane hydrocarbons, were detected in samples collected during these episodes at various mountain-top locations and by aircraft. Other studies have documented the movement of industrial dust and smoke aerosols out of Asia that impact air quality throughout the Pacific and in North America (Jaffe *et al.*, 1999; Liang *et al.*, 2004; Jaffe *et al.*, 2005; Weiss-Penzias *et al.*, 2006; Weiss-Penzias *et al.*, 2007; Zhang *et al.*, 2008a). In these studies, Earth-observing sensor data and models were employed to identify pollutant sources and regions of impact. Atmospheric samples were used to identify sources but satellite observations provided the technology for tracking down-wind plume dispersion. In 2003, export of atmospheric pollutants from China across the Pacific was estimated at twenty million tons, of which 5.6 million tons were estimated to have reached the west coast of North America (Yu *et al.*, 2008).

Aerosolized dust on smaller scales in non-arid regions also pose a risk to human health (Griffin 2007). Clean-up following Hurricane Katrina in New Orleans revealed that contaminated dry muds aerosolized into dust containing toxic metals, wastewater pollutants and pathogenic microorganisms. Other sources of hazardous toxic metals from dust followed the Aznalcollar mine tailing accident and the World Trade Centre attacks of September 2011 (Grimalt *et al.*, 1999; Plumlee & Ziegler 2005; Plumlee *et al.*, 2006; Plumlee *et al.*, 2007; Griffin *et al.*, 2009).

4.2 *Chemical warfare*

Chemicals weapons in warfare are intended to expose combatant forces to fatal or disabling doses of air-borne contaminants. In World War I, there were approximately 100,000 fatalities caused by releases of chlorine and mustard gas, and another 1.2 million non-fatal injuries. Approximately eighty-five per cent of the fatalities were due to mustard gas. The French were the first to deploy a toxic chemical weapon (tear gas), but the attack had no impact on the German Army. Similarly, the German military attempted to gas the Russian Army in January, 1915 near Warsaw, but the chemical quickly froze and had no effect. A prime example of the danger of using such weapons occurred in September 1915, when the British released a chemical attack at the Battle of Loos. A change in wind direction first stalled the gas cloud over no-man's-land, then pushed the cloud back over British positions (Heller 1984).

During the eight-year Iran-Iraq war (1980–1988), mustard gas and nerve agents were used against Iran and its own civilian population, resulting in an estimated 100,000 casualties and approximately 20,000 deaths. In contrast biological weapons have so far been relatively ineffective. This is due primarily to flawed delivery mechanisms and issues in dose response with various pathogens. Releasing harmful chemicals into the atmosphere as a military strategy seems to be not only indiscriminate, but highly risky. Their use in the early 20th Century proved only that chemical and biological warfare is sinister. More problematical in today's world are exposures resulting from unintentional industrial accidents.

4.2.1 *Agent Orange*

One of the best known cases of herbicide use impacting human health was Agent Orange during the Vietnam War. This program utilized several different herbicides in addition to Agent Orange to clear foliage around bases, roads, and trails, and to kill crops to limit food production. Agent Orange was a mixture of two chemicals, 2,4-dichlorophenoxyacetic acid and 2,4,5-trichlorophenoxyacetic acid that contained the dioxin 2,3,7,8-tetrachlorodibenzodioxin (aka TCDD). It is a by-product of 2,4,5-trichlorophenoxyacetic-acid production and is a known human carcinogen (Schecter *et al.*, 2001). Approximately 50 million litres were sprayed over approximately 2.6 million acres on multiple occasions (Ngo *et al.*, 2006). TCDD exposure has been shown to induce physiological responses such as shape changes, cause membrane damage in red blood cells, and has been linked to an increased prevalence of diabetes and insulin resistance (Suwalsky *et al.*, 1996; Duchnowicz *et al.*, 2005). There has been a number of studies that have suggested or linked TCDD exposure to birth defects; but also, there have been a number that challenged these findings and concluded that the link is questionable (Erickson *et al.*, 1984; Friedman 2005; Ngo *et al.*, 2006; Schecter & Constable 2006). Obviously, many military personnel and civilians were exposed to TCDD during the Vietnam War. In 1970, one human breast-milk sample was reported to contain 1832ppt. Subsequent analyses in 1973–1995 showed a decline in concentrations, but persistence in exposed populations over time. Tissue-sample concentrations collected in 1984 from an area that was not sprayed were less than three parts per thousand. Recent studies have shown that TCDD is still present in soil and water samples and in current residential tissue/fluid samples in areas where this chemical was utilized (Schecter *et al.*, 2001; Dwernychuk *et al.*, 2002).

Two metre high spatial resolution, declassified satellite photography collected between 1960 and 1972 provide data that can be utilized to map 'use areas'. One reason for doing this is to identify contaminated regions that might serve as sites for long-term human health exposure studies, and to design remediation projects (Hatfield-Consultants 2000). A GIS database has been developed for agent orange and other pesticides used in Vietnam as a tool to supplement epidemiological and sensor-based studies (Stellman *et al.*, 2003).

4.3 *Industrial accidents*

In the US between 1994 and 2001, there were 696 ammonia, 534 chlorine, 100 flammable mixtures, 98 hydrogen fluoride/hydrofluoric acid, 59 chlorine dioxide, and 447 other reported accidents with

the twenty-five most commonly involved chemicals and mixtures (Kleindorfer *et al.*, 2003). In July, 2003 a cloud of chlorine gas was released from a plant in Baton Rouge, Louisiana, that resulted in eight employees requiring medical attention and causing residents within a half-mile radius to seek in-door shelter. Morbidity and mortality in incidents such as these within the United States have occurred primarily within manufacturing facilities and have not caused significant risk to local populations. This is not the case everywhere.

4.3.1 *Bhopal industrial leak*

Two devastating incidents marked the 1980's: Bhopal, India in December, 1984 and Chernobyl, Ukraine in April, 1986. The Bhopal incident involved a leak of almost twenty-seven tons of methyl isocyanate and other chemical gases from a pesticide production facility that ultimately exposed hundreds of thousands of people. Immediate deaths were estimated at 3800 individuals with total fatalities climbing to an estimated 6000 due to post-exposure medical complications (Dhara *et al.*, 2002; Broughton 2005). Approximately 50,000 injured still suffer from exposure injuries. For a review of chemical accidents in industrializing countries (de Souza Porto & Freitas 1996). The limited availability of satellites capable of data acquisition from industrial accidents following the Bhopal disaster was recognized (Chrysoulakis & Cartalis 2003). Currently, this need is driving the development of software capable of utilizing satellite data to track and monitor the release of toxic plumes in the atmosphere (Chrysoulakis *et al,* 2005).

4.3.2 *Three Mile Island, Chernobyl, and Fukushima radiation leaks*

Accidental release of radioactive particles into the atmosphere is another source of human health risk. Two of the most familiar events are the nuclear power plant accidents at Three Mile Island in the US and Chernobyl, in the Ukraine. The Three Mile Island accident occurred in March, 1979 near Middletown, Pennsylvania. That accident was caused by a loss of reactor coolant due to a pilot-operated relief valve that stuck open, and a failure of reactor personnel to recognize the loss of coolant when system alarms sounded (Walker 2004). The event released approximately thirteen million curies of radioactive gas. Of the thirteen million curies, only about fifteen curies (carcinogenic iodine-131) were believed to be harmful (Walker 2004). Approximately 140,000 residents within a five-mile radius of the power plant temporarily evacuated the area in the following days. Exposure from the event was reported to be less than that adsorbed from a chest X-ray. Although there were later reports of elevated cases of infant mortality and effects on wildlife in exposed populations, epidemiological investigations found no evidence of event-related morbidity or mortality in exposed populations (USNRC 2009). Fortunately, there were no identified cases of morbidity or mortality in plant personnel or residents who lived close to the plant. This was not the case with the Chernobyl event.

The Chernobyl incident released several forms of particulate and gaseous radioisotopes into the atmosphere. It is the most significant unintentional release of radiation into the environment to date. It remains a problem because radioactive particulates deposited far downwind persist in soils subject to atmospheric entrainment. It took ten days to contain the event during which fifty million curies of noble gases and fifty million curies of non-noble gases were released into the atmosphere (Ginsburg & Reis 1991). Dispersion of these materials occurred throughout the Northern Hemisphere. During the first three months following the event, thirty-one individuals (most were first responders) died out of 237 individuals who acquired acute radiation sickness (Hallenbeck 1994). One hundred and thirty-five thousand residents within thirty kilometres of the immediate site of the power plant were permanently evacuated (Chesser & Baker 2006). The International Atomic Energy Agency (IAEA) has estimated that cancer deaths may reach 4,000 out of 600,000 who received the greatest exposure. Thyroid cancer is the primary long-term concern, but fortunately this disease is very treatable. Outside of the exclusion zone, fatal cancer risk from the event is believed to be minor. Within the exclusion zone, surface and ground waters were heavily contaminated. Forests within this zone are now known as the red forests due to the discoloured and dead pine trees (Arkhipov *et al.*, 1994). Initial radiation levels were fatal to indigenous animals and abandoned livestock. Interestingly, wildlife currently flourishes within the exclusion zone, although

bone and tissue samples show elevated radioactivity (current radiation levels are only about three per cent of those directly following the event). Genetic analyses of voles captured within the exclusion zone showed no evidence of mutation and there is currently no evidence that elevated rates of morbidity or mortality occur in animal populations within the exclusion zone. Although human health risk outside of the exclusion-zone is believed to be minimal, there is concern about atmospheric remobilization of radioactive material from this event in both the exclusion zone and in down-wind regions of deposition where arid zone surface soils are susceptible to atmospheric entrainment. Remobilization of cesium-137 and dispersion to downwind environments have been noted (Hao *et al.*, 2008). Scientists in Greece detected elevated cesium-137 during a Saharan desert dust event that demonstrated remobilization and long-range dispersion of previously deposited Chernobyl radio nucleotides (Papastefanou *et al.*, 2001). Although availability of Earth-observing satellites was limited at the time of that accident, the Landsat Program provided images of the region, which highlight the change in cropland cover from one month to six years post-accident.

The more recent Fukushima Daiichi nuclear power plant incident started on 11 March 2011 following the Tohoku 9.0 magnitude earthquake and succeeding tsunami. While the operational reactors shutdown following the earthquake, the fourteen meter tsunami (This coastal plant was designed to withstand a 5.7 meter tsunami) that hit the plant knocked out backup generator systems used for emergency cooling operations, causing the subsequent event. Failures in three of the six reactors were rated Level 7, the highest level on the International Nuclear Event Scale (Three Mile Island was rated Level 5 and Chernobyl Level 7). Between the onslaught of the incident and 12 April 2011, an estimated ten million curies of radiation were released into surrounding and downwind environments. While this incident fortunately did not cause any direct casualties, due in part to a much more effective response than was documented with the Chernobyl incident, it has been estimated that total radiation leakage could eventually surpass Chernobyl levels. Approximately 200,000 people were displaced due to mandatory (twenty kilometre exclusion zone) and recommended evacuations (Dauer *et al.*, 2011). Early economic cost estimates including remediation and compensation range from roughly $100 to $250 billion US dollars. Historical and current information on this event can be found at the International Atomic Energy Agency Fukushima Nuclear Accident (IAEA 2012).

4.3.3 *Sverdlovsk biological release*

An accidental release of a virulent strain of *Bacillus anthracis* (causative agent of anthrax) from a bioweapon production facility occurred near Sverdlovsk in 1979. It caused sixty-four human deaths and outbreaks of the disease in local livestock populations (Meselson *et al.*, 1994). In the early 20th Century ground observation was limited to planes, balloons, and blimps; and images of a number of the World War-I gas attacks show smoke-like clouds of vapour being carried downwind from their points of origin. Modern Earth observing platforms are capable of imaging these types of clouds, as can be seen in numerous archived 'fire-smoke' images. LiDAR (light detection and ranging) is an optical sensing (light scattering) technology being used on satellites to study atmospheric aerosols. They are being used also to investigate and to monitor the release and movement of aerosolized biological weapons (Immler *et al.*, 2005; Glennon *et al.*, 2009).

4.4 *Pesticides and herbicides*

The historical public health concern related to pesticide exposure, which includes herbicides has been restricted to individuals involved in their application, and to those in close proximity to application sites. An 1990 estimate for the quantity of pesticides used globally was reported to be about 2.5 million tons (Pimentel *et al.*, 1992). Such widespread use of these chemicals is due to annual crop-loss estimates of thirteen per cent from insects, twelve per cent from plant pathogens, and ten per cent from weeds (Cramer 1967). The primary means of large-scale application of either group of chemicals is through hand sprayers, automobiles, or aircraft. Risks from these classes of chemicals are obvious. Just look at a package at your local store and read the application and exposure warning labels. While residential use of pesticides and herbicides present health risks, it is the more potent variants of these that are utilized by government organizations for agricultural

purposes that are the main health concern in downwind environments. The governments of Canada and the US (like many other national, state and regional governments) provide guidelines or laws for using these chemicals, and numerous documents addressing their acquisition, use, and storage can be found at their respective websites. Guidelines for hand and vehicle application include limiting application to wind-speed conditions of less than 15 km/hour to protect those in downwind environments and ten metre buffer zones around wells and surface waters to protect potential drinking water supplies and aquatic ecology. Agency guidelines on aerial application (crop dusting) include limiting application to wind speeds of less than 4.4 m/second and an altitude of five metres or less if near a no-spray zone. Health risk from exposure to these chemicals was recognized early, and scientific data addressing this issue have been reviewed periodically (Hallenbeck & Cunningham-Burns 1985; Oehme 1991; Ecobichon & Joy 1994; Safe 1995; Margni *et al.*, 2002).

Civilian uses of pesticides pose significant health risks. In South Africa there are approximately 100 to 200 cases of pesticide poisoning annually, and approximately ten per cent of these cases are fatal (London & Bailie 2000). In India, injuries from sprayer-applied chemical exposure is about 4.5 per 1,000 sprayers per year (Nag & Nag 2004). In Sri Lanka, there were approximately 10,000 to 20,000 pesticide poisonings per year with a fatality rate of nearly ten per cent between 1986 and 2000 (Roberts *et al.*, 2003). Sri Lanka banned class-I organophosphate pesticides in 1995 resulting in a drop in fatalities from this form of pesticide, but there was a marked increase in fatalities from toxic replacements. The annual incident rate of acute pesticide poisoning in developing countries is approximately 18.2 per 100,000 agricultural workers and 7.4 per million school children (Thundiyil *et al.*, 2008). In 1993, twenty-seven Provinces in China reported approximately 52,000 cases of acute pesticide poisoning, of which some 6,000 were fatal (He *et al.*, 1999). Between 1985 and 1990, US poison centres reported about 338,000 cases and ninety-seven deaths from pesticide, herbicide, fungicide, and rodenticide exposure (Klein-Schwartz & Smith 1997). The data reported here from the various countries include cases of self-poisoning, but most are related to handling and application.

Health risk from handling (mixing, loading sprayers) and to the applicators can be minimized with protective breathing devices but risk to individuals in downwind environments is not as easy to mitigate. It has been estimated that less than 0.1 per cent of pesticides reach their target organisms and thus present risk through penetration into ground-waters, precipitation run-off to surface waters, spray-drift, and remobilization into the atmosphere via field dust as crops are harvested and/or the fields are later prepared for their next crop (Pimentel 1995). Applicator unit nozzle selection (that is, the size of the spray droplets) is the main factor influencing drift. Aerosol droplets larger than 100 μm are less susceptible to drift, regardless of the application technique used. Low-volume ground sprayers have been shown to be the most susceptible to drift (Salyani & Cromwell 1992). Small-spray droplets in the size range of 10–50 μm can drift distances exceeding thirteen kilometres (Akesson & Yates 1964). Computer programs have been developed as tools to calculate spray-drift in different geographical and atmospheric conditions (Zhu *et al.*, 1995; Teske *et al.*, 2002). As with most diseases, the young, old, and immune-compromised are at greatest health-risk. The US/EPA and the University of Washington's Center for Child Environmental Health Risks Research conduct studies on pesticide exposure pathways, and health outcomes. They provide a database and related publications on exposure and prevention (UW 2012). Researchers have utilized a combination of geospectral and geospatial techniques to successfully demonstrate the feasibility of looking at historical and current pesticide use to identify potentially exposed populations for epidemiological studies (Ward *et al.*, 2000). A similar combined approach was utilized that included land-use, atmospheric conditions, and pesticide-use data to determine exposure for cancer research (Maxwell *et al.*, 2009). This same publication provides a review of the current state of knowledge for this genre of pesticide exposure assessments, including the pros and cons of the methodologies.

4.5 *Urban air contaminants (persistent organic pollutants)*

As planet Earth becomes increasingly urbanized, critical research is needed that addresses links between global atmospheric processes and air pollutant exposures to these growing populations. The

health effects of vehicle emissions on urban life are well investigated and are being supported by sensor data from ground, air, and satellite platforms. Satellites deployed over the past few decades carry a very sophisticated array of measurement instruments to monitor atmospheric trace gases (e.g. O_3, NO, NO_2, HCHO, CO_2, and SO_2) and particulates generated at scales relevant to urban ecosystems (one to ten kilometre). These measurements are useful for characterizing pollution source areas and detecting transient events, as well as for delineating and tracking of pollutant plumes. There is also considerable interest in using sensor observations to estimate ground level concentrations of toxic air pollutants such as nitrogen dioxide (NO_2) and respirable aerosols and particulates. This is done by comparing satellite observations of pollutant levels in tropospheric air columns with ground-level (boundary layer) concentrations obtained from direct measurements, and modelling the results. NO_2 is particularly amenable to satellite observation because it is present at high levels in the surface boundary layer relative to the free troposphere; and it, therefore, produces a strong boundary layer signal (Martin 2008). Satellite observation of tropospheric NO_2 columns began in 1995 with the Global Ozone Monitoring Experiment (GOME-1), and has continued since then with the SCanning Imaging Absorption spectroMetre for Atmospheric CHartographY (SCIAMACHY), OMI, and GOME-2 (Lamsal *et al.*, 2008). Observations from GOME and SCIAMACHY have been used to demonstrate the correlation between ground-level NO_x emissions and tropospheric column measurements of NO_2 (Leue *et al.*, 2001; Martin *et al.*, 2003; Jaeglé *et al.*, 2005; Richter *et al.*, 2005; Zhang *et al.*, 2007). Petritoli (*et al.*, 2004) and Ordóñez (*et al.*, 2006) found a significant correlation ($R2 \geq 0.78$) between ground-level NO_2 measurements and GOME tropospheric NO_2 columns. Figure 14 shows a one-year average of tropospheric NO_2 columns over Western Europe retrieved from OMI. Pronounced enhancements are evident over major urban and industrial areas. From the high degree of spatial heterogeneity, it is evident that the dominant signals are from the boundary layer. Martin (*et al.*, 2004) estimate that seventy five per cent of the NO_2 column occurs in the lowest 1500 m of the atmosphere. Panel (a) shows the region with an overlay of the main roads and regional topography. The Rhine, Rhone, and Seine river valleys are also enumerated as 1, 2, & 3, respectively. Details of Randstad in the Netherlands (panel b), the Ruhr area in Germany (panel c), and Paris (panel d) and also shown. The colour scales have been adjusted for each region, as compared to the colour scale of Panel (a).

Satellite observation of AOD, a measure of light scattering by atmospheric particles, began in 1999 with MISR, and has continued with MODIS, the Cloud and Aerosol LiDAR with Orthogonal Polarization (CALIOP, pronounced calîopç), and OMI (Martin 2008; Hoff & Christopher 2009). A growing body of literature suggests that AOD can be used as a predictor of ground-based $PM_{2.5}$ mass concentrations. For example, Gupta *et al.*, (2006) compared MODIS AOD and $PM_{2.5}$ mass concentration in several locations including Sydney, Delhi, Hong Kong, and New York City and obtained a linear correlation coefficient ($R^2 = 0.96$) between daily mean AOD and ground-based $PM_{2.5}$. However, they found that the $PM_{2.5}$–AOD relationship strongly depended on aerosol concentrations, RH, cloud cover and mixing height. The highest correlation was found for clear sky conditions with RH less than 40–50 per cent and mixing height from 100 m to 200 m. Engle-Cox (*et al.*, 2004) compared MODIS/AOD with ground-based $PM_{2.5}$ and PM_{10} mass concentration measurements from across the US, and found relatively poor correlations for western parts of the US compared to the east and Midwest. This was attributed to differences between MODIS and ground-based sensor measurements, regression artefacts, and terrain variations as well as the MODIS cloud mask and aerosol optical depth algorithms. In a comprehensive review of the subject, Hoff & (Carpenter 2009) estimated that the precision in measuring AOD is about twenty per cent, and the relationship to $PM_{2.5}$ is at best thirty per cent in controlled measurements. They concluded that, although this precision is insufficient to meet regulatory needs in terms of air quality prediction, other information provided by orbiting sensors fill gaps in areas where there are few ground-based monitors, or for delineating plumes, and for assessing plume dispersion.

Studies by the National Research Council (2007), Martin (2008), and references therein have identified needs for improving sensor design parameters for use at the urban scale. Some of the most pressing needs include: (1) developing instruments and data processing algorithms to achieve higher spatial and temporal resolution for urban areas; (2) improving validation processes,

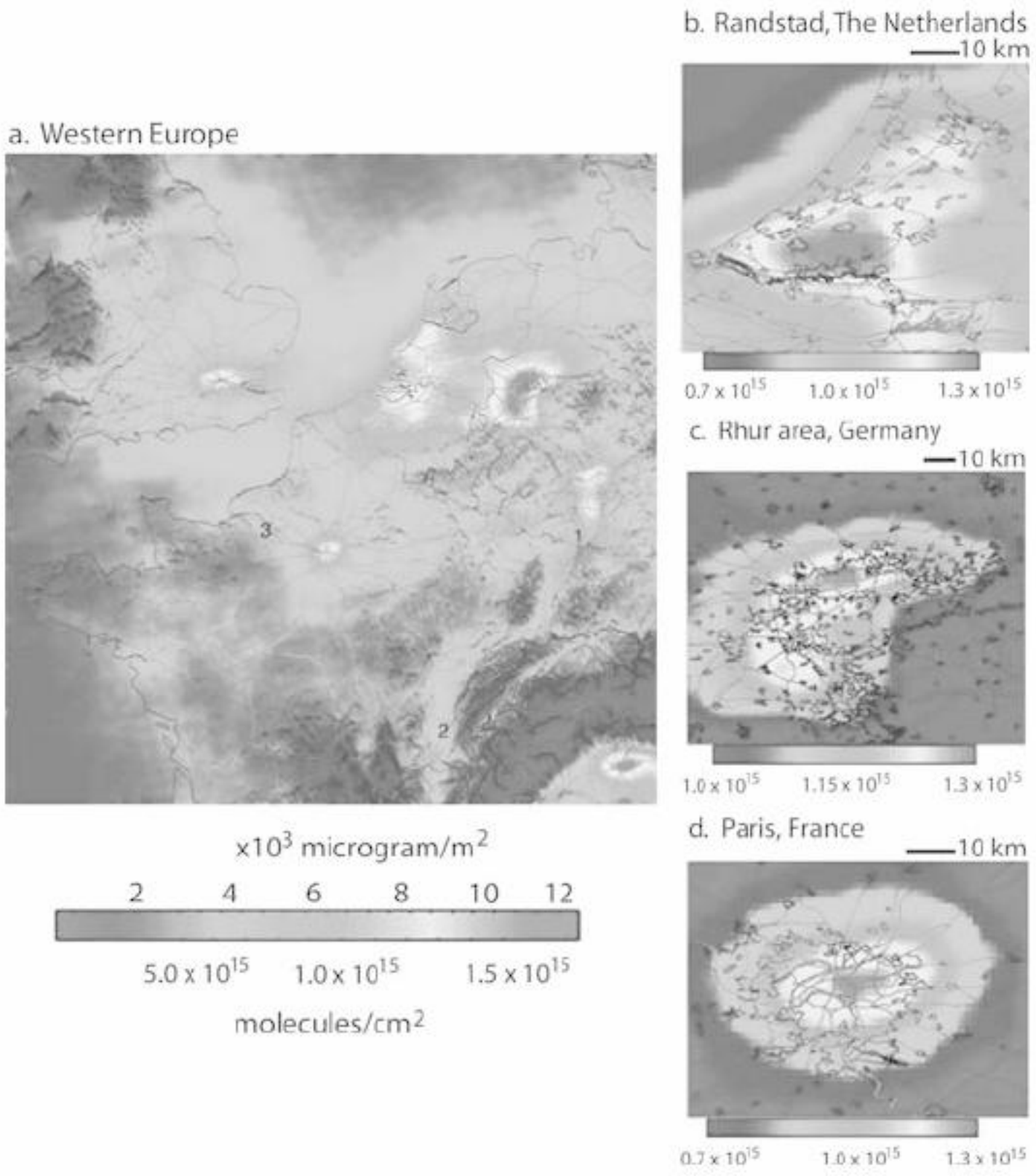

Figure 14. Mean tropospheric NO_2 from OMI over Western Europe December 2004-November 2005. Data from Boersma *et al.*, 2007 (Courtesy J.P. Veefkind). (see colour plate 31)

especially for tropospheric NO_2 (e.g. different terrain, seasons, and boundary layer concentrations); and (3), improving characterization of geophysical fields (e.g. cloud contamination, surface reflectivity).

Finally, effective utilization of novel sources of information calls for inter-, intra-, and multi-disciplinary research; and, policy development in data manipulation, archiving, analysis, sharing, and dissemination. Of necessity, emerging global and local health surveillance systems will be built upon analytical approaches and techniques that enable data processing and their more timely use for public health practice and research (Jajai *et al.*, 2009; McEntee *et al.*, 2010; Fefferman & Naumova 2010).

5 EMERGING EARTH OBSERVING SENSORS AND DATA

Key factors for many public health incidents are the environmental conditions leading to the specific public health issue under consideration. The information on those environmental conditions typically come from non-medical sources and involve estimating parameters such as the abundance of air-borne particulates, water inundation etc. Trying to address these factors comprehensively over a large area is a challenge. Addressing the challenge involves EO data, numerical modeling, and machine learning. Machine learning is a subfield of artificial intelligence that is concerned with the design and development of algorithms that allow computers to learn the behaviour of data sets empirically. Since environmental conditions change across all temporal scales of reference,

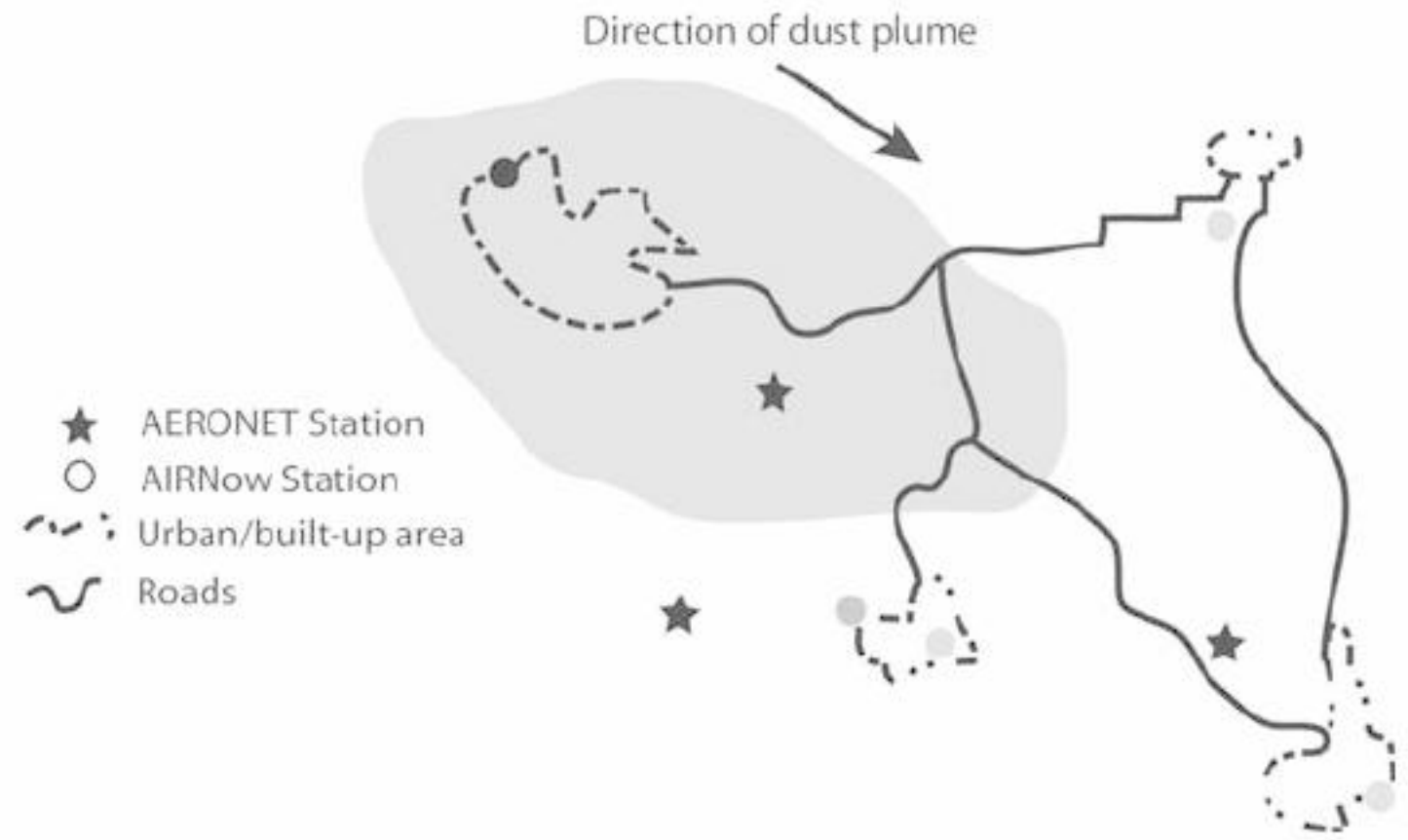

Figure 15. Relationships between anthropogenic (fugitive) dust/aerosols and atmospheric dust. Courtesy, Earth Data Analysis Center, University of New Mexico.

it should be possible to provide timely alerts of health issues through environmental forecasting systems. Hence, remote sensing, numerical modelling and machine learning are the focus of this Section.

Satellite and aerial observations contribute a wide variety of data to better understanding how natural environments relate to various disease categories. Key to the effective use of these data is identifying the appropriate sensors and the properties of their acquired data sets that can be used to improve models and to enhance surveillance systems, decision support tools, and early warning systems. To illustrate the roles these data sets can play, an example is provided for particle matter less than 2.5 μm in aerodynamic diameter ($PM_{2.5}$). Data on $PM_{2.5}$ are useful for studying asthma and respiratory conditions. Frequent, if not continuous, monitoring of fine particulate concentrations removes a critical barrier in studying health impacts, especially in the vast majority of rural and remote areas where there are no *in situ* monitors. Results from repetitive, synoptic measurements can assist public policy decisions for coping with $PM_{2.5}$ events and episodes.

5.1 *$PM_{2.5}$ information for asthma studies*

Today there are twenty-two million people in the US alone with asthma, and one of the environmental triggers for asthma is the concentration of air-borne particulates such as $PM_{2.5}$. Various networks of ground-based sensors provide routine measurements of $PM_{2.5}$, but their spatial coverage is sparse, especially in the developing world. Moreover, ground observation sites do not necessarily represent their broader surrounding areas. Many of the EPA ground-based monitors in the US are located near roads where air quality is influenced by local dust entrainment and vehicle exhaust that is not representative of surrounding neighbourhoods. Multiple space-borne sensors provide an array of data products on atmospheric aerosols. There is growing interest in using these data for air quality and health purposes, but there is also a growing realization that currently available products do not provide what is often needed, the near surface $PM_{2.5}$ abundance.

Simulating both windblown dust and anthropogenic air pollution events is intensive computationally in dusty regions. Figure 15 is a schematic illustrating this complexity. The diagram is a hypothetical region within a model domain that has a low level of ambient dust and aerosols. In this region there are five hypothetical AIRNow monitors (circles) and three AERONET Stations (stars). Each of these sites has a shade of grey indicating its observed concentration of dust and aerosol measured at a specific time, as contributed by its respective local population and economic activities. Each of the population centres (irregular shapes) has a shade of grey to indicate its ambient level of anthropogenic dust and aerosols at the moment of measurement. A dust cloud (pale brown)

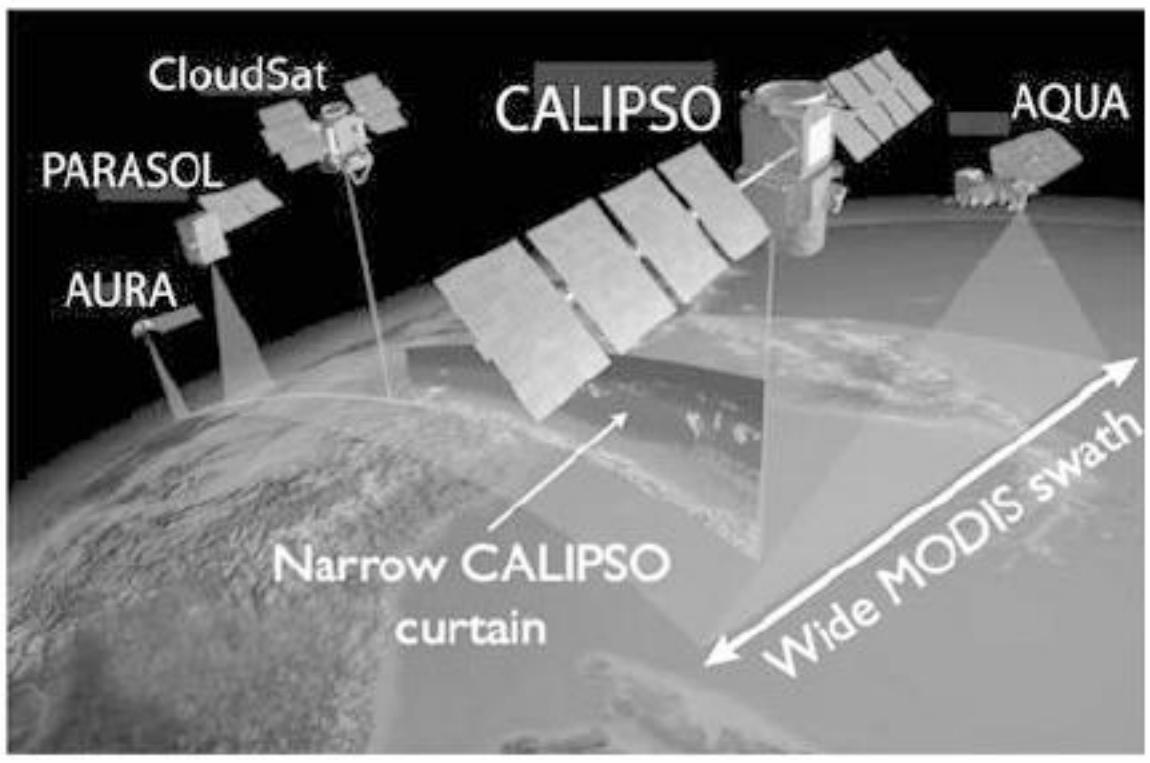

Figure 16. Visualization of the two complimentary types of aerosol information obtained by NASA's A-TRAIN constellation, detailed vertical information from CALIPSO curtains and global coverage of the total optical depth from MODIS. (see colour plate 32)

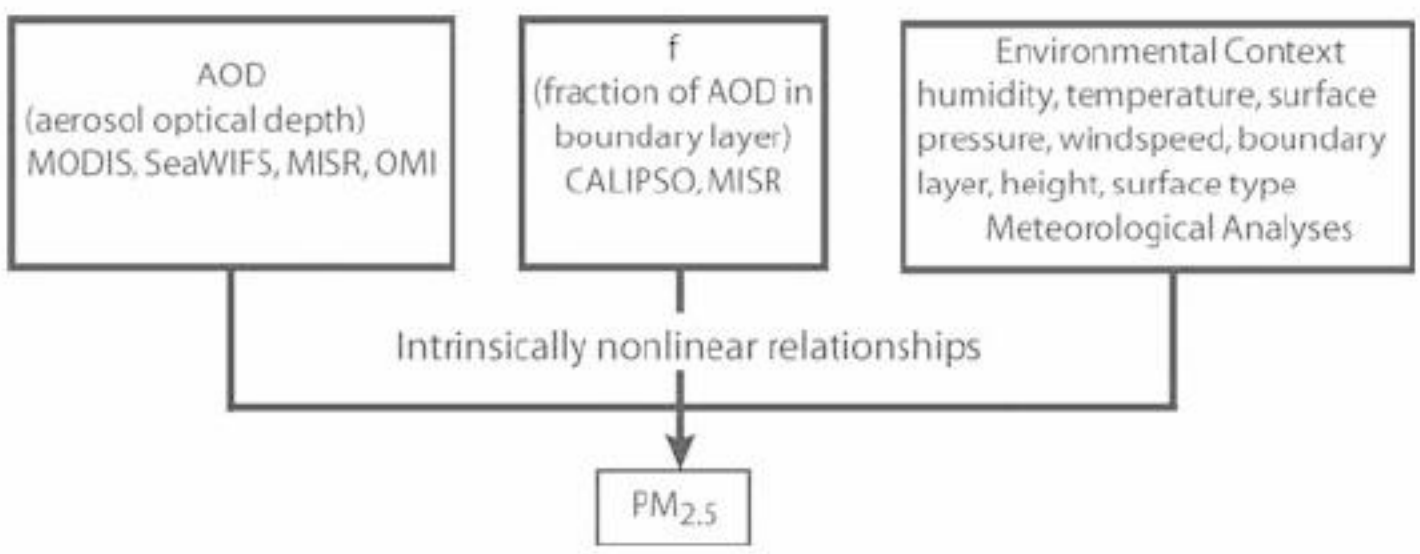

Figure 17. Schematic of the complexity surrounding multi-variate, non-linear relationships between satellite platforms and sensors for measuring AOD, humidity, temperature, surface pressure, wind speed, boundary layer height, and surface type to measure $PM_{2.5}$.

is shown moving toward the northeast that will add an atmospheric dust component to the ambient anthropogenic signal. The population centre in the upper left of the domain shows a particularly heavy concentration of atmospheric dust mixed with the ambient anthropogenic dust/aerosol load. One can imagine that levels of air contaminants will rise in the population centre near the centre of the image as the dust cloud passes through. Modelled dust concentrations can therefore consist of three different phenomena: atmospheric dust only; the ambient level of urban dust only; or a combination of both. To separate the atmospheric from the ambient concentrations, one must know the dust loads of each.

An approach to overcoming this limitation is to bring together data from multiple sensors, models of their meteorological context, and advanced machine learning. The suites of observations used include LiDAR data from CALIOP on-board the CALYPSO platform. CALIOP provides global vertical profiles of the atmosphere and fuses them into their appropriate meteorological context to provide three-dimensional vertical curtains of aerosol distribution (Figure 16).

Figure 17 is another schematic showing how multiple data sets converge on $PM_{2.5}$ measurements. This prototype system involves several components. The approach takes into account the cardinally multi-variate, non-linear relationship between currently available EO data products and the parameters needed to estimate $PM_{2.5}$ routinely. The absence of such an approach has been a stumbling block in using satellite observations to infer $PM_{2.5}$ for health studies.

Science is close to delivering global $PM_{2.5}$ analyses on a $0.1° \times 0.1°$ lat/lon grid. These analyses can then be used in several ways: 1) to display a daily global visualization of the $PM_{2.5}$ abundance in Google Earth, so that for any day and location for which there are data, an estimate of the breathable $PM_{2.5}$ abundance with an associated uncertainty can be provided; 2) the analyses could

be used to provide personalized $PM_{2.5}$ accumulated dosage if a timeline of locations is provided; and 3), people with respiratory issues could check the history of $PM_{2.5}$ for any location. This would be of use if they are considering moving to a new location. This is just the first of many examples envisioned for an integrated environmental health system. The goal is to provide people with optimized personal alerts relevant to their health to enable smart lifestyle choices based on timely environmental information.

5.1.1 *Realizing the goal*

Realizing the goal requires two components. The first uses the appropriate temporally and spatially varying meteorological context of the latest version of each satellite product, as well as *in-situ* ground truth observations of $PM_{2.5}$ abundance. The precise context of observations is critical, as there is significant temporal and spatial variability in the abundance of $PM_{2.5}$. Careful attention must be paid to ingesting/fusing satellite observations in both time and place. The second component uses nonlinear, nonparametric, multivariate machine learning to address the issues for which there is not yet a complete theoretical description. Ideally, science will eventually have a complete theoretical understanding of the multivariate, nonlinear relationships between $PM_{2.5}$ and AOD, in which case machine learning would not be required. Currently, the array of tools for multivariate, nonlinear, nonparametric machine learning has proven to be valuable for a variety of applications. For estimating $PM_{2.5}$, the three nonlinear, multivariate issues that must be addressed are: 1) the inter-instrument bias between satellite AOD products and ground truth (e.g. from AERONET); 2) the inter-instrument bias between the suite of satellite AOD products (MODIS Terra, MODIS Aqua, MISR, SeaWiFS and OMI); and 3) the multivariate, nonlinear dependence of the abundance of $PM_{2.5}$ in the atmospheric boundary layer on humidity, temperature, boundary-layer height, surface pressure, wind speed, and surface type.

A major focus of machine-learning research is to produce (induce) empirical models from data automatically. This approach is usually used because of the absence of adequate and complete theoretical models that are more desirable conceptually. Currently there is not an adequate and complete theoretical model describing the complex relationships between AOD, as retrieved by satellite instruments, and the near-surface abundance of $PM_{2.5}$ in $\mu g/cm^3$. Neither is there an adequate and complete theoretical explanation for the inter-instrument biases that are present between the suite of AOD satellite products and ground truth data such as AERONET. Both of these factors have hindered use of EO data to estimate near-surface abundance of $PM_{2.5}$ in $\mu g/cm^3$.

Machine learning assists construction of a more complete theoretical model and offers two important advantages relative to more traditional statistical prediction models. These advantages are: 1) they use traditional statistical prediction models; and 2) they specify *a priori* that the relation between the predictors and the outcome is linear. In many cases, however, the form of the relationship is unknown or poorly understood. Machine-learning models offer a nonparametric alternative to parametric modelling. In addition, they are capable of learning relations in the data that may not be evident in *a priori* model specification. Machine-learning models include the capability for identifying and simulating nonlinear relations among variables. Support vector machines (SVM) are a type of machine learning found to be useful in this discussion (Lary *et al.*, 2009).

SVMs were used initially for classification. They are based on a concept of decision planes that define decision boundaries (Vapnik 1995; 1998). SVMs were subsequently extended to include support vector regression (SVR) (Scholkopf *et al.*, 2000; Smola & Scholkopf 2004). SVM and SVR use kernel functions to map data into a different space. The concept of a kernel mapping function is powerful. The SVM model algorithmic process utilizes a higher dimensional space to achieve excellent predictive power and offers an important advantage compared with neural network approaches. Specifically, neural networks can suffer from multiple local minima; in contrast, the solution to an SVM is global and unique.

5.1.2 *Technical approach and methodology*

NASA has a constellation of satellites flying in close formation called the A-Train (see Figure 16). Several of these satellites host instruments that make aerosol observations. These include Terra

MODIS and MISR launched in 1999, and Aqua MODIS launched in 2002, Aura OMI launched in 2004, and CALIOP launched in 2006 (Kahn *et al.*, 2005; Remer *et al.*, 2005; Mcgill *et al.*, 2007; Torres *et al.*, 2007; *Winker et al.*, 2007). Aerosol observations from SeaWiFS are also available from GeoEye OrbView-2 satellite launched in 1997 (Hooker & Mcclain 2000).

Several of these instruments provide a daily global picture of AOD. It is a measure of the total light extinction by atmospheric aerosols in a vertical column at a given wavelength from Earth's surface to the top of the atmosphere. For example, MODIS provides AOD across its swath at a spatial resolution of ten kilometres; SeaWiFS' resolution is 1.1 kilometre. A new MODIS product at three kilometre spatial resolution should soon be available. MODIS, OMI and SeaWiFS provide the total global aerosol burden, but not how it is vertically distributed. Other instruments provide detailed vertical aerosol structure while not providing the contiguous global coverage of MODIS, OMI and SeaWiFS. CALIPSO provides corrected backscatter and extinction profiles at 120 metre vertical resolution at altitudes below twenty kilometres, but does not provide contiguous horizontal coverage. MISR provides some vertical information for cases with higher optical depths and distinct plume boundaries but at a coarser resolution than CALIPSO. The CALIPSO observations provide a set of high vertical resolution, narrow swath curtains underneath the satellite overpass. These curtains span the globe daily, but there are substantial gaps between them. Since CALIPSO completes fewer than fifteen orbits per day, there is a longitudinal separation of 24.7° between successive curtains at the equator.

The horizontal resolution of the raw CALIPSO data depends on the altitude. From the surface to eight kilometres, it is 0.33 km; from eight to twenty kilometres, it is one kilometre; from twenty to thirty kilometres, it is 1.66 kilometres; and above thirty kilometres, it is five kilometres. However, the resolution of the corrected CALIPSO backscatter and extinction is a minimum five kilometres and as much as twenty to forty kilometres, if the aerosol loading is light. In Figure 16, one can imagine two complimentary types of aerosol information: a wide swath of Aqua MODIS at the head of the A-Train; followed immediately by a narrow curtain of vertical information collected by CALIPSO.

5.2 *Relating aerosol extinction to $PM_{2.5}$ abundance*

The relationship between $PM_{2.5}$ abundance at Earth's surface and the boundary layer optical depth or aerosol extinction depends on a variety of factors that change both seasonally and geographically. These factors include humidity, temperature, boundary layer height, surface pressure, wind speed and surface type (Liu *et al.*, 2004a; Liu *et al.*, 2004b; Hutchison *et al.*, 2005; Gupta *et al.*, 2006; Koelemeijer *et al.*, 2006; Liu *et al.*, 2007a; Liu *et al.*, 2007b; *Liu et al.*, 2007c; Pelletier *et al.*, 2007; Gupta & Christopher 2008; Hutchison *et al.*, 2008; Zhang *et al.*, 2009).

If the relationship between the AOD observed by MODIS and $PM_{2.5}$ are analysed, it is found that the best correlations are mostly observed over the eastern US in summer and fall (Zhang *et al.*, 2009). The south eastern US has the highest correlation coefficients of more than 0.6. The south western US has the lowest correlation coefficient of approximately 0.2. Several factors are at work. One is that the entire aerosol load does not usually reside within the boundary layer, hence using AOD alone as a proxy for $PM_{2.5}$ introduces a significant error. For example, on the Pacific coast a, a significant fraction of the AOD is due to smoke events in which substantial amounts of aerosol are above the boundary layer. This issue can be addressed by estimating what fraction of the total AOD comes from the boundary layer for each satellite data pixel as described later in Section 5.4.1. In addition, the correlation depends on the version of the satellite retrieval, for example, MODIS v5.2.6 AOD retrievals demonstrate better correlation with $PM_{2.5}$ than v4.0.1 retrievals; but they have much less coverage because of the differences in the cloud-screening algorithm (Zhang *et al.*, 2009). The correlation between AOD and $PM_{2.5}$ is also related to the surface pressure and wind-speed (Smirnov *et al.*, 1995; Lyamani *et al.*, 2006; Choi *et al.*, 2008; Rajeev *et al.*, 2008). This issue can be addressed by using the surface pressure and wind-speed contemporary with each observation used. The surface pressure and wind-speed comes from the meteorological analyses.

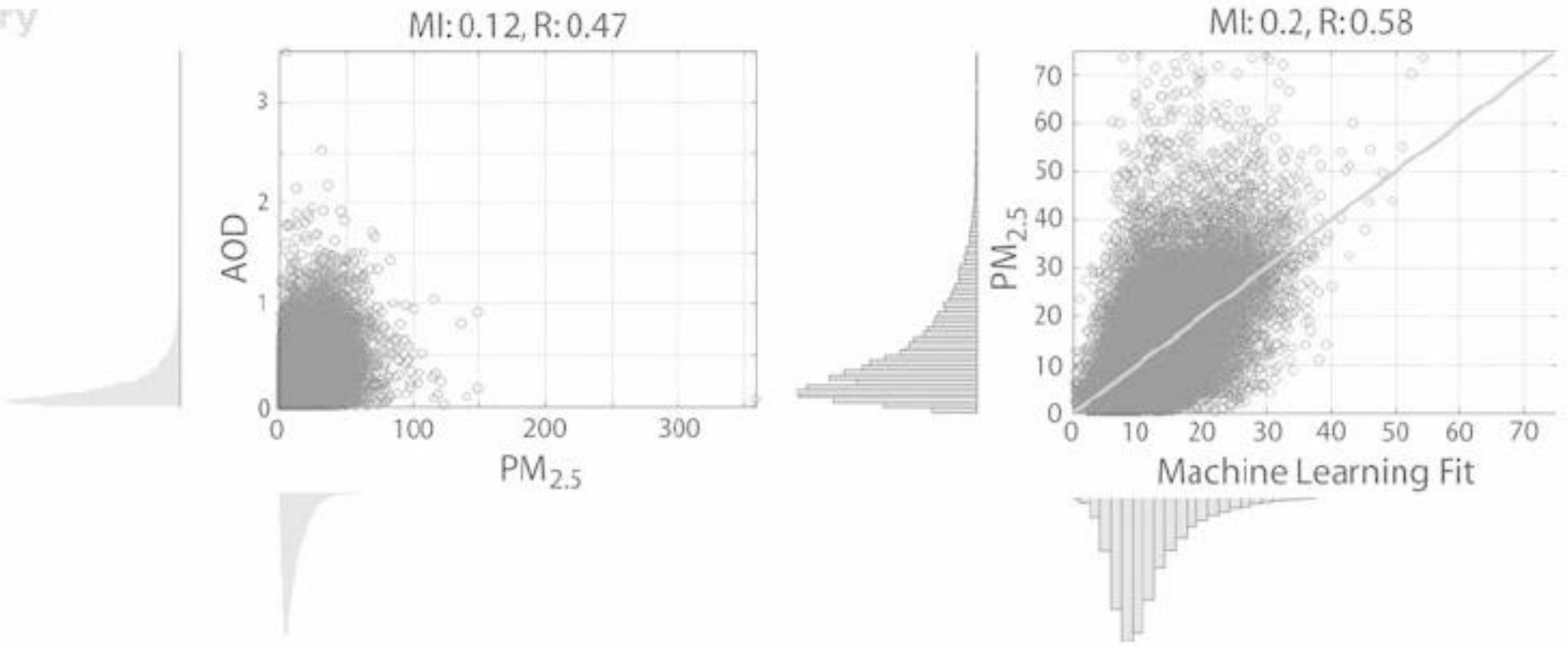

Figure 18. (Left) scatter diagram comparison between MODIS AOD and EPA $PM_{2.5}$; (Right) scatter diagram obtained by machine learning and inferring $PM_{2.5}$ to be a function of the AOD, surface pressure, surface temperature, surface humidity, and planetary boundary layer height.

It has been found that the correlation between AOD and $PM_{2.5}$ increases as the mixing layer height decreases (Gupta *et al.*, 2006). Also higher wind speeds can induce higher mixing layer height, which changes the correlation. Relative humidity (RH) can affect the AOD-$PM_{2.5}$ correlation by changing the optical properties of the aerosols. The higher the relative humidity, the larger the proportion of light scattered, and the larger AOD (Hoff & Christopher 2009). This issue can be addressed by using the humidity and boundary layer height together with each observation used. The humidity comes from the meteorological analyses. The boundary layer height comes from the meteorological analyses and can be verified from the available LiDAR data. The meteorological analyses are available from the modern era retrospective analysis for research and applications (MERRA) system housed at the Goddard Space Flight Centre (GSFC) global modelling and assimilation office (GMAO).

As can be seen from Figure 18, a machine learning multivariate estimate of $PM_{2.5}$ as a function of the AOD, surface pressure, surface temperature, surface humidity, and planetary boundary layer height is more successful at estimating $PM_{2.5}$ than using the AOD alone. The correlation coefficient for Figure 18 (left) is 0.47 and the mutual information 0.12. The correlation coefficient for Figure 18 (right) is 0.58 and the mutual information 0.2. A prototype study conducted by the authors indicates that accounting for the shape of the aerosol vertical profile and estimating the fraction of the total AOD in the boundary layer, f, is important.

Determination of the fraction of total aerosol extinction due to aerosols in the boundary layer is an important missing parameter needed to improve accuracy in the estimate of the $PM_{2.5}$ abundance. To determine the fraction of the total AOD close to the surface for each grid point it is necessary to combine the CALIOP extinction profile curtains in their appropriate meteorological context. There are typically two or three CALIPSO curtains obtained over the US every day. These can be modelled to extend the aerosol height information to the entire grid. The fraction can be estimated in two ways. The first is to use the NAAPS transport model in a reanalysis mode that includes operational MODIS AOD assimilation as well as CALIOP 3D-variational data assimilation (Zhang *et al.*, 2008b; Campbell *et al.*, 2009; Reid *et al.*, 2009; Xian *et al.*, 2009). Several groups have used three-dimensional models to study long-range aerosol transport (Karyampudi *et al.*, 1999; Colarco *et al.*, 2003a; Colarco *et al.*, 2003b; Colarco *et al.*, 2004; Hoff *et al.*, 2005; Hoff *et al.*, 2006; Matichuk *et al.*, 2007; 2008). The fraction can also be estimated by using the Lagrangian/trajectory approach adopted by a variety of NOAA operational forecasts; for example, the smoke forecasting system, the volcanic ash transport and dispersion system, and the emergency assistance activities system. Each of these systems uses a trajectory/dispersion approach to track the motion of air parcels utilizing the HYbrid Single-Particle Lagrangian Integrated Trajectory (HYSPLIT) model.

Several groups have been using trajectory models and CALIPSO data to study long-range aerosol transport (Escudero *et al.*, 2006; Kovacs 2006; Charles *et al.*, 2007; Huang *et al.*, 2007; Feldman *et al.*, 2008; Huang *et al.*, 2008; Hutchison *et al.*, 2008; Liu *et al.*, 2008).

5.2.1 *Data gaps in the AOD products*

While the primary physical challenge in relating $PM_{2.5}$ to AOD observations concerns partitioning total column measurements into vertical components, observational and retrieval challenges of the satellite sensors remain and must be addressed. AOD information provided by an individual sensor might be spatially incomplete, or in some other way insufficient to generate daily global or regional maps. In such cases, judicious merging of co-located data from MODIS, OMI, MISR or SeaWiFS, can fill in many of the data gaps created by missing data, and can create a consistent, reliable, and complete global or regional map. AOD data from these sensors can be optimally combined with error estimates to produce improved AOD estimates. Missing data from one sensor can be provided by available co-located data from another sensor, thus increasing the total data coverage spatially.

The GES-DISC has studied data merging methods for daily AOD from MODIS Terra and Aqua (Leptoukh *et al.*, 2007; Levy *et al.*, 2009; Zubko *et al.*, 2009). They experimented with three methods for pure merging (no interpolation): simple arithmetic averaging (SIM), maximum likelihood estimate (MLE), and weighting by pixel counts (WPC). They applied them to both the global maps and regional subsets and found that the methods produce comparable AODs. The MLE is slightly better with respect to the AOD standard deviation, and the SIM is slightly better with respect to the AOD mean. Other techniques could include data interpolation with empirical orthogonal functions (DINEOF) and independent component analysis (ICA).

5.2.2 *Data biases between AOD products*

Before merging the data as just described one needs to ensure that the various merged outputs agree within the measurement uncertainties and are not biased relative to each other. As part of the joint ESA ENVISAT/NASA Aura validation, a framework has been developed to detect and correct inter-instrument bias effectively as a multi-variate non-linear function of many explanatory factors. What the explanatory factors are depends on the data product being considered.

While progress has been made in understanding the biases between MODIS and AERONET, there is still an imperfect understanding of all the root causes of bias. Biases in a variety of EO data sets have been corrected by using an empirical machine learning approach (Lary *et al.*, 2007; Brown *et al.*, 2008; Lary & Aulov 2008; Lary *et al.*, 2009). As shown in Figure 18 machine-learning algorithms are able to adjust the AOD bias effectively between the MODIS instruments and AERONET (Lary *et al.*, 2009). SVMs performed the best, improving the correlation coefficient between the AERONET AOD and the MODIS AOD from 0.86 to 0.99 for MODIS Aqua and from 0.84 to 0.99 for MODIS Terra. Key in allowing the machine-learning algorithms to correct the MODIS bias was provision of the surface type and other ancillary variables that explain the variance between MODIS and AERONET AOD.

The same techniques can be applied to adjust and merge different EO data sets. Different sensors provide different measurements and make different sets of assumptions. Some data sets have smaller uncertainties under specific conditions than others, and these differences can be using machine learning techniques to optimize a merged product. A partial optimization using this approach was achieved by combining MODIS and MISR AOD, taking into account MISR's superiority in the North American west and MODIS's superior spatial coverage (Van Donkelaar *et al.*, 2006).

5.3 *Public health implications*

The public health implication from this discussion is that a global data product of boundary layer $PM_{2.5}$ may one day be possible. Such a product is useful for a variety of public health applications from long-term epidemiological studies of respiratory conditions, to pro-active real time alerts for people with asthma.

5.3.1 *Classification*

There are numerous occasions in public health when classification based on the information available must be made. In optimal situations there is *a priori* information that makes classification possible. Most often, however, situations arise that require a classification but there is no *a priori* basis for making it. In such situations unsupervised machine learning proves very useful. In the first part of this Section a global $PM_{2.5}$ data product was described based on observations. A similar forecast product could be derived also based on model simulations. A key factor to providing a good $PM_{2.5}$ prediction would be to delineate surface dust and aerosol sources accurately. Providing such a classification is non-trivial. Machine learning takes a radically different approach to provide an unsupervised multi-variate and non-linear classification of surface types using multi-spectral satellite data. The process would allow automatic identification of dust sources that, in turn, lead to air-borne particulates and their associated health impacts.

5.3.2 *Self-organizing maps*

Self-organizing maps (SOMs) are created by a data visualization and unsupervised classification technique that reduce the dimensions of data through self-organizing neural networks (Kohonen 1982; 1990). They help address the issue that humans simply cannot visualize high dimensional data. The way SOMs reduce dimensionality is by producing a map, usually with two dimensions, that plots the similarities of the data objectively by grouping similar data items together. SOMs learn to classify input vectors according to how they are grouped in the input space. They differ from competitive layers in that neighbouring neurons in the self-organizing map learn to recognize neighbouring sections of the input space. Thus, self-organizing maps learn both the distribution and topology of the input vectors they are trained on. This approach allows SOMs to accomplish two things, reduce dimensions and display similarities.

A SOM attempts to replicate the computational power of biological neural networks, with the following important features: 1) non-linearity – the ability to represent non-linear functions or mappings; 2) non-parametric – they do not presume *a priori* a functional form for the data being analysed; 3) adaptability – the ability to change the internal representation (connection weights, network structure) if new data or information are available; 4) robustness – ability to handle missing, noisy or otherwise confusing data; and 5), power/speed – the ability to handle large data volumes in acceptable time due to inherent parallelism (Kohonen 1995; 1997; 2001).

5.4 *EO data for dust source classification*

For many environmental applications, satellite spectral imaging has become a tool of preference for collecting information about Earth's surface. These multi-wavelength data provide signatures relevant for a wide variety of applications. However, classifying these intricate and high-dimensional data sets is far from trivial. Discriminating among many surface cover classes and discovering spatially small but interesting spectral categories has proved to be an insurmountable challenge to many traditional clustering and classification methods (Villmann *et al.*, 2003). By customary measures, such as principal component analysis, the intrinsic spectral dimensionality of hyperspectral images appears to be surprisingly low. Yet, dimensionality reduction has not always been successful in terms of preservation of important surface class distinctions. The spectral bands, many of which are highly correlated, may lie on a low-dimensional but non-linear manifold, which is a scenario that eludes many classical approaches. In addition, these data comprise enormous volumes and are frequently noisy. This motivates research into advanced and novel approaches for image analysis and, in particular, machine learning using neural network self-organizing maps (Merenyi *et al.*, 1996).

Data from the two MODIS instruments aboard the Terra (EOS AM) and Aqua (EOS PM) satellites are the basis for this case study (NASA 2012b). Terra and Aqua MODIS are viewing the entire Earth's surface every one to two days, acquiring data in thirty-six spectral bands. These data are used to provide an albedo product of both directional hemispherical reflectance (black-sky albedo, BSA) and bi-hemispherical reflectance (white-sky albedo, WSA). The output product is based on

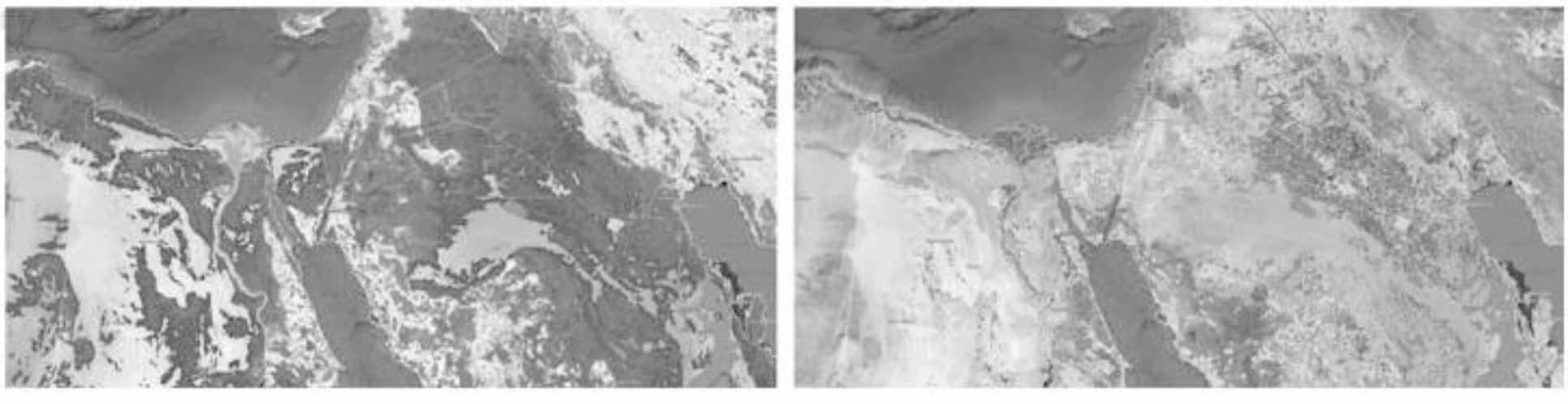

Figure 19. (Left) shows a region centred on Iraq. All the land pixels that could contain dust sources were classified by a SOM into 1000 classes. (Right) shows the small subset of SOM classes (shown in red) that have the largest overlap with regions identified as dust sources by NRL. (see colour plate 33)

the level-3 gridded data product containing sixteen days of data projected onto a 0.05° (5.6 km) lat/lon grid.

5.4.1 *Methodology*

The goal was to identify all the surface locations on the planet that are dust sources. A SOM was used to classify all land surface locations into a set of categories, a subset of which encompasses regions that are dust sources. There are many types of dust sources ranging in size, physiographic position, elevation and land use practices that were delineated. For example in Figure 19 the Nile delta is in a different class from mountainous regions. The SOM did an acceptable job of distinguishing the surface types, even placing Chad's Bodele in a class all of its own.

To achieve a comprehensive classification it was necessary to consider surface conditions throughout the year. An entire year of daily data at 0.05° (roughly 7.5 km^2) was therefore created. A massive data set was generated from which to calculate the mean, μ, for each grid point. Attention was first restricted to those broad MODIS surface categories that could include dust sources. Those are barren or sparsely vegetated surfaces, croplands, savannah, grasslands, and open and closed shrub lands. For each of these cover types an input vector was constructed that contained seven values, one for each of the seven bands provided in the MODIS product the mean, μ, of the WSA. When training the SOM, the Euclidean distance was used to compare the input vectors.

To provide a fine gradation of categories the SOM grouped the surface locations into 1000 classes, only a small subset of which actually correspond to regions that are dust sources (Figure 19). Once the classes corresponding to potential dust sources were identified, an automated method that could be executed routinely was used to identify actual dust sources. Figure 19 (left) shows all the land surface pixels over a region centred on Africa classified by a SOM into 1000 classes. Figure 19 (right) shows a subset of those 1000 classes that have the largest overlap with regions that were selected laboriously by an analyst as dust sources. There is a high degree of overlap between a subset of the SOM classes shown in blue and cyan, and those selected by the analyst shown in red. The regions are hard to identify manually so the red regions have an associated uncertainty.

Now that the signatures for potential dust sources have been identified using the SOM, areas having the same signature can be selected automatically for other land areas of the globe. An example of this is shown in Figure 20. The regions identified are very plausible dust sources, typically around the periphery of desert regions. These selections were regarded as very impressive by the same analyst that manually created the red regions in Figure 19 (right). From these data, there seems to be a method for automatically identifying global dust sources, and monitoring how they change with time. These sources can then be used in the forecast models used to produce $PM_{2.5}$ forecasts, with obvious public health applications (e.g. for personalized alerts for the twenty-two million plus asthma sufferers in the US).

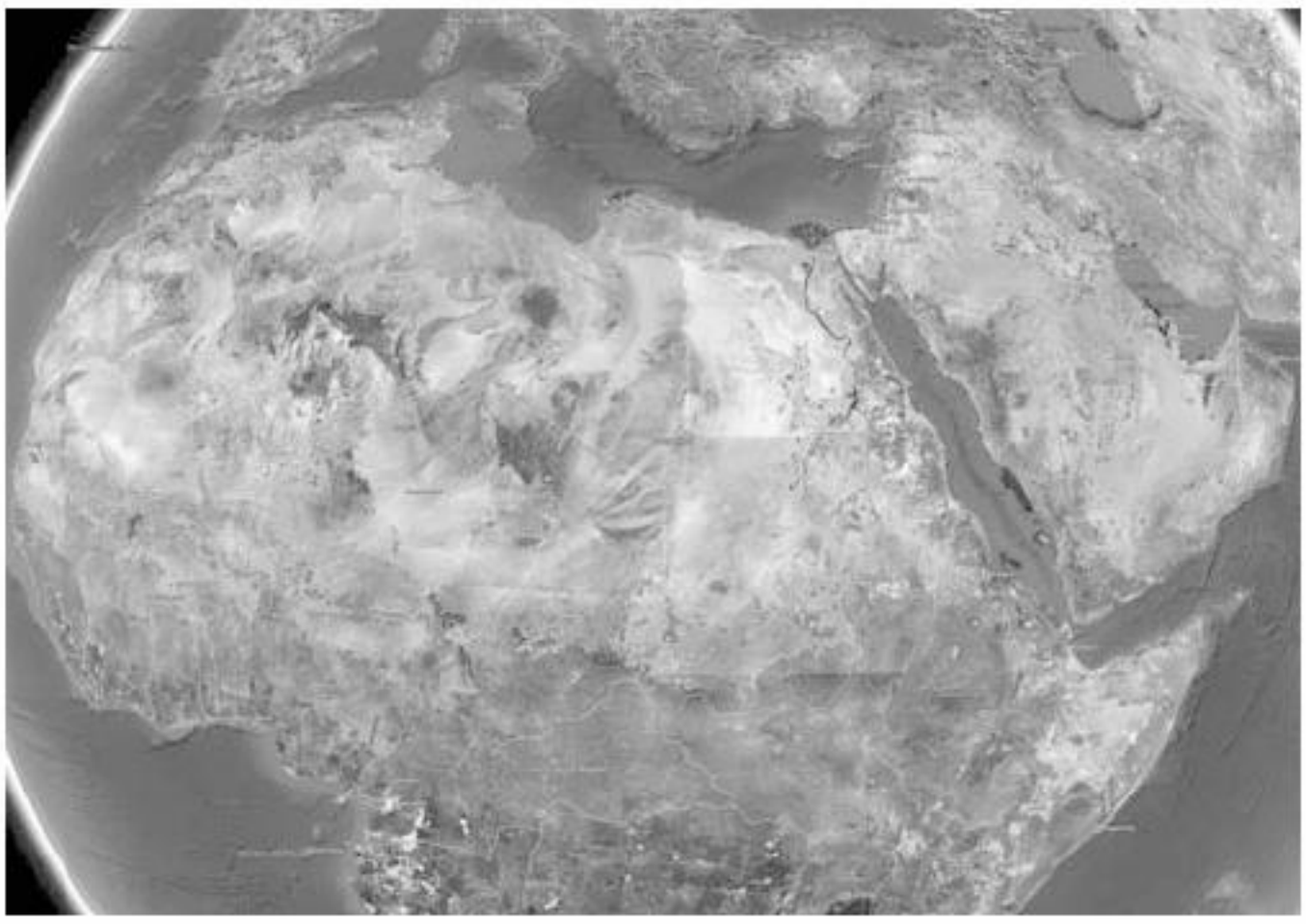

Figure 20. The shaded pixels (blue and cyan) show all the land surface pixels in the SOM classes identified as dust sources. These classes were the same SOM classes displayed in Figure 19 (right). (see colour plate 34)

6 FUTURE DIRECTIONS

Current and future Earth-observing satellite systems will enable scientists to more accurately track and study atmospheric events (Haynes 2009). Several countries have used data from these systems to formulate actions for improving data collection, access, and analysis capabilities (Williamson & Obermann 2002). As a result of growing evidence and concern for global air quality impacts on health, the Group on Earth Observations was created in 2003. The developing world suffers most from severe consequences of natural disasters and also faces inadequacies in accessing satellite sensor data that can aid in disaster warning, relief mobilization, and telemedical support (Jayaraman *et al.*, 1997). The volcanic eruption of Eyjafjallajökull in Iceland was a sharp reminder of the far reaching economic, social, and health-related impacts of volcanoes (Laursen 2010). Based on recent estimates, the Eyjafjallajökull eruptions have cost airlines upward of two billion $USD (Batty 2010). Currently, WMO is developing a sand and dust storm warning advisory and assessment system (SDSWAS) which, when fully implemented, will provide global data accessible through regional processing centres in Spain, China, and Japan. The WMO website provides links that report current global weather events as they might impact human and societal health. There are numerous websites that provide very specific, current and archived environmental data from Earth-observing platforms, as well as a growing toolbox of models designed for use by health communities of practice. What is needed regarding public health are studies on the presence of pathogenic microorganisms, naturally occurring toxic metals, and pollutants such as pesticides, herbicides, and industrial emissions that utilize model-derived data. Validation of models is needed to advance their use as public health tools that may one day provide widespread real-time data to healthcare and public-health protection personnel, and the public in general.

A growing number of research groups utilize model and satellite data to illustrate relationships between atmospheric constituents, their sources, impacts on humans, and transmission pathways. More of these types of projects are needed to advance aerosol monitoring for public health (Jaffe *et al.*, 2003; Griffin 2007). Limitations of current methodologies will diminish in time. Advances will continue to be made in computing, molecular biology, chemistry, and sensor system technologies. Existing capabilities are already sufficiently robust to advance public-health studies at all geographic scales from local to global. Although there are toxicology programs, a few aerobiology programs, and numerous meteorology programs, most are discipline-specific and do not offer the opportunity to investigate global scale questions that require integrated approaches. A

broadening of research areas in meteorology programs is needed. The need for research to address the movement of particles in the atmosphere was recognized in 1935 by Meier & Lindbergh in which they state…*The potentialities of world-wide distribution of spores of fungi and other organisms caught up and carried abroad by trans-continental winds may be of tremendous economic consequence.*

REFERENCES

Akesson, N.B. & Yates, W.E. 1964. Problems relating to application of agricultural chemicals and resulting drift residues. *Ann. Rev. Entom.* 9(1): 285–318.

Al Frayh, A.R., Shakoor, Z., Gad El Rab, M.O. & Hasnain, S.M. 2001. Increased prevalence of asthma in Saudi Arabia. *Ann. Allerg. Asth. & Immun.* 86(3): 292–296.

Amann, R.I., Ludwig, W. & Schleifer, K.H. 1995. Phylogenetic identification and in situ detection of individual microbial cells without cultivation. *Microbio. Rev.* 59(1): 143–169.

Andronico, D., Spinetti, C., Cristaldi, A. & Buongiorno, M.F. 2009. Observations of Mt. Etna volcanic ash plumes in 2006: An integrated approach from ground-based and polar satellite NOAA-AVHRR monitoring system. *J. Volcan. & Geoth. Res.* 180(2–4): 135–147.

Arkhipov, N.P., Kuchma, N.D. Askbrant, S., Pasternak, P.S. & Musica, V.V. 1994. Acute and long-term effects of irradiation on pine (*Pinus silvestris*) stands post-Chernobyl. *Sci. Total Environ.* 157: 383–386.

Aronson, N.E., Sanders, J.W. & Moran, K.A. 2006. In harm's way: Infection in deployed American military forces. *Clin. Infect. Dis.* 43: 1045–1051.

AVO. 2010. Alaska Volcano Observatory. Available from: http://www.avo.alaska.edu [Accessed 20th March 2012].

Batty, D. 2010. Icelandic volcano now appears to be dormant say scientists. *Guardian Weekly 23May2010*

Baxter, P.J. 2003. The eruption of El Reventador volcano 2002: Health hazards and the implications for volcano risk management in Ecuador. Washington DC: PAHO

Baxter, P.J., Ing, R., Falk, H., French, J., Stein, G.F., Bernstein, R.S., Merchant, J.A. & Allard, J. 1981. Mount St. Helens eruptions, May 18 to June 12, 1980. An overview of the acute health impact. *J. Amer. Med. Assoc.* 246(22): 2585–2589.

Baxter, P.J., Ing, R., Falk, H. & Plikaytis, B. 1983. Mount St. Helens eruptions: The acute respiratory effects of volcanic ash in a North American community. *Arch. Environ. Health* 38(3): 138–143.

Baxter, P.J., Bonadonna, Dupree, C.R., Hards, V.L., Kohn, S.C., Murphy, M.D., Nichols, A., Nicholson, R.A., Norton, G., Searl, A., Sparks, R.S. & Vickers, B.P. 1999. Cristobalite in volcanic ash of the Soufriere Hills volcano, Montserrat, British West Indies. *Science* 283(5405): 1142–1145.

Becker, S., Soukup, J.M. & Gallagher, J.E. 2002. Differential particulate air pollution induced oxidant stress in human granulocytes, monocytes and alveolar macrophages. *Toxicol. in Vitro* 16(3): 209–218.

Becker, S., Mundandhara, S., Devlin, R.B. & Madden, M. 2005. Regulation of cytokine production in human alveolar macrophages and airway epithelial cells in response to ambient air pollution particles: Further mechanistic studies. *Toxicol. & Appl. Pharmacol.* 207(2): 269–275.

Belser, J.A., Blixt, O., Chen, L.M., Pappas, C., Maines, T.R., Van Hoeven, N., Donis, R., Busch, J., Mcbride, R., Paulson, J.C., Katz, J.M. & Tumpey, T.M. 2008. Contemporary North American influenza H7 viruses possess human receptor specificity: Implications for virus transmissibility. *Proc. Nat. Acad. Sci.* 105(21): 7558–7563.

Bener, A., Abdulrazzaq, Y.M., Al-Mutawwa, J. & Debuse, P. 1996. Genetic and environmental factors associated with asthma. *Human Biology* 68(3): 405–414.

Betzer, P.R., Carder, K.L., Duce, R.A., Merrill, J.T., Tindale, N.W., Uematsu, M., Costello, D.K., Young, R.W., Feely, R.A., Freland, J.A., Bernstein, R.E. & Greco, A.M. 1988. Long-range transport of giant mineral aerosol particles. *Nature* 336(6199): 568–571.

Bluth, G.J.S., Schnetzler, C.C. Krueger, A.J. & Walter, L.S. 1993. The contribution of explosive volcanism to global atmospheric sulphur dioxide concentrations. *Nature* 366(6453): 327–329.

Broecker, W.S. 2000. Abrupt climate change: Causal constraints provided by the paleoclimate record. *Earth-Sci. Rev.* 51(1–4): 137–154.

Broughton, E. 2005. The Bhopal disaster and its aftermath: A review. *Environ. Health* 4(1): 6.

Brown, E.G., Gottlieb, S. & Laybourn, R.L. 1935. Dust storms and their possible effect on health. *Public Health Repts.* 50(40): 1369–1383.

Brown, J.H., Cook, K.M., Ney, F.G. & Hatch, T. 1950. Influence of particle size upon the retention of particulate matter in the human lung. *Amer. J. Pub. Health* 40(4): 450–458.

Brown, J.S., Zeman, K.L. & Bennett, W.D. 2002. Ultrafine particle deposition and clearance in the healthy and obstructed lung. *Amer. J. Respir. & Criti. Care Med.* 166 (9):1240–1247.

Brown, M.E., Lary, D.J., Vrieling, A., Stathakis D. & Mussa, H. 2008. Neural networks as a tool for constructing continuous NDVI time series from AVHRR and MODIS. *Int. J. Rem. Sens* 29(24): 7141–7158.

Cahill, T.A., Gill, T.E., Reid, J.S., Gearhart, E.A. & Gillette, D.A. 1998. Saltating particles, playa crusts and dust aerosols at Owens (dry) Lake, California. *Earth Surf. Proc. & Landforms* 21(7): 621–639.

Campbell, J.R., Reid, J.S. Westphal, D.L., Zhang, J., Hyer, E.J. & Welton, E.J. 2010. CALIOP aerosol subset processing for global aerosol transport model data assimilation. *J. Sel. Topics in Appl. Earth Obs. & Rem. Sens.* 3(2): 203–214.

Carapezza, M.L., Badalamenti, B., Cavarra, L. & Scalzo, A. 2003. Gas hazard assessment in a densely inhabited area of Colli Albani volcano (Cava dei Selci, Roma). *J. Volcan. & Geoth. Res.* 123(1–2): 81–94.

Carter, A.J. & Ramsey, M.S. 2009. ASTER- and field-based observations at Bezymianny Volcano: Focus on the 11 May 2007 pyroclastic flow deposit. *Rem. Sens. Environ.* 113(10): 2142–2151.

Casadevall, T.J. 1994. The 1989–1990 eruption of Redoubt volcano, Alaska: Impacts on aircraft operations. *J. Volcan. & Geoth. Res.* 62(1–4): 301–316.

Castranova, V., Bowman, L. Shreve, J.M., Jones, G.S. & Miles, P.R. 1982. Volcanic ash: Toxicity to isolated lung cells. *J. Toxicol. & Environ. Health,* 9(2*Part* A): 317–325.

Castronovo, D., Chui, K. & Naumova, E. 2009. Dynamic maps: A visual-analytic methodology for exploring spatio-temporal disease patterns. *Environ. Health* 8(1): 61–70.

Chan, C.C., Chuang, K.J., Chen, W.J., Chang, W.T., Lee, C.T. & Peng, C.M. 2008. Increasing cardiopulmonary emergency visits by long-range transported Asian dust storms in Taiwan. *Environ. Res.* 106(3): 393–400.

Chang, C.C., Lee, I.M., Tsai, S.S. & Yang, C.Y. 2006. Correlation of Asian dust storm events with daily clinic visits for allergic rhinitis in Taipei, Taiwan. *J. Toxicol. & Environ. Health* A 69(3): 229–235.

Charles, L., Gross, B., Moshary, F., Wu, Y., Vladutescu, V. & Ahmed, S. 2007. Atmospheric transport of smoke and dust particulates and their interaction with the planetary boundary layer as observed by multi-wavelength lidar and supporting instrumentation. *Lidar Rem Sens. Environ. Monitor.* VIII. UN Singh. 6681: U157–U167.

Chen, P.S., Tsai, F.T., Lin, C.K., Yang, C.Y., Chan, C.C., Young, C.Y. & Lee, C.H. 2010. Ambient influenza and avian influenza virus during sandstorm days and background days. *Environ. Health Perspec.* 118(9): 1211–1216.

Chesser, R.K. & Baker, R.J. 2006. Growing up with Chernobyl. *Amer. Sci.* 94(6): 542–549.

Chiu, H.F., Tiao, M.M., Ho, S.C., Kuo, H.W., Wu, T.N. & Yang, C.Y. 2008. Effects of Asian dust storm events on hospital admissions for chronic obstructive pulmonary disease in Taipei, Taiwan. *Inhal. Toxicol.* 20(9): 777–781.

Choi, Y.S., Ho, C.H., Chen Ho, D., Noh,Y.H. & Song, C.K. 2008. Spectral analysis of weekly variation in PM10 mass concentration and meteorological conditions over China. *Atmosph. Environ.* 42(4): 655–666.

Chrysoulakis, N. & Cartalis, C. 2003. A new algorithm for the detection of plumes caused by industrial accidents, based on NOAA/AVHRR imagery. *Int. J. Rem. Sens.* 24(17): 3353–3368.

Chrysoulakis, N., Adaktylou, N. & Cartalis, C. 2005. Detecting and monitoring plumes caused by major industrial accidents with JPLUME, a new software tool for low-resolution image analysis. *Environ. Model. & Software* 20(12): 1486–1494.

Chrysoulakis, N., Herlin, I., Prastacos, P., Yahia, H., Grazzini, J. & Cartalis, C. 2007. An improved algorithm for the detection of plumes caused by natural or technological hazards using AVHRR imagery. *Rem. Sens. Environ.* 108(4): 393–406.

Chui, K.H., Castronovo, D.A., Jagai, J.S., Kosheleva, A.A. & Naumova, E.N. 2006. Gastroenteritis infections in the U.S. elderly and extreme weather events: Exposures to Atlantic tropical storms of 1998–2002. *Epidemiology* 17(6): S477.

Cifuentes, L.A., Krupnick, A.J. 2005. Urban air quality and human health in Latin America and the Caribbean. Inter Amer. Dev. Bank. Available from: http://www.iadb.org/sds/env [Accessed 20th March 2012].

Colarco, P.R., Toon, O.B. & Holben, B.N. 2003a. Saharan dust transport to the Caribbean during PRIDE: 1. Influence of dust sources and removal mechanisms on the timing and magnitude of downwind aerosol optical depth events from simulations of in situ and remote sensing observations. *J. Geophys. Res. Atmosph.* 108(D19): 8589.

Colarco, P.R., Toon, O.B., Reid, J.S., Livingston, J.M., Russell, P.B., Redemann, J., Schmid, B., Maring, H.B., Savoie, D., Welton, E.J., Campbell, J.R., Holben, B.N. & Levy, R. 2003b. Saharan dust transport to the Caribbean during PRIDE: 2. Transport, vertical profiles, and deposition in simulations of in situ and remote sensing observations. *J. Geophys. Res. Atmosph. 108(D19):*8590.

Cook, A.G., Weinstein, P. & Centeno, J.A. 2005. Health effects of natural dust – Role of trace elements and compounds. *Biol. Trace Element Res.* 103(1): 1–15.

Corbett, E.L., Churchyard, G.J., Clayton, T., Herselman, P., Williams, B., Hayes, R., Mulder, D. & De Cock, K.M. 1999. Risk factors for pulmonary mycobacterial disease in South African gold miners. A case-control study. *Amer. J. Respir. Criti. Care Med.* 159(1): 94–99.

Cramer, H.H. 1967. Plant protection and world crop production.*Pflanzenschutz-Nachrichten 'Bayer'*20: 1–524.

Crowley, J.K., Hubbard, B.E. & Mars, J.C. 2003. Analysis of potential debris flow source areas on Mount Shasta, California, by using airborne and satellite remote sensing data. *Rem. Sens. Environ.* 87(2–3): 345–358.

Cullen, R.T., Jones, A.D., Miller, B.G., Tran, C.L., Davis, J.M.G., Donaldson, K., Wilson, M., Stone, V. & Morgan, A. 2002. Toxicity of volcanic ash from Montserrat. *Edinburgh. Inst. Occupat. Med.* Research Report TM/02/01.

Daigle, C.C., Chalupa, D.C., Gibb, F.R., Morrow, P.E., Oberdorster, G., Utell, M.J. & Frapton, M.W. 2003. Ultrafine particle deposition in humans during rest and exercise. *Inhal. Toxicol.* 15(6): 539–552.

Dalton, M.P., Bluth, G.J.S., Prata, A.J., Watson, I.M. & Carn, S.A. 2006. Ash, SO_2, and aerosol analysis of the November 2002 eruption of Reventador volcano, Equador, using TOMS, HIRS, and MODIS satellite sensors. *Cities on Volcanoes, Fourth Conference*. Quito, Ecuador.

Dauer, L.T., Zanzonico, P., Tuttle, R.M., Quinn, D.M. & Strauss, H.W. 2011. The Japanese tsunami and resulting nuclear emergency at the Fukushima Daiichi power facility: Technical, radiologic, and response perspectives. *J. Nucl. Med.* 52:1423–1432.

de Deckker, P., Abed, R.M.M., de Beer, D., Hinrichs, K.U., O'loingsigh, T., Schefufl, E., Stuut, J.B.W., Tapper, N.J. & van der Kaars, S. 2008. Geochemical and microbiological fingerprinting of airborne dust that fell in Canberra, Australia in October 2002. *Geochem. Geophy. Geosyst.* 9, Q12Q10, doi:10.1029/2008GC002091.

de la Cadena, M. 2006. Risk management of volcanic crises in Quito's metropolitan area. *Cities on Volcanoes, Fourth Conference*. Quito, Ecuador.

de Souza Porto, M.F. & Freitas, C.M. 1996. Major chemical accidents in industrializing countries: The social-political amplification of risk. *Risk Anal.* 16(1): 19–29.

Dean, K.G., Dehn, J., Papp, K.R., Smith, S., Izbekov, P., Peterson, R., Kearney, C. & Steffke, A. 2004. Integrated satellite observations of the 2001 eruption of Mt. Cleveland, Alaska. *J. Volcan. & Geoth. Res.* 135(1–2): 51–73.

Delmelle, P., Stix, J., Bourque, C.P., Baxter, P.J., Garcia-Alvarez, J. & Barquero, J. 2001. Dry deposition and heavy acid loading in the vicinity of Masaya volcano, a major sulfur and chlorine source in Nicaragua. *Environ. Sci. & Tech.* 35(7): 1289–1293.

Dhara, V.R., Dhara, R., Acquilla, S.D. & Cullinan, P. 2002. Personal exposure and long-term health effects in survivors of the Union Carbide disaster at Bhopal. *Environ. Health Perspec.* 110(5): 487–500.

Diaz, V., Parra, R., Ibarra, B. & Paez, C. 2006. Monitoring of ash from volanic eruptions in Quito, Ecuador. *Cities on Volcanoes, Fourth Conference*. Quito, Ecuador.

Dockery, D. 2006. Concentration and acidity of airborne particulate matter in communities of the big island of Hawaii. *Cities on Volcanoes, Fourth Conference*. Quito, Ecuador.

Doebbeling, B.N., Clarke, W.R., Watson, D., Torner, J.C., Woolson, R.G., Boelker, M.D., Barrett, D.H. & Schwartz., D.A. 2000. Is there a Persian Gulf War syndrome? Evidence from a large population-based survey of veterans and nondeployed controls. *Amer. J. Med.* 108(9): 695–704.

Donaldson, K., Stone, V., Gilmour, P.S., Brown, D.M. & Macnee, W. 2000. Ultrafine particles: Mechanisms of lung injury. *Phil. Trans. Roy. Soc. Lond. Series A: Math., Phys. & Engin. Sci.* 358(1775): 2741.

Dowd, S.E. & Maier, R.M. 2000. Aeromicrobiology. In: R.M. Maier, I.L Pepper. & C.P. Gerba, (eds.), *Environmental microbiology*. San Diego: Academic Press.

Draxler, R.R. & Hess, G.D. 1998. An overview of the HYSPLIT_4 modelled system for trajectories, dispersion, and deposition. *Austral. Meteorol. Mag.* 47(4): 295–308.

Driscoll, K.E. 1996. Role of inflammation in the development of rat lung tumors in response to chronic particle exposure. In J.J.L. Mauderly & R.J. McCunney (eds), *Particle overload in the rat lung and lung cancer: Implications for human risk assessment*: 139–153. Philadelphia: Taylor & Francis.

Duchnowicz, P., Szczepaniak, P. & Koter, M. 2005. Erythrocyte membrane protein damage by phenoxyacetic herbicides and their metabolites. *Pestic. Biochem. & Physiol.* 82(1): 59–65.

Durry, E., Pappagianis, D., Werner, S.B., Hutwagner, L., Sun, R.K., Maurer, M., Mcneil, M.M. & Pinner, R.W. 1997. Coccidioidomycosis in Tulare County, California, 1991: Reemergence of an endemic disease. *Med. Mycol.* 35(5): 321–326.

Dwernychuk, L.W., Cau, H.D., Hatfield, C.T., Boivin, T.G., Hung, T.M., Dung, P.T. & Thai, N.D. 2002. Dioxin reservoirs in southern Vietnam–A legacy of Agent Orange. *Chemosphere* 47(2): 117–137.

Ecobichon, D.J. & Joy, R.M. 1994. *Pesticides and Neurological Diseases*. Boca Raton: CRC Press.
Egan, T. 2006. *The worst hard time*. New York: Houghton Mifflin.
Ellrod, G.P. 2003. Development of volcanic ash image products using MODIS multi-spectral data. *Amer. Met. Soc. Ann. Mtg*. Long Beach, CA.
Ellrod, G.P., Connell, B.H. & Hillger, D.W. 2003. Improved detection of airborne volcanic ash using multispectral infrared satellite data. *J. Geophys. Res.* 108(D12): 4356.
EO. 2012. Available from: http://earthobservatory.nasa.gov [Accessed 4th February 2012].
Erickson, J.D., Mulinare, J., Mcclain, P.W., Fitch, T.G., James, L.M., Mcclearn, A.B. & Adams Jr., M.J. 1984. Vietnam veterans' risks for fathering babies with birth defects. *J. Amer. Med. Assoc.* 252(7): 903–912.
Escudero, M., Stein, A. Draxler, R.R., Querol, X., Alastuey, A., Castillo, S. & Avila, A. 2006. Determination of the contribution of northern Africa dust source areas to PM10 concentrations over the central Iberian peninsula using the hybrid single-particle Lagrangian integrated trajectory model (HYSPLIT) model. *J. Geophys. Res. Atmosph.* 111(D6): 210.
Estrella, B., Estrella, R., Oviedo, J., Narvez, X., Reyes, M.T., Gutierrez, M. & Naumova, E.N. 2005. Acute respiratory diseases and carboxyhemoglobin status in school children of Quito, Ecuador. *Environ. Health Perspec.* 113(5): 607–611.
Fiese, M.J. 1958. *Coccidioidomycosis*. Springfield: Charles C. Thomas.
Filizzola, C., Lacava, T., Marchese, F., Pergola, N., Scaffidi, I. & Tramutoli, V. 2007. Assessing RAT (Robust AVHRR Techniques) performances for volcanic ash cloud detection and monitoring in near real-time: The 2002 eruption of Mt. Etna (Italy). *Rem. Sens. Environ.* 107(3): 440–454.
Friedman, J.M. 2005. Does Agent Orange cause birth defects? *Teratology* 29(2): 193–221.
Fukuda, K., Nisenbaum, R., Stewart, B., Thompson, W.W., Robin, L., Washko, R.M., Noah, D.L., Barrett, D.H., Randall, B., Herwaldt, B.L., Mawle, A.C. & Reeves, W.C. 1998. Chronic multisymptom illness affecting Air Force veterans of the Gulf War. *J. Amer. Med. Assoc.* 280(11): 981–988.
Fung, I.Y., Meyn, S.K., Tegen, I., Doney, S.C., John, J.G. & Bishop, J.K.B. 2000. Iron supply and demand in the upper ocean. *Global Biogeochem. Cycles* 14(1): 281–295.
Gangale, G., Prata, A.J. & Clarisse, L. 2009. The infrared spectral signature of volcanic ash determined from high-spectral resolution satellite measurements. *Rem. Sens. Environ.* 114(2): 414–425.
Gans, J., Wolinsky, M. & Dunbar, J. 2005. Computational improvements reveal great bacterial diversity and high metal toxicity in soil. *Science* 309: 1387–1390.
Gao, T., Yu, X., Ma, Q., Li, H., Li, X. & Si, Y. 2003. Climatology and trends of the temporal and spatial distribution of sandstorms in Inner Mongolia. *Water, Air, & Soil Pollu.* 3(2): 51–60.
Garcia-Aristizabal, A., Kumagai, H., Samaniego, P., Mothes, P., Yepes, H. & Monzier, M. 2007. Seismic, petrologic, and geodetic analyses of the 1999 dome-forming eruption of Guagua Pichincha volcano, Ecuador. *J. Volcan. Geoth. Res.* 161(4): 333–351.
Giannini, A., Saravanan, R. & Chang, P. 2003. Oceanic forcing of Sahel rainfall on interannual to interdecadal time scales. *Science* 302: 1027–1030.
Giggenbach, W.F. 1990. Water and gas chemistry of Lake Nyos and its bearing on the eruptive process. *J. Volcan. & Geoth. Res.* 42(4): 337–362.
Giggenbach, W.F., Sano, Y. & Schmincke, H.U. 1991. CO_2-rich gases from Lakes Nyos and Monoun, Cameroon; Laacher See, Germany; Dieng, Indonesia, and Mt. Gambier, Australia–Variations on a common theme. *J. Volcan. & Geoth. Res.* 45(3–4): 311–323.
Gillette, D., Ono, D. & Richmond, K. 2004. A combined modeling and measurement technique for estimating windblown dust emissions at Owens (dry) Lake, California. *J. Geophys. Res. – Earth* 109(F1): 337–362.
Ginzburg, H.M. & Reis, E. 1991. Consequences of the nuclear power plant accident at Chernobyl. *Pub. Health Repts.* 106(1): 32.
Giraudi, C. 2005. Eolian sand in peridesert northwestern Libya and implications for Late Pleistocene and Holocene Sahara expansions. *Palaeogeo., Palaeoclim., Palaeoecol.* 218(1–2): 161–173.
Glaze, L.S. & Baloga, S.M. 2003. DEM flow path prediction algorithm for geologic mass movements. *Environ. & Engin. Geosci.* 9(3): 225–240.
Glennon, J.J., Nichols, T., Gatt, P., Baynard, T., Marquardt, J.H. & Vanderbeek, R.G. 2009. *System performance and modeling of a bioaerosol detection lidar sensor utilizing polarization diversity*. Laser Radar Technology & Applications XIV, Orlando, FL.
Goklany, I.M. 2007. Death and death rates due to extreme weather events: Global and U.S. trends, 1900–2004. In: *The Civil Society Report on Climate Change*:47–59. London: International Policy Press.
Gong, S.L., Zhang, X.Y., Zhao, T.L., Zhang, X.B., Barrie, L.A., Mckendry, I.G. & Zhao, C.S. 2006. A simulated climatology of Asian dust aerosol and its trans-Pacific transport. Part II: Interannual variability and climate connections. *J. Climate* 19(1): 104–122.

Goudie, A.S. & Middleton, N.J. 2001. Saharan dust storms: Nature and consequences. *Earth Sci. Rev.* 56: 179–204.

Graham, W.F. & Duce, R.A. 1979. Atmospheric pathways of the phosphorus cycle. *Geochim. et Cosmochim. Acta* 43: 1195–1208.

Gray, G.C., Reed, R.J., Kaiser, K.S., Smith, T.C. & Gastanaga, V.M. 2002. Self-reported symptoms and medical conditions among 11,868 Gulf War-era veterans: The Seabee health study. *Amer. J. Epidem.* 155(11): 1033.

Gregory, P.H. 1961. *The Microbiology of the Atmosphere*. London: Leonard Hill Books Ltd.

Griffin, D.W. 2004. Terrestrial microorganisms at an altitude of 20,000 m in Earth's atmosphere. *Aerobiologia* 20: 135–140.

Griffin, D.W. 2007. Atmospheric movement of microorganisms in clouds of desert dust and implications for human health. *Clin. Microbio. Rev.* 20(3): 459–477.

Griffin, D.W. 2008. Non-spore forming eubacteria isolated at an altitude of 20,000 m in Earth's atmosphere: extended incubation periods needed for culture-based assays. *Aerobiologia* 24(1): 19–25.

Griffin, D.W., Garrison, V.H., Herman, J.R. & Shinn, E.A. 2001. African desert dust in the Caribbean atmosphere: Microbiology and public health. *Aerobiologia* 17(3): 203–213.

Griffin, D.W., Kellogg, C.A. & Shinn, E.A. 2001. Dust in the wind: Long-range transport of dust in the atmosphere and its implications for global public and ecosystem health. *Global Change & Human Health* 2(1): 20–33.

Griffin, D.W., Kellogg, C.A., Garrison, V.H. & Shinn, E.A. 2002. The global transport of dust. *Amer. Sci.* 90(3): 228–235.

Griffin, D.W., Kellogg, C.A., Garrison, V.H., Lisle, J.T., Borden, T.C. & Shinn, E.A. 2003. African dust in the Caribbean atmosphere. *Aerobiologia* 19(3–4): 143–157.

Griffin, D.W., Westphal, D.L. & Gray, M.A. 2006. Airborne microorganisms in the African desert dust corridor over the mid-Atlantic ridge, Ocean Drilling Program, Leg 209. *Aerobiologia* 22(3): 211–226.

Griffin, D.W., Kubilay, N., Kocak, M., Gray, M.A., Borden, T.C. & Shinn, E.A. 2007. Airborne desert dust and aeromicrobiology over the Turkish Mediterranean coastline. *Atmosph. Environ.* 41(19): 4050–4062.

Griffin, D.W., Petrosky, T., Morman, S.A. & Luna, V.A. 2009. A survey of the occurrence of *Bacillus anthracis* in North American soils over two long-range transects and within post-Katrina New Orleans. *Appl. Geochem.* 24(8): 1464–1471.

Grimalt, J.O., Ferrer, M. & Macpherson, E. 1999. The mine tailing accident in Aznalcollar. *Sci. Total Environ.* 242(1–3): 3–11.

Grini, A. & Zender C.S. 2004. Roles of saltation, sandblasting, and wind speed variability on mineral dust aerosol size distribution during the Puerto Rican Dust Experiment (PRIDE). *J. Geophys. Res.* 109: D07202.

Grousset, F.E., Ginoux, P., Bory, A. & Biscaye, P.E. 2003. Case study of a Chinese dust plume reaching the French Alps. *Geophys. Res. Lett.* 30(6): 1277–1277.

Gu, Y., Rose, W.I., Schneider, D.J., Bluth, G.J.S. & Watson, I.M. 2005. Advantageous GOES IR results for ash mapping at high latitudes: Cleveland eruptions 2001. *Geophys. Res. Lett.* 32(2): L02305.

Gudmundsson, G. 2011. Respiratory health effects of volcanic ash with special reference to Iceland: A review. *Clin. Respir. J.* 5: 2–9.

Guffanti, M., Ewert, J.W., Gallina, G.M., Bluth, G.J.S. & Swanson, G.L. 2005. Volcanic-ash hazard to aviation during the 2003–2004 eruptive activity of Anatahan volcano, Commonwealth of the Northern Mariana Islands. *J. Volcan. & Geoth. Res.* 146(1–3): 241–255.

Gupta, P. & Christopher, S.A. 2008. Seven year particulate matter air quality assessment from surface and satellite measurements. *Atmosph. Chem. & Phys.* 8(12): 3311–3324.

Gupta, P., Christopher, S.A., Wang, J., Gehrig, R., Lee, Y. & Kumar, N. 2006. Satellite remote sensing of particulate matter and air quality assessment over global cities. *Atmosph. Environ.* 40(30): 5880–5892.

Gyan, K., Henry, W., Lacaille, S., Laloo, A., Lamesee-Eubanks, C., Mckay, S., Antoine, R.M. & Monteil, M.A. 2005. African dust clouds are associated with increased paediatric asthma accident & emergency admissions on the Caribbean island of Trinidad. *Int. J. Biomet.* 49(6): 371–376.

Haley, R.W., Kurt, T.L. & Hom, J. 1997. Is there a Gulf War syndrome? Searching for syndromes by factor analysis of symptoms. *J. Amer. Med. Assoc.* 277(3): 215–222.

Hallenbeck, W.H. 1994. *Radiation Protection*. Boca Raton: CRC.

Hallenbeck, W.H. & Cunningham-Burns, K.M. 1985. *Pesticides and Human Health*. New York: Springer-Verlag.

Halonen, M., Stern, D.A., Wright, A.L., Taussig, L.M. & Martinez, F.D. 1997. *Alternaria* as a major allergen for asthma in children raised in a desert environment. *Amer. J. Respir. Criti. Care Med.* 155(4): 1356–1361.

Hammond, G.W., Raddatz, R.L. & Gelskey, D.E. 1989. Impact of atmospheric dispersion and transport of viral aerosols on the epidemiology of influenza. *Revs. Infect. Dis.* 11(3): 494–497.

Hansell, A.L., Horwell, C.J. & Oppenheimer, C. 2006. The health hazards of volcanoes and geothermal areas. *Brit. Med. J.* 63(2): 149–156.

Hao, W.M., Bondarenko, O.O., Zibtsev, S. & Hutton, D. 2008. Vegetation fires, smoke emissions, and dispersion of radionuclides in the Chernobyl exclusion zone. *Dev. Environ. Sci.*: 8: 265–275.

Hara, Y., Uno, I. & Wang, Z. 2006. Long-term variation of Asian dust and related climate factors. *Atmos. Environ.* 40(35): 6730–6740.

Hatfield Consultants. 2000. Development of Impact Mitigation Strategies Related to the Use of Agent Orange Herbicide in the Aluoi Valley, VietNam. Volume 1: Report; Volume 2: Appendices. Hatfield Consultants Ltd., West Vancouver, BC, Canada; 10-80 Committee, Ha Noi, Viet Nam.

Haynes, J.A. 2009. *NASA satellite observations for climate research and applications for public health:* 407–414. Int. Sem. Nuclear War & Planetary Emergencies, 42th Session, Erice, Italy. Singapore:World Scientific.

He, F., Chen, S. & China, P.R. 1999. Health impacts of pesticide exposure and approaches to prevention. *Asian Pac. Newsletter Occup. Health Safety* 6: 60–63.

Hector, R.F. & Laniado-Laborin, R. 2005. Coccidioidomycosis – A fungal disease of the Americas. *PLoS Med.* 2(1): e2.

Herman, J.R., Krotkov, N., Celarier, E., Larko, D. & Labow, G. 1999. The distribution of UV radiation at the Earth's surface from TOMS measured UV-backscattered radiances. *J. Geophys. Res.* 104: 12059–12076.

Hoff, R.M. & Christopher, S.A. 2009. Remote sensing of particulate pollution from space: Have we reached the promised land? *J. Air & Waste Manage. Assoc.* 59(6): 645–675.

Hoff, R.M., Palm, S.P., Engel-Cox, J.A. & Spinhirne, J. 2005. GLAS: A long-range transport observation of the 2003 California forest fire plumes to the northeastern US. *Geophys. Res. Letts.* 32(22): 08.

Hoff, R.M., Huff, A.K. & Szykman, J.J. 2006. Three-dimensional air quality system: 3D-AQS. Available from: http://appliedsciences.nasa.gov/pdf/AQ-3D- AQS_Final_BenchmarkReport.pdf [Accessed 18th March 2012].

Holasek, R.E., Self, S. & Woods, A.W. 1996. Satellite observations and interpretation of the 1991 Mount Pinatubo eruption plumes. *J. Geophys. Res.* 101(27): 27635–27655.

Holt, G. 2007. Repair of facial fractures in the Iraq war combat theater. *J. Amer. Med. Assoc.* 298(24): 2905.

Honrath, R.E., Owen, R.C., Val Martin, M., Reid, J.S., Lampina, K., Fialho, P., Dziobak, M.P., Kleissl, J. & Westphal, D.L. 2004. Regional and hemispheric impacts of anthropogenic and biomass burning emissions on summertime CO_2 and O_3 in the North Atlantic lower free troposphere. *J. Geophys. Res.* 109(D24310): doi:10.1029/2004JD005147.

Hooker, S.B. & Mcclain, C.R. 2000. The calibration and validation of SeaWiFS data. *Prog. Oceanogra.* 45(3–4): 427–465.

Hooper, K., Petreas, M.X., Chuvakova, T., Kazbekova, G., Durz, N., Seminova, G., Sharmanov, T., Hayward, D., She, J.W., Visita, P., Windler, J., Mckinnery, M., Wade, T.J., Grassman, J. & Stephens, R.D. 1998. Analysis of breast milk to assess exposure to chlorinated contaminants in Kazakstan: High levels of 2,3,7,8-tetrachlorodibenzo-p-dioxin (TCDD) in agricultural villages of southern Kazakstan. *Environ. Health Perspec.* 106(12): 797–806.

Hooper, T.I., DeBakey, S.F., Nagaraj, B.E., Bellis, K.S., Smith, T.C. & Gackstetter, G.D. 2008. The long-term hospitalization experience following military service in the 1991 Gulf War among veterans remaining on active duty, 1994–2004. *BMC Public Health* 8: 60.

Horwell, C.J. 2007. Grain-size analysis of volcanic ash for the rapid assessment of respiratory health hazard. *J. Environ. Monitor.* 9(10): 1107–1115.

Horwell, C.J. & Baxter, P.J. 2006. The respiratory health hazards of volcanic ash: A review for volcanic risk mitigation. *Bull.Volcan.* 69(1): 1–24.

Howitt, M.E., Naibu, R. & Roach, T.C. 1998. The prevalence of childhood asthma and allergy. In Barbados. The Barbados National Asthma and Allergy Study. *Amer. J. Respir. & Criti. Care Med.* 157: A624.

Hsu, N.C., Tsay, S.C., King, M.D. & Herman, J.R. 2006. Deep blue retrievals of Asian aerosol properties during ace-asia. *IEEE Trans. Geos. & Rem. Sens.* 44(11): 3180–3195.

Huang, J.P., Minnis, P., Yi, Y., Tang, Q., Wang, X., Hu, Y., Liu, Z., Ayers, K., Trepte, C. & Winker, D. 2007. Summer dust aerosols detected from CALIPSO over the Tibetan Plateau. *Geophys. Res. Letts.* 34(18): 805.

Huang, J., Minnis, P., Chen, B., Huang, Z., Liu, Z., Zhao, Q., Yi, Y. & Ayers, J.K. 2008. Long-range transport and vertical structure of Asian dust from CALIPSO and surface measurements during PACDEX. *J. Geophys. Res. Atmosph.* 113(D23): 212.

Husar, R.B., Tratt, D.M., Schichtel, B.A., Falke, S.R., Li, F., Jaffe, D., Gasso, S., Gill, T., Laulainen, N.S., Lu, F., Reheis, M.C., Chun, Y., Westphal, D., Holben, B.N., Gueymard, C., Mckendry, I., Kuring, N., Feldman, G.C., Mcclain, C., Frouin, R.J., Merrill, J., Dubois, D., Vignola, F., Murayama, T., Nickovic, S.,

Wilson, W.W., Sassen, K., Sugimoto, N. & Malm, W.C. 2001. Asian dust events of April 1998. *J. Geophys. Res.-Atmosph.* 106(D16): 18317–18330.

Hutchison, K.D., Smith, S. & Faruqui, S.J. 2005. Correlating MODIS aerosol optical thickness data with ground-based PM2.5 observations across Texas for use in a real-time air quality prediction system. *Atmosph. Environ.* 39(37): 7190–7203.

Hyams, K.C., Riddle, J., Trump, D.H. & Graham, J.T. 2001. Endemic infectious diseases and biological warfare during the Gulf War: A decade of analysis and final concerns. *Amer. J. Trop. Med. & Hyg.* 65(5): 664–670.

IAEA 2012. Available from: www.iaea.org/About/japan-infosheet.html [Accessed 18th March 2012].

Immler, F., Engelbart, D. & Schrems, O. 2005. Fluorescence from atmospheric aerosol detected by a lidar indicates biogenic particles in the lowermost stratosphere. *Atmosph. Chem. & Phys.* 5: 345–355.

Inhorn, M.C. & Brown, P.J. 2000. The anthropology of infectious disease. *Ann. Rev. Anthro.* 19(1): 89–117.

Ismail, K., Everitt, B., Blatchley, N., Hull, L., Unwin, C., David, A. & Wessely, S. 1999. Is there a Gulf War syndrome? *The Lancet* 353(9148): 179–182.

Jaffe, D., Anderson, T., Covert, D., Kotchenruther, R., Trost, B., Danielson, J., Simpson, W., Berntsen, T., Karlsdottir, S. & Blake, D. 1999. Transport of Asian air pollution to North America. *Geophys. Res. Lett.* 26(6): 711–714.

Jaffe, D., McKendry, I., Adnerson, T. & Price, H. 2003. Six 'new' episodes of trans-Pacific transport of air pollutants. *Atmos. Environ.* 37(3): 391–404.

Jaffe, D., Prestbo, E., Swartzendruber, P., Weiss-Penzias, P., Kato, S., Takami, A., Hatakeyama, S. & Kajii, Y. 2005. Export of atmospheric mercury from Asia. *Atmos. Environ.* 39(17): 3029–3038.

Jagai, J.S., Monchakb, J., Mcentee, J.C., Castronovo, D.A. & Naumova, E.N. 2007. The use of remote sensing to assess global trends in seasonality of cryptosporidiosis. *32nd Int. Symp. Rem. Sens. Environ.*, San Jose, Costa Rica.

Janssen, P.H. 2006. Identifying the dominant soil bacterial taxa in libraries of 16S rRNA and 16S rRNA genes. *Appl. & Environ. Microb.* 72(3): 1719–1728.

Jayaraman, V., Chandrasekhar, M.G. & Rao, U.R. 1997. Managing the natural disasters from space technology inputs. *Acta Astronaut.* 40(2–8): 291–325.

Jensen, J.R. 2000. *Remote Sensing of the Environment*. Upper Saddle River, NJ: Prentice Hall.

Jinadu, B.A. 1995. Valley Fever Task Force Report on the control of *Coccidioides immitis*. Bakersfield: California: Kern County Health Department.

Johnson, K.G., Loftsgaarden, D.O. & Gideon, R.A. 1982. The effects of Mount St. Helens volcanic ash on the pulmonary function of 120 elementary school children. *Amer. Rev. Respir. Dis.* 126(6): 1066–1089.

Johnson, K.S., Elrod, V.A., Fitzwater, S.E., Plant, J.N., Chavez, F.P., Tanner, S.J., Gordon, R.M., Westphal, D.L., Perry, K.D., Wu, J. & Karl, D.M. 2003. Surface ocean-lower atmosphere interactions in the Northeast Pacific Ocean Gyre: Aerosols, iron and the ecosystem response. *Global Biogeochem. Cycles* 17(2): 1063. doi:1010.1029/2000JC000555.

Jurado, J. & Southgate, D. 2001. Dealing with air pollution in Latin America: The case of Quito, Ecuador. *Environ. & Devel. Econ.* 4(03): 375–388.

Kahn, R.A., Gaitley, B.J. Martonchik, J.V., Diner, D.J., Crean, K.A. & Holben, B. 2005. Multi-angle imaging spectroradiometer (MISR) global aerosol optical depth validation based on 2 years of coincident aerosol robotic network (AERONET) observations. *J. Geophys. Res. Atmosph.* 110(D10): S04.

Kan, H., London, S.J., Chen, G., Zhang, Y., Song, G., Zhao, N., Jiang, L. & Chen, B. 2007. Differentiating the effects of fine and coarse particles on daily mortality in Shanghai, China. *Environ. Int.* 33(3): 376–384.

Kang, H.K., Mahan, C.M., Lee, K.Y., Murphy, F.M., Simmens, S.J., Young, H.A. & Levine, P.H. 2002. Evidence for a deployment-related Gulf War syndrome by factor analysis. *Arch. Environ. Health* 57(1): 61–68.

Karyampudi, V.M., Palm, S.P., Reagen, J.A., Fang, H., Grant, W.B., Hoff, R.M., Moulin, C., Pierce, H.F., Torres, O., Browell, E.V. & Melfi, S.H. 1999. Validation of the Saharan dust plume conceptual model using Lidar, Meteosat, and ECMWF data. *Bull. Amer. Meteorol. Soc.* 80(6): 1045–1075.

Kellogg, C.A., Griffin, D.W., Garrison, V.H., Peak, K.K., Royall, N., Smith, R.R. & Shinn, E.A. 2004. Characterization of aerosolized bacteria and fungi from desert dust events in Mali, West Africa. *Aerobiol.* 20(2): 99–110.

Kienle, J. & Shaw, G.E. 1979. Plume dynamics, thermal energy and long-distance transport of vulcanian eruption clouds from Augustine volcano, Alaska. *J. Volcan. & Geoth. Res.* 6(1–2): 139–164.

Klein-Schwartz, W. & Smith, G.S. 1997. Agricultural and horticultural chemical poisonings: Mortality and morbidity in the United States. *Ann. Emerg. Med.* 29(2): 232–238.

Kleindorfer, P.R., Belke, J.C., Elliott, M.R., Lee, K., Lowe, R.A. & Feldman, H.I. 2003. Accident epidemiology and the U.S. chemical industry: Accident history and worst-case data from RMP*Info. *Risk Anal.* 23(5): 865–881.

Kling, G.W., Clark, M.A., Wagner, G.N., Compton, H.R., Humphrey, A.M., Devine, J.D., Evans, W.C., Lockwood, J.P., Tuttle, M.L. & Koenigsberg, E.J. 1987. The 1986 Lake Nyos gas disaster in Cameroon, West Africa. *Science* 236(4798): 169.

KMA 2008. Available from: http://www.korea.amedd.army.mil/webapp/yellowSand/Default.asp [Accessed 4th February 2012].

Knoke, J.D., Smith, T.C., Gray, G.C., Kaiser, K.S. & Hawksworth, A.W. 2000. Factor analysis of self-reported symptoms: Does it identify a Gulf War syndrome? *Amer. J. Epidem.* 152(4): 379–388.

Koelemeijer, R.B.A., Homan, C.D. & Matthijsen, J. 2006. Comparison of spatial and temporal variations of aerosol optical thickness and particulate matter over Europe. *Atmosph. Environ.* 40(27): 5304–5315.

Koren, I., Kaufman, Y.J., Washington, R., Todd, M.C., Rudich, Y., Martins, J.V. & Rosenfeld, D. 2006. The Bodele Depression: A single spot in the Sahara that provides most of the mineral dust to the Amazon forest. *Environ. Res. Lett.* 1: 014005.

Korenyi-Both, A.L. 2000. Al Eskan disease and no gaming please. *Military Medicine* 165(11): 3–4.

Korenyi-Both, A.L., Molnar, A.C. & Fidelus-Gort, R. 1992. Al Eskan disease: Desert Storm pneumonitis. *Military Med.* 157(9): 452–462.

Kovacs, T. 2006. Comparing MODIS and AERONET aerosol optical depth at varying separation distances to assess ground-based validation strategies for spaceborne Lidar. *J. Geophys. Res. Atmosph.* 111(D24): 203.

Krotkov, N.A., Torres, O., Seftor, C., Krueger, A.J., Kostinski, A., Rose, W.I., Bluth, G.J.S., Schneider, D.J. & Schaifer, S.J. 1999. Comparison of TOMS and AVHRR volcanic ash retrievals from the August 1992 eruption of Mt. Spurr. *Geophys. Res. Lett.* 26(4): 455–458.

Krueger, A.J., Walter, L.S., Bhartia, P.K., Schnetzler, C.C., Krotkov, N.A., Sprod, I. & Bluth, G.J.S. 1995. Volcanic sulfur dioxide measurements from the total ozone mapping spectrometer instruments. *J. Geophys. Res.* 100(14): 14057–14076.

Kwon, H.J., Cho, S.H. & Chun, Y.S. 2000. The effects of the Asian dust events on daily mortality in Seoul, Korea. *Epidem.* 11(4): 243.

Kwon, H.J., Cho, S.H., Chun, Y., Lagarde, F. & Pershagen, G. 2002. Effects of the Asian dust events on daily mortality in Seoul, Korea. *Environ. Res.* 90 (Sect. A): 1–5.

Lambert, F., Delmonte, B., Petit, J.R., Bigler, M., Kaufmann, P.R., Hutterli, M.A., Stocker, T.J., Ruth, U., Steffensen, J.P. & Maggi, V. 2008. Dust – climate couplings over the past 800,000 years from the EPICA Dome C ice core. *Nature* 452: 616–619.

Lary, D.J. 2010. Artificial intelligence in aerospace. In: T.A. Thawar (ed.), *Aerospace Technologies Advancements*: 492–516. Vukovar, Croatia: INTECH.

Lary, D.J. 2010. Artificial Intelligence in geoscience and remote sensing. In: P. Imperatore & D. Riccio (eds.), *Geoscience & Remote Sensing. New Achievements*: 105–128. Vukovar, Croatia: INTECH.

Lary, D.J. & Aulov, O. 2008. Space-based measurements of HCl: Inter-comparison and historical context. *J. Geophys. Res. Atmosph.* 113(D15): S04.

Lary, D.J., Muller, M.D. & Mussa, H.Y. 2004. Using neural networks to describe tracer correlations. *Atmosph. Chem. & Phys.* 4: 143–146.

Lary, D.J., Waugh, D.W., Douglass, A.R., Stolarski, R.S., Newman, P.A. & Mussa, H. 2007. Variations in stratospheric inorganic chlorine between 1991 and 2006. *Geophys. Res. Letts* 34(21): 811.

Lary, D.J., Remer, L.A., Macneill, D., Roscoe, B. & Paradise, S. 2009. Machine learning and bias correction of MODIS aerosol optical depth. *IEEE Geos. & Rem. Sens. Letts.* 6(4): 694–698.

Laursen, L. 2010. Iceland eruptions fuel interest in volcanic gas monitoring. *Science* 328: 410–411.

Le Pennec, J.L., Ruiz, A.G., Hidalgo, S., Samaniego, P., Ramon, P., Eissen, J.P., Yepes, H., Hall, M.L., Mothes, P., Vallee, A. & Vennat, J. 2006. Characteristics and impacts of recent ash falls produced by Tungurahua and El Reventador volcanoes, Ecuador. *Cities on Volcanoes, Fourth Conference*. Quito, Ecuador.

Lee, H.A., Gabriel, R., Bolton, J.P.G., Bale, A.J. & Jackson, M. 2002. Health status and clinical diagnoses of 3000 UK Gulf War veterans. *J. Roy. Soc. Med.* 95: 491–497.

Lehnert, B.E. 1993. Defense mechanisms against inhaled particles and associated particle-cell interactions. *Revs. Mineral. & Geochem.* 28(1): 427–469.

Lenes, J.M., Darrow, B.P., Cattrall, C., Heil, C.A., Callahan, M., Vargo, G.A., Byrne, R.H., Prospero, J.M., Bates, D.E., Fanning, K.A. & Walsh, L.J. 2001. Iron fertilization and the *Trichodesmium* response on the West Florida shelf. *Limnol. & Oceanogra.* 46(6): 1261–1277.

Leptoukh, G., Zubko, V. & Gopolan, A. 2007. Spatial aspects of multi-sensor data fusion: Aerosol optical thickness. *IGARSS: Int. Geos. & Rem. Sens. Symp. vols 1–12: Sensing & Understanding Our Planet*: 3119–3122.

Levy, R.C., Leptoukh, G.G., Kahn, R., Zubko,V., Gopalan, A. & Remer, L.A. 2009. A critical look at deriving monthly aerosol optical depth from satellite data. *IEEE Trans. Geos. Rem. Sens.* 47(8): 2942–2956.

Liang, Q., Jaegle, L., Jaffe, D.A., Weiss-Penzias, P., Heckman, A. & Snow, J.A. 2004. Long-range transport of Asian pollution to the northeast Pacific: Seasonal variations and transport pathways of carbon monoxide. *J. Geophys. Res.* 109: D23S07.

Liu, Y., Franklin, M., Kahn, R. & Koutrakis, P. 2007a. Using aerosol optical thickness to predict ground-level PM2.5 concentrations in the St. Louis area: A comparison between MISR and MODIS. *Rem. Sens. Environ.* 107(1–2): 33–44.

Liu, Y., Koutrakis, P. & Kahn, R. 2007b. Estimating fine particulate matter component concentrations and size distributions using satellite-retrieved fractional aerosol optical depth: Part 1 – method development. *J. Air & Waste Manag. Assoc.* 57(11): 1351–1359.

Liu, Y., Koutrakis, P., Kahn, R., Turquety, S. & Yantosca, R.M. 2007c. Estimating fine particulate matter component concentrations and size distributions using satellite-retrieved fractional aerosol optical depth: Part 2 – a case study. *J. Air & Waste Manag. Assoc.* 57(11): 1360–1369.

Liu, Y., Park, R.J., Jacob, D.J.Q., Li, B., Kilaru, V. & Sarnat, J.A. 2004a. Mapping annual mean ground-level PM2.5 concentrations using multiangle imaging spectroradiometer aerosol optical thickness over the contiguous United States. *J. Geophys. Res. Atmosph.* 109(D22): 10.

Liu, Y., Sarnat, J.A., Coull, B.A., Koutrakis, P. & Jacob, D.J. 2004b. Validation of multiangle imaging spectroradiometer (MISR) aerosol optical thickness measurements using aerosol robotic network (AERONET) observations over the contiguous United States. *J. Geophys. Res. Atmosph.* 109(D6): 9.

Liu, Z., Liu, D. Huang, J., Vaughan, M., Uno, I., Sugimoto, N., Kittaka, C., Trepte, C., Wang, Z., Hostetler, C. & Winker, D. 2008. Airborne dust distributions over the Tibetan Plateau and surrounding areas derived from the first year of CALIPSO Lidar observations. *Atmosph. Chem. & Phys.* 8(16): 5045–5060.

Loehr, A., Bogaard, T., Heikens, A., Hendriks, M., Suarti, S., Bergen, M., van Gestel, K.C.A.M., Straalen, N., Vroon, P. & Widianarko, B. 2005. Natural pollution caused by the extremely acid crater lake Kawah Ijen, East Java, Indonesia. *Environ. Sci. & Poll. Res.* 12(2): 89–95.

London, L. & Bailie, R. 2001. Challenges for improving surveillance for pesticide poisoning: Policy implications for developing countries. *Int. J. Epidem.* 30(3): 564.

Lyles, M.B., Fredrickson, H.L., Bednar, A.J., Fannin, H.B. & Sobecki, T.M. 2005. The chemical, biological, and mechanical characterization of airborne micro-particulates from Kuwait. *8th Annual Force Health Protection Conference*. Louisville, Kentucky. Session #2586. Available from: http://www.apgea.army.mil/fhp/Archives/FHP2005/Users/ConferenceAgenda_Pop.aspx [Accessed 20th March 2012].

Lyamani, H., Olmo, F.J., Alcántara, A. & Alados-Arboledas, L. 2006. Atmospheric aerosols during the 2003 heat wave in southeastern Spain-I: Spectral optical depth. *Atmosph. Environ.* 40(33): 6453–6464.

Lyons, J.J., Waite, G.P., Rose, W.I. & Chigna, G. 2010. Patterns in open vent, strombolian behavior at Fuego volcano, Guatemala, 2005–2007. *Bull. Volcan.* 72(1): 1–15.

Malilay, J., Real, M.G., Vanegas, A.R., Noji, E. & Sinks, T. 1997. Public health surveillance after a volcanic eruption: Lessons from Cerro Negro, Nicaragua, 1992. *Rev. Panam. Sal. Publ.* 1: 213–219.

Margni, M., Rossier, D., Crettaz, P. & Jolliet, O. 2002. Life cycle impact assessment of pesticides on human health and ecosystems. *Agric. Ecosys. & Environ.* 93(1–3): 379–392.

Martin, T.R., Ayars, G., Butler, J. & Altman, L.C. 1984. The comparative toxicity of volcanic ash and quartz. Effects on cells derived from the human lung. *Amer. Rev. Respir. Dis.* 130(5): 778–782.

Martin, T.R., Wehner, A.P. & Butler, J. 1986. Evaluation of physical health effects due to volcanic hazards: The use of experimental systems to estimate the pulmonary toxicity of volcanic ash. *Amer. J. Publ. Health* 76(Suppl): 59–65.

Matichuk, R.I., Colarco, P.R., Smith, J.A. & Toon, O.B. 2007. Modeling the transport and optical properties of smoke aerosols from African savanna fires during the southern African regional science initiative campaign (Safari 2000). *J. Geophys. Res. Atmosph.* 112(D8): 203.

Matichuk, R.I., Colarco, P.R. Smith, J.A. & Toon, O.B. 2008. Modeling the transport and optical properties of smoke plumes from South American biomass burning. *J. Geophys. Res. Atmosph.* 113(D7): 208.

Maxwell, S.K., Meliker, J.R. & Goovaerts, P. 2009. Use of land surface remotely sensed satellite and airborne data for environmental exposure assessment in cancer research. *J. Exp. Sci. & Environ. Epidem.* 20: 176–185.

Mcgill, M.J., Vaughan, M.A., Trepte, C.R., Hart, W.D., Hlavka, D.L., Winker, D.M., & Kuehn, R. 2007. Airborne validation of spatial properties measured by the CALIPSO Lidar. *J. Geophys. Res. Atmosph.* 112(D20): 201.

McGonigle, A.J.S. 2005. Volcano remote sensing with ground-based spectroscopy. *Philos. Trans. Roy. Soc. Lond. – Series A: Mathematical, Physical & Engineering Sciences* 363(1837): 2915–2929.

McKendry, I.G., Strawbridge, K.B., Oneill, N.T., Macdonald, A.M., Liu, P.S.K., Leaitch, W.R., Anlauf, K.G., Jaegle, L., Gairlie, T.D. & Westphal, D.L. 2007. Trans-Pacific transport of Saharan dust to western North America: A case study. *J. Geophys. Res.* 112: D01103.

Meier, F.C. & Lindbergh, C.A. 1935. Collecting micro-organisms from the Arctic atmosphere. *Sci. Monthly* 40: 5–20.

Meng, Z. & Lu, B. 2007. Dust events as a risk factor for daily hospitalization for respiratory and cardiovascular diseases in Minqin, China. *Atmosph. Environ.* 41(33): 7048–7058.

Meselson, M., Guillemin, J., Hugh-Jones, M., Langmuir, A., Popova, I., Shelokov, A. & Yampolskaya, O. 1994. The Sverdlovsk anthrax outbreak of 1979. *Science.* 266(5188): 1202.

Micklin, P.P. 1988. Desiccation of the Aral Sea: A water management disaster in the Soviet Union. *Science* 241: 1170–1176.

Micklin, P.P. 2007. The Aral Sea disaster. *Ann. Rev. Earth & Planetary Sci.* 35: 47–72.

Mills, N.L., Amin, N., Robinson, S.D., Anand, A., Davies, J., Patel, D., De La Fuente, J.M., Cassee, F.R., Boon, N.A. & Macnee, W. 2006. Do inhaled carbon nanoparticles translocate directly into the circulation in humans? *Amer. J. Respir. & Criti. Care Med.* 173(4): 426.

Mims, S.A. & Mims, F.M. 2004. Fungal spores are transported long distances in smoke from biomass fires. *Atmosph. Environ.* 38(5): 651–655.

MMWR 2003a. Increase in coccidioidomycosis – Arizona, 1998–2001. *Morb. & Mort. Wkly. Rept.* 52(6): 109–112.

MMWR 2003b. Severe acute pneumonitis among deployed U.S. military personnel – southwest Asia, March – August 2003. *Morb. & Mort. Wkly. Rept.* 290(14): 1845–1846.

MODVOC. 2009. Near-real-time thermal monitoring of global hot-spots. Available from: http://modis.higp.hawaii.edu [Accessed 19th March 2012].

Mohr, A.J. 1997. Fate and transport of microorganisms in air. In C.J. Hurst, G.R. Knudsen, M.J. McInerney, L.D. Stetzenbach & M.V. Walter (eds.), *Manual of Environmental Microbiology*: 641–650. Washington: ASM Press.

Molesworth, A.M., Cuevas, L.E., Morse, A.P., Herman, J.R. & Thomson, M.C. 2002. Dust clouds and spread of infection. *Lancet.* 359(9300): 81–82.

Molesworth, A.M., Cuevas, L.E., Conner, S.J., Morse, A.P. & Thomson, M.C. 2003. Environmental risk and meningitis epidemics in Africa. *Emerg. Infect. Dis.* 9(10): 1287–1293.

Morain, S.A. & Budge A.M. 2010. Suggested practices for forecasting dust storms and intervening their health effects. In O. Altan, R. Backhaus, P. Boccardo & S. Zlatanova (eds.), *Geoinformation for Disaster and Risk Management*: 45–50. Copenhagen: Joint Board of Geospatial Information Societies & United Nations Office of Outer Space Affairs.

Morain, S.A., Sprigg, W.A., Benedict, K., Budge, A., Budge, T., Hudspeth, W., Barbaris, B., Yin, D. & Shaw, P. 2007. Public Health Applications in Remote Sensing: Verification and Validation Report. NASA Cooperative agreement NNS04AA19A.

Morain, S.A., Sprigg, W.A., Benedict, K., Budge, A., Budge, T., Hudspeth, W., Sanchez, G., Barbaris, B., Catrall, C., Chandy, B., Mahler, A.B., Shaw, P., Thome, K., Nickovic, S., Yin, D., Holland, D., Spear, J., Simpson, G. & Zelicoff, A. 2009. Public Health Applications in Remote Sensing: Final Benchmark Report. NASA Cooperative agreement. NNS04AA19A.

Morawska, L. & Zhang J.F. 2002. Combustion sources of particles. 1. Health relevance and source signatures. *Chemosphere* 49(9): 1045–1058.

Morrow, P.E. 1992. Dust overloading of the lungs: Update and appraisal. *Toxicol. & Appl. Pharmacol.* 113(1): 1–12.

Moulin, C., Lambert, C.E., Dulac, F. & Dayan, U. 1997. Control of atmospheric export of dust from North Africa by the North Atlantic Oscillation. *Nature.* 387: 691–694.

Nadkarni, N.M., McIntosh, A.C.S. & Cushing, J.B. 2008. A framework to categorize forest structure concepts. *For. Ecol. & Mangmnt.* 256(5): 872–882.

Nag, P.K. & Nag, A. 2004. Drudgery, accidents and injuries in Indian agriculture. *Indust. Health* 42(2): 149–162.

Nandalal, K.D.W. & Hipel, K.W. 2007. Strategic decision support for resolving conflict over water sharing among countries along the Syr Darya River in the Aral Sea Basin. *J. Water Res. Plan. & Mangmnt.* 133: 289–299.

Nania, J. & Bruya, T.E. 1982. In the wake of Mount St. Helens. *Annals Emerg. Med.* 11(4): 184–191.

NASA 2012a. Available from: http://www.nasascience.nasa.gov/earth-science/mission_list [Accessed 23rd February 2012.

NASA 2012b. Available from: http://lpdaac.usgs.gov/lpdaac/products/modis_products_table/albedo/16_day_l3_global_0_05deg_cmg/mcd43c3 [Accessed 18th March 2012].

Naumova, E.M., Haas, T.C. & Morris, R.D. 1997. *Estimation of Individual Exposure Following a Chemical Spill in Superior, Wisconsin*. New York: Springer-Verlag.

NCDC 2010. Available from: http://www.ncdc.noaa.gov/oa/reports/billionz.html [Accessed 19th March 2012].

Nemmar, A., Hoet, P.H.M., Vanquickenborne, B., Dinsdale, D., Thomeer, M., Hoylaerts, M.F., Vanbilloen, H., Mortelmans, L. & Nemery, B. 2002. Passage of inhaled particles into the blood circulation in humans. *Circulation* 105(4): 411.

Ngo, A.D., Taylor, R., Roberts, C.L. & Nguyen, T.V. 2006. Association between Agent Orange and birth defects: Systematic review and meta-analysis. *Int. J. Epidem.* 35(5): 1220–1230.

Nickovic, S., Kallos, G., Papadopoulos, A. & Kakaliagou, O. 2001. A model for prediction of desert dust cycle in the atmosphere. *J. Geophys. Res.* 106: 18113–18130.

NOAA 2012. Available from: http://www.ssd.noaa.gov/VAAC/ARCH11/archive.html. [Acessed 4th February 2012].

Norboo, T., Angchuk, P.T., Yahya, M., Kamat, S.R., Pooley, F.D., Corrin, B., Kerr, I.H., Bruce, N. & Ball, K.P. 1991. Silicosis in a Himalayan village population: Role of environmental dust. *Thorax* 46: 861–863.

Novak, M.A., Watson, I.M., Delgado-Granados, H., Rose, W.I., Cardenas-Gonzalez, L. & Realmuto, V. 2008. Volcanic emissions from Popocatepetl volcano, Mexico, quantified using Moderate Resolution Imaging Spectroradiometer (MODIS) infrared data: A case study of the December 2000–January 2001 emissions. *J. Volcan. & Geoth. Res.* 170(1–2): 76–85.

Oehme, M. 1991. Dispersion and transport paths of toxic persistent organochlorides to the Arctic: Levels and consequences. *Sci. Total Environ.* 106(1–2): 43–53.

O'Hara, S.L., Wiggs, G.F.S., Mamedov, B., Davidson, G. & Hubbard, R.B. 2000. Exposure to airborne dust contaminated with pesticide in the Aral Sea region. *The Lancet* 355(9204): 627.

Olenchock, S.A., Mull, J.C., Mentnech, M.S., Lewis, D.M. & Bernstein, R.S. 1983. Changes in humoral immunologic parameters after exposure to volcanic ash. *J. Toxicol. & Environ. Health.* Part A 11(3): 395–404.

O'Malley, M.A. & McCurdy, S.A. 1990. Subacute poisoning with phosalone, an organophosphate insecticide. *Western J. Med.* 153(6): 619–624.

OMISDG 2007. Ozone Monitoring Instrument Sulfur Dioxide Group. Available from: http://so2.gsfc. nasa.gov [Accessed 4th February 2012].

Oppenheimer, C. 1998. Review article: Volcanological applications of meteorological satellites. *Int. J. Rem. Sens.* 19(15): 2829–2864.

OPS 2005. Eruciones volcanicas y proteccion de la salud. Quito, Ecuador, Organization Panamercana de la Salud. Available from: http://www.ops-oms.org/Spanish/DD/PED/gv_modulo2-1.pdf?vm=r [Accessed 19th March 2012].

Papastefanou, C., Manolopoulou, M., Stoulos, S., Ioannidou, A. & Gerasopoulos, E. 2001. Coloured rain dust from Sahara Desert is still radioactive. *J. Environ. Radioact.* 55: 109–112.

Papayannis, A., Zhang, H.Q., Amiridis, V., Ju, H.B., Chourdakis, G., Georgoussis, G., Perez, C., Chen, H.B., Goloub, P. & Mamouri, R.E. 2007. Extraordinary dust event over Beijing, China, during April 2006: Lidar, Sun photometric, satellite observations and model validation. *Geophys. Res. Lett.* 34, L07806. doi: 10.1029/2006GL029125.

Park, J.W., Lim, Y.H., Kyung, S.Y., An, C.H., Lee, S.P., Jeong, S.H. & Ju, Y.S. 2005. Effects of ambient particulate matter on peak expiratory flow rates and respiratory symptoms of asthmatics during Asian dust periods in Korea. *Respirology* 10: 470–476.

Pelletier, B., Santer, R. & Vidot, J. 2007. Retrieving of particulate matter from optical measurements: A semiparametric approach. *J. Geophys. Res. Atmosph.* 112(D6): 18.

Pergola, N., Tramutoli, V., Marchese, F., Scaffidi, I. & Lacava, T. 2004. Improving volcanic ash cloud detection by a robust satellite technique. *Rem. Sens. Environ.* 90(1): 1–22.

Peterson, R., Webley, P.W., D'Amours, R., Servranckx, R., Stunder, R. & Papp, K. 2012. Volcanic ash cloud dispersion models. In K. Dean & J. Dehn (eds.) *Volcanoes of the North Pacific: Observations from Space*: Chapter 7. London: Praxis.

Pieri, D. & Abrams, M. 2004. ASTER watches the world's volcanoes: A new paradigm for volcanological observations from orbit. *J.Volcan. & Geoth. Res.* 135(1–2): 13–28.

Pimentel, D. 1995. Amounts of pesticides reaching target pests: Environmental impacts and ethics. *J. Agric. & Environ. Ethics* 8(1): 17–29.

Pimentel, D., Acquay, H., Biltonen, M., Rice, P., Silva, M., Nelson, J., Lipner, V., giordano, S., Horowitz, A. & D'amore, M. 1992. Environmental and economic costs of pesticide use. *BioScience* 42(10): 750–760.

Plumlee, G.S. & Ziegler, T.L. 2005. The medical geochemistry of dusts, soils, and other earth materials. In B.S. Lollar (ed.), *Environmental Geochemistry*: 263. Oxford: Elsevier.

Plumlee, G.S., Morman, S.A. & Zeigler, T.L. 2006. The toxicological geochemistry of Earth materials: An overview of processes and the interdisciplinary methods used to understand them. *Revs. Mineral. & Geochem.* 64(1): 5–57.

Plumlee, G.S., Foreman, W.T., Meeker, G.P., Demas, C.R., Lovelace, J.K., Hageman, P.L., Morman, S.A., Lamothe, P.J., Breit, G.N., Furlong, E.T. & Goldstein, H. 2007. Sources, mineralogy, chemistry, environmental reactivity, and metal bioaccessibility of flood sediments deposited in the New Orleans area by Hurricanes Katrina and Rita. USGS Open-File Report 2006–1023.

Prata, A.J. 1989. Observations of volcanic ash clouds in the 10–12 μm window using AVHRR/2 data. *Int. J. Rem. Sens.* 10(4): 751–761.

Prata, A.J. & Bernardo, C. 2009. Retrieval of volcanic ash particle size, mass and optical depth from a ground-based thermal infrared camera. *J. Volcan. & Geoth. Res.* 186(1–2): 91–107.

Prospero, J.M. & Nees, R.T. 1986. Impact of the North African drought and El Niño on mineral dust in the Barbados trade winds. *Nature* 320(6064): 735–738.

Prospero, J.M. 1999. Long-range transport of mineral dust in the global atmosphere: Impact of African dust on the environment of the southeastern United States. *Proc. Nat. Acad. Sci.* 96: 3396–3403.

Prospero, J.M. & Lamb, P.J. 2003. African droughts and dust transport to the Caribbean: Climate change implications. *Science* 302(5647): 1024–1027.

Pudykiewicz, L. 1989. Simulation of the Chernobyl dispersion with a 3-D hemispheric tracer model. *Tellus* 41(B): 391–412.

Pugnaghi, S., Gangale, G., Corradini, S. & Buongiorno, M.F. 2006. Mt. Etna sulfur dioxide flux monitoring using ASTER-TIR data and atmospheric observations. *J. Volcan. & Geoth. Res.* 152(1–2): 74–90.

Rajeev, K., Parameswaran, K., Nair, S.K. & Meenu, S. 2008. Observational evidence for the radiative impact of Indonesian smoke in modulating the sea surface temperature of the equatorial Indian Ocean. *J. Geophys.Res. Atmosph.* 113(D17): 201.

Realmuto, V.J. 2000. The potential use of Earth observing system data to monitor the passive emission of sulfur dioxide from volcanoes. In P.J. Mouginis-Mark, J.A. Crisp & J.H. Fink (eds.), *Remote Sensing of Active Volcanism*: 101–115. Washington DC: American Geophysical Union

Realmuto, V.J., Abrams, M.J., Fabrizia Buongiorno, M. & Pieri, D.C. 1994. The use of multispectral thermal infrared image data to estimate the sulfur dioxide flux from volcanoes: A case study from Mount Etna, Sicily *J. Geophys. Res.* 99(1): 481–488.

Realmuto, V.J., Sutton, A.J. & Elias, T. 1997. Multispectral thermal infrared mapping of sulfur dioxide plumes: A case study from the East Rift Zone of Kilauea volcano, Hawaii. *J. Geophys. Res.* 102(B7): 15057–15072.

Reid, J.S., Prins, E.M., Westphal, D.L., Schmidt, C.C., Richardson, K.A., Christopher, S.A., Eck, T.F., Reid, E.A., Curtis, C.A. & Hoffman, J.P. 2004. Real-time monitoring of South American smoke particle emissions and transport using a coupled remote sensing/box-model approach. *Geophys. Res. Lett.* 31(L06107). doi:10.1029/2203GL018845.

Reid, J.S., Hyer, E.J. Prins, E.M., Westphal, D.L., Zhang, J., Wang, J., Christopher, S.A., Curtis, C.A., Schmidt, C.C., Eleuterio, D.P., Richardson, K.A. & Hoffman, J.P. 2009. Global monitoring and forecasting of biomass-burning smoke: Description of and lessons from the Fire Locating and Modeling of Burning Emissions (FLAMBE) program. *IEEE J. Sel. Topics Appl. Earth Obs. & Rem. Sens.* 2(3): 144–162.

ReliefWeb. 2010. Efectos en la salud por les erupciones del Tungurahua. Available from: http://www.reliefweb.int/rw/dbc.nsf/doc108?OpenForm&rc=2&emid=VO-1999-0584-ECU [Accessed 4th February 2012.

Remer, L.A., Kaufman, Y.J. Tanre, D., Mattoo, S., Chu, D.A., Martins, J.V., Li, R.R., Ichoku, C., Levy, R.C., Kleidman, R.G., Eck, T.F., Vermote, E. & Holben, B.N. 2005. The MODIS aerosol algorithm, products, and validation. *J. Atmosph. Sci.* 62(4): 947–973.

Reynolds, K.A. & Pepper, I. L. 2000. Microorganisms in the environment. In R.M. Maier, I.L. Pepper & C.P. Gerba (eds.), *Environmental Microbiology*: 585. San Diego: Academic Press

Ridgwell, A.J. 2003. Implications of the glacial CO_2 iron hypothesis for Quarternary climate change. *Geochem. Geophys. Geosyst.* 4(9): 1076.

Risebrough, R.W., Huggett, R.J., Griffin, J.J. & Goldberg, E.D. 1968. Pesticides: Transatlantic movements in the Northeast Trades. *Science* 159(3820): 1233–1236.

Roberts, D.M., Karunarathna, A., Buckley, N.A., Manuweera, G., Sheriff, M.H.R. & Eddleston, M. 2003. Influence of pesticide regulation on acute poisoning deaths in Sri Lanka. *Bull. WHO* 81(11): 789–798.

Robock, A. 2000. Volcanic eruptions and climate. *Revs. Geophys.* 38(2): 191–219.

Rogie, J.D., Kerrick, D.M., Sorey, M.L., Chiodini, G. & Galloway, D.L. 2001. Dynamics of carbon dioxide emission at Mammoth Mountain, California. *Earth & Planetary Sci. Lett.* 188(3–4): 535–541.

Rook, G.A. & Zumla, A. 1997. Gulf War syndrome: Is it due to a systemic shift in cytokine balance towards a Th2 profile? *Lancet* 349(9068): 1831–1833.

Safe, S.H. 1995. Environmental and dietary estrogens and human health: Is there a problem? *Environ. Health Perspec.* 103(4): 346–351.

Sait, M., Hugenholtz, P. & Janssen, P.H. 2002. Cultivation of globally distributed soil bacteria from phylogenetic lineages previously only detected in cultivation-independent surveys. *Environ. Microbio.* 4(11): 654–666.

Saiyed, H.N., Sharma, Y.K., Sadhu, H.G., Norboo, T., Patel, P.D., Patel, T.S., Vendaiah, K. & Kashyap, S.K. 1991. Non-occupational pneumoconiosis at high altitude villages in central Ladakh. *Brit. J. Indian Med.* 48: 825–829.

Salyani, M. & Cromwell, R.P. 1992. Spray drift from ground and aerial applications. *Trans. Amer. Soc. Agric. & Biolog. Engin.* 35(4): 1113–1120.

Samuelsen, M., Nygaard, U.C. & Lovik, M. 2009. Particle size determines activation of the innate immune system in the lung. *Scandin. J. Immunol.* 69(5): 421–428.

Sanders, J.W., Putnam, S.D., Frankart, C., Frenck, R.W., Monteville, M.R., Riddle, M.S., Rockabrand, D.M., Sharp, T.W. & Tribble, D.R. 2005. Impact of illness and non-combat injury during operations Iraqi Freedom and Enduring Freedom (Afghanistan). *Amer. J. Trop. Med. & Hyg.* 73(4): 713–719.

Schecter, A., Dai, C., Papke, O., Prange, J., Constable, J.D., Matuda, M., Duc Thao, V. & Piskac, A. 2001. Recent dioxin contamination from Agent Orange in residents of a southern Vietnam city. *J. Occup. & Environ. Med.* 43(5): 435–443.

Schecter, A. & Constable, J.D. 2006. Commentary: Agent Orange and birth defects in Vietnam. *Int. J. Epidem.* 35(5): 1230–1232.

Schiff, L.J., Byrne, M.M., Elliott, S.F., Moore, S.J., Ketels, K.V. & Graham, J.A. 1981. Response of hamster trachea in organ culture to Mount St. Helens volcano ash. *Scan. elect. microsc.* (Pt 2): 169–178.

Schneider, D.J., Rose, W.I., Coke, L.R., Bluth, G.J.S., Sprod, U.E. & Krueger, A.J. 1999. Early evolution of a stratospheric volcanic eruption cloud as observed with TOMS and AVHRR. *J. Geophys. Res.* 104: 4037–4050.

Schneider, E., Hajjeh, R.A., Spiegel, R.A., Jibson, R.W., Harp, E.L., Marshall, G.A., Gunn, R.A., McNeil, M.M., Pinner, R.W., Baron, R.C., Hutwagner, L.C., Crump, C., Kaufman, L., Reef, S.E., Feldman, G.M., Pappagianis, D. & Werner, S.B. 1997. A coccidioidomycosis outbreak following the Northridge, California earthquake. *J. Amer. Med. Assoc.* 277(11): 904–908.

Schölkopf, B., Smola, A.J., Williamson, R.C. & Bartlett, P.L. 2000. New support vector algorithms. *Neural Computation* 12(5): 1207–1245.

Schollaert, S.E., Yoder, J.A., Westphal, D.L. & O'reilly, J.E. 2003. The influence of dust and sulfate aerosols on ocean color spectra and chlorophyll-*a* concentrations derived from SeaWiFS of the U.S. Coast. *J. Geophy. Res.* 108(C6): 3191. doi:3110.1029/2000JC000555.

Searcy, C., Dean, K., Stringer, W. 1998. PUFF: A high-resolution volcanic ash tracking model. *J. Volcan. & Geoth. Res.* 80(1–2): 1–16.

Seftor, J. & Hsu, N., 1997. Detection of volcanic ash clouds from Nimbus 7/total ozone mapping spectrometer. *J. Geophys. Res.* 102(D14): 16,749–16,759.

Shoor, A.F., Scoville, S.L., Cersovsky, S.B., Shanks, D., Ockenhouse, C.F., Smoak, B.L., Carr, W.W. & Petruccelli, B.P. 2004. Acute eosinophilic pneumonia among U.S. military personnel deployed in or near Iraq. *J. Amer. Med. Assoc.* 292(24): 2997–3005.

Simkin, T. & Siebert, L. 1994. *Volcanoes of the World*. Tucson: Geoscience Press & Smithsonian Institution Global Volcanism Program.

Simpson, J.J., Hufford, G., Pieri, D. & Berg, J. 2000. Failures in detecting volcanic ash from a satellite-based technique. *Rem. Sens. Environ.* 72(2): 191–217.

Sinigalliano, C.D., Gidley, M.L., Shibata, T., Whitman, D., Dixon, T.H., Laws, E., Hou, A., Bachoon, D., Brand, L., Amaral-Zettler, L., Gast, R.J., Steward, G.F., Nigro, O.D., Fujioka, R., Betancourt, W.Q., Vithanage, G., Mathews, J., Fleming, L.E. & Solo-Gabriele, H.M. 2007. Impacts of Hurricanes Katrina and Rita on the microbial landscape of the New Orleans area. *Proc. Nat. Acad. Sci. USA* 104(21): 9029–9034.

Small, C. & Naumann, T. 2001. The global distribution of human population and recent volcanism. *Global Environmental Change Part B: Environmental Hazards* 3(3–4): 93–109.

SMD 2012. Available from: www.nasascience.nasa.gov/earth-science/mission_list [Accessed 4th February 2012].

Smirnov, A., Villevalde, Y., O'Neill, N.T., Royer, A. & Tarussov, A. 1995. Aerosol optical depth over the oceans – analysis in terms of synoptic air-mass types. *J. Geophys. Res. Atmosph.* 100(D8): 16639–16650.

Smith, B., Wong, C.A., Smith, T.C., Boyko, E.J., Gackstetter, G.D. & Margaret, A.K. 2009. Newly reported respiratory symptoms and conditions among military personnel deployed to Iraq and Afghanistan: A prospective population-based study. *Amer. J. Epidem.* 170(11): 1433–1442.

Smith, D.B., Cannon, W.F., Woodruff, L.G., Garrett, R.G., Klassen, R., Kilburn, J.E., Horton, J.D., King, J.D., Goldhaber, M.B. & Morrison, J.M. 2005. Major-and trace-element concentrations in soils from two continental-scale transects of the United States and Canada. USGS Open File Report 2005-1253: 1–20.

Smith, D.J., Griffin, D.W. & Schuerger, A.C. 2010. Stratospheric microbiology at 20 km over the Pacific Ocean. *Aerobiologia* 26(1): 35–46.

Smithsonian. 2009. Smithsonian Institute's Global Volcanism Program Archives of Natural History. Available from: http://www.volcano.si.edu/world/ [Accessed 4th February 2012].

Smola, A.J. & Scholkopf, B. 2004. A tutorial on support vector regression. *Stats. & Comput.* 14(3): 199–222.

Sprigg, W., Barbaris, B., Morain, S.A., Budge, A.M., Hudspeth, W. & Pejanovic, G. 2009. Public-health applications in remote sensing. Available from: http://www.spie.org/x33688.xml?highlight=x2416&ArticleID=x33688 [Accessed 4th February 2012].

SSEC. 2005. Space Science and Engineering Center. Available from: http://www.ssec.wisc.edu/mcidas [Accessed 4th February 2012].

Stellman, J.M., Stellman, S.D., Weber, T., Tomasallo, C., Stellman, A.B. & Christian Jr., R. 2003. A geographic information system for characterizing exposure to Agent Orange and other herbicides in Vietnam. *Environ. Health Perspec.* 111(3): 321.

Stevens, N.F., Manville, V. & Heron, D.W. 2003. The sensitivity of a volcanic flow model to digital elevation model accuracy: Experiments with digitised map contours and interferometric SAR at Ruapehu and Taranaki volcanoes, New Zealand. *J. Volcan. & Geoth. Res.* 119(1–4): 89–105.

Sultan, B., Labadi, K., Guegan, J.F. & Janicot, S. 2005. Climate drives the meningitis epidemics onset in West Africa. *PLoS Med.* 2(1): e6.

Sutton, A.J., Elias, T., Kauahikaua, J.P. & Moniz-Nakamura, J. 2006. Increased CO_2 emissions from Kilauea: A newly appreciated health hazard at Hawaii Volcanoes National Park, USA. *Cities on Volcanoes, Fourth Conference*. Quito, Ecuador.

Suwalsky, M., Benites, M., Villena, F., Aguilar, F. & Sotomayor, C.P. 1996. Interaction of 2,4-dichlorophenoxyacetic acid (2,4-D) with cell and model membranes. *Biochim. et Biophys. Acta (BBA)-Biomembranes* 1285(2): 267–276.

Swap, R., Garstang, M., Greco, S., Talbot, R. & Kallberg, P. 1992. Saharan dust in the Amazon Basin. *Tellus* 44(B): 133–149.

Swap, R., Ulanski, S., Cobbertt, M. & Garstang, M. 1996. Temporal and spatial characteristics of Saharan dust outbreaks. *J. Geophys. Res.* 101(D2): 4205–4220.

Symonds, R.B., Rose, W.I., Bluth, G.J.S. & Gerlach, T.M. 1994. Volcanic-gas studies: Methods, results, and applications. *Revs. Mineral. & Geochem.* 30(1): 1–66.

Takenaka, S., Karg, E., Kreyling, W.G., Lentner, B., Moller, W., Behnke-Semmler, M., Jennen, L., Walch, A., Michalke, B. & Schramel, P. 2006. Distribution pattern of inhaled ultrafine gold particles in the rat lung. *Inhal. Toxicol.* 18(10): 733–740.

Tan, K. 2010. Available from: http://shanghaiist.com/2010/04/26/gansu-sandstorm.php [Accessed 22nd February 2012].

Tank, V., Pfanz, H. & Kick, H. 2008. New remote sensing techniques for the detection and quantification of earth surface CO2 degassing. *J. Volcan. & Geoth. Res.* 177(2): 515–524.

Tassi, F., Vaselli, O., Capaccioni, B., Giolito, C., Duarte, E., Fernandez, E., Minissale, A. & Magro, G. 2005. The hydrothermal-volcanic system of Rincon de la Vieja volcano (Costa Rica): A combined (inorganic and organic) geochemical approach to understanding the origin of the fluid discharges and its possible application to volcanic surveillance. *J. Volcan. & Geoth. Res.* 148(3-4): 315–333.

Tate, R.L. III. 2000. *Soil Microbiology*. New York: John Wiley.

Teske, M.E., Bird, S.L., Esterly, D.M., Curbishley, T.B., Ray, S.L. & Perry, S.G. 2002. AgDRIFT®: A model for estimating near-field spray drift from aerial applications. *Environ. Toxicol. & Chem.* 21(3): 659–671.

Thundiyil, J.G., Stober, J., Besbelli, N. & Pronczuk, J. 2008. Acute pesticide poisoning: A proposed classification tool. *Bull. WHO* 86(3): 205–209.

Tobin, G.A. & Whiteford L.M. 2002a. Community resilience and volcano hazard: The eruption of Tungurahua and evacuation of the faldas in Ecuador. *Disasters* 26(1): 28–48.

Tobin, G.A. & Whiteford, L.M. 2002b. Economic ramifications of disaster: Experiences of displaced persons on the slopes of Mount Tungurahua, Ecuador. In *25th Appl. Geogr. Conf.* 316–324. Binghamton, NY.